Food and Agriculture Organization of the United Nations

International Institute for Applied Systems Analysis
IIASA www.iiasa.ac.at

The Islamic Republic of

AFGHANISTAN

AGRO-ECOLOGICAL ZONING ATLAS

PART 1

Agro-climatic indicators

The Islamic Republic of AFGHANISTAN

AGRO-ECOLOGICAL ZONING ATLAS

PART 1 / *Agro-climatic indicators*

A study of the International Institute for Applied Systems Analysis (IIASA) in collaboration with FAO

Edited by Günther Fischer and Harrij van Velthuizen (IIASA)

Published by

THE FOOD AND AGRICULTURE ORGANIZATION OF THE UNITED NATIONS
and
INTERNATIONAL INSTITUTE FOR APPLIED SYSTEMS ANALYSIS

Rome, 2019

FAO and IIASA. 2019. *The Islamic Republic of Afghanistan — Agro-ecological zoning atlas. Part 1: Agro-climatic indicators*. Rome.

ISBN 978-92-5-131925-3

Cover photograph:
©FAO/ Giulio Napolitano

Contents

Maps

Foreword

Agriculture is crucial for the national economy of the Islamic Republic of Afghanistan and in particularly so for the agriculturally dependent population which is constituting 60 percent of the total population.

Adoption of new strategies for agriculture monitoring, rural land use planning and land management are urgently required to reduce hunger and poverty among rural population and to assure sustainable food and feed production for future generations. The availability of reliable information on natural resources and agriculture for its monitoring and analysis is indispensable to development and implementation of such strategies.

However, productivity in the agricultural sector has been relatively low. Afghanistan has the potential to increase its output of cereals, fruits and vegetables.

For this purpose the project "Strengthening Afghanistan Institutions' Capacity for the Assessment of Agriculture Production and Scenario Development" (GCP/AFG/087/EC), funded by the European Union (EU), is implemented by the Ministry of Agriculture, Irrigation and Livestock (MAIL) and the Food and Agriculture Organization of the United Nations (FAO). Among the project objectives are improving the understanding of the country's national resources endowment and limitations as well as assessing agricultural production capacities under current climatic conditions and likely impacts of climate change.

Within the context of this project the Food and Agriculture Organization of the United Nations (FAO) and the International Institute for Applied Systems Analysis (IIASA) support and implement a national agro-ecological zoning activity in Afghanistan (NAEZ) which assesses quality and availability of land resources and identifies crop cultivation potentials under given current or future agro-climatic conditions.

One of the outputs of the NAEZ activities is this agro-ecological zones atlas which is based on applications of the FAO/IIASA national agro-ecological zoning system for current and future climates. The Atlas provides two distinct parts, namely:

- Part 1: Agro-climatic indicators
- Part 2: Agro-ecological assessments.

Nasir Ahmad Durrani
Minister of Agriculture, Irrigation
and Livestock of Afghanistan

Rajendra Kumar Aryal
FAO Representative
Country Director in Afghanistan

Acknowledgements

The publication of the agro-ecological zoning atlas of the Islamic Republic of Afghanistan is the result of the great joint efforts of many institutions and individuals working in close partnership.

The publication of the atlas was made possible by the contributions (financial and in-kind) of the partner organizations involved in the Afghanistan programme: the Government of the Islamic Republic of Afghanistan, the Food and Agriculture Organization of the United Nations (FAO) and the European Commission (EC), which funds the Programme.

FAO Afghanistan greatly acknowledges the initiative taken by the Ministry of Agriculture, Irrigation and Livestock (MAIL) for delegating the study on national agro-ecological zoning.

Significant valued management for this work was provided by Rajendra Aryal. Guidance, support and oversight in his current role as FAO Representative/Country Director is highly appreciated.

The collaboration and assistance of the International Institute for Applied System Analysis (IIASA) and its experts (Günther Fischer and Harrij van Velthuizen) are acknowledged in implementation of the national agro-ecological zoning (NAEZ) system for Afghanistan including data collection/verification, database creation, coding and scenario analysis, soil/crop/climate results classification and map production.

For in-country and International consultations, technical guidance, formal and informal peer reviews, local knowledge, and insights, thanks are due to: Sabawoon Chakhansuri (Director of Statistics and MIS-MAIL), Moeen Uddin Siraj (Head of Operation - FAO Afghanistan), and Muhammad Ishaq Safi (National Project Manager – FAO Afghanistan).

We acknowledge the keen interest and support provided by Douglas Muchoney (Project Lead Technical Officer, FAO-CBDS) and graphic design developed by Lucia Moro (FAO-CBDS). In addition, we also thank the technical interactions and inputs of all colleagues in FAO and many other individuals and government agencies (MAIL, MEW, NSIA, AMD, ARAZI and NEPA) at all administrative levels of Afghanistan.

Abbreviations and acronyms

AEZ	Agro-ecological zones
AR5	IPCC Fifth assessment report, 2014
BADC	British Atmospheric Data Centre
CMIP5	Coupled model intercomparison project phase 5
GFDL-ESM2M	Geophysical fluid dynamics laboratory earth system model 2
GPCC	Global Precipitation Climatology Centre
CRU	Climate Research Unit
CVR	Coefficient of variation
Ensamble mean	Mean value outcomes of multi-model simulation experiments
ERA-40	Re-analysis of methodological observations from September 1957 to August 2002 produced by the European Centre for Medium-Range Weather Forecasts (ECMWF)
ETo	Reference potential evapotranspiration
ETa	Reference actual evapotranspiration
FAO	Food and Agriculture Organization of the United Nations
HadGEM2-ES	Hadley Centre global environmental model 2 - earth system
IIASA	International Institute for Applied Systems Analysis
IPCC	Intergovernmental panel on climate change
IPSL-CM5A-LR	Institut Pierre Simon Laplace earth system model for the 5th IPCC report
ISI-MIP	Intersectoral impact model intercomparison project
LGP	Lenght of growing period
LGPt	Lenght of temperature growing period
MIROC-ESM-CHEM	Earth system model developed by Japan Agency for Marine-Earth Science and Technology and Centre for Climate System Research / National Institute for Environmental Studies, Japan
NAEZ	National agro-ecological zoning
NDR	Number of rain-days
NHUM	Number of humid months
NorESM1-M	Norwegian earth system model
NPP	Net primary production
RCP	Representative concentration pathway
SD	Standard deviation
WATCH	Water and global change, EU-funded integrated project
WDe	Reference water deficit
2020s	Period 2011–2040
2050s	Period 2014–2070
2080s	Period 2071–2100

Selected agro-ecological zoning (AEZ) agro-climatic indicators

1. Climate data

For the Agro-ecological zones (AEZ), historical assessment time-series data were used from three main sources: the Climate research unit (CRU) at the University of East Anglia, the Global precipitation climatology centre (GPCC) and the EU WATCH Integrated project.

Climatic research unit (CRU) TS v3.21 (time-series) datasets were obtained from British atmospheric data centre (BADC). These are month-by-month variations in climate over the last century. CRU TS v3.21 data used in national agro-ecological zones (NAEZ) Afghanistan are mean monthly temperatures, diurnal temperature range, cloud cover, vapour pressure and wet-day frequency.

For monthly precipitation, the GPCC Full data re-analysis product version 6 is used. In the current version of NAEZ-Afghanistan, the gridded historical precipitation data cover the period from 1961 to 2010. Global sub-daily meteorological forcing data were provided in WATCH[1] for use with land surface and hydrological models. The data are derived from the ERA-40 and ERA-Interim re-analysis products via sequential interpolation, elevation correction and monthly scale adjustments based on CRU (temperature, diurnal temperature range) and GPCC (precipitation) monthly observations.

Year-by-year climatic data analysis was undertaken for 1961 to 2010 and time series data were used to compile three 30-year baseline data sets, for the periods 1961–1990, 1971–2000 and 1981–2010, respectively; and for compiling associated CV/SD statistics.

2. Climate scenarios

International panel on climate change (IPCC) Assessment report 5 (AR5) climate model outputs for four Representative concentration pathways (RCPs) are used to characterize a range of possible future climate distortions for the 2020s (period 2011–2040), the 2050s (period 2041–2070) and the 2080s (period 2070–2099).

RCPs are a set of four greenhouse-gas concentration trajectories developed for the climate modeling community as a basis for long-term and near-term modeling experiments adopted by the IPCC for its AR5.

The four RCPs together span the range of years 2100 radiative forcing values found in the open literature, i.e. from 2.6 W/m^2 under stringent emission mitigation measures to 8.5 W/m^2. The four RCPs – RCP2.6, RCP4.5, RCP6, and RCP8.5 – are named after a future level of radiative forcing values in the year 2100 (2.6, 4.5, 6.0, and 8.5 W/m^2, respectively). These concentration pathways are documented in a special issue of climatic change (van Vuuren *et al.*, 2011), and climate model simulations based on them were undertaken as part of the Coupled model intercomparison project phase 5 (CMIP5) (Taylor *et al.*, 2011).

Multi-model ensembles for each of the climate-forcing levels of the RCPs were analysed, based on spatial data from the IPCC's AR5 CMIP5 process, data bias-corrected and downscaled to 0.5 degree as used in the Intersectoral impact model intercomparison project (ISI-MIP) (Hempel *et al.*, 2013). ISI-MIP data of five climate models (GFDL-ESM2M, HadGEM2-ES, IPSL-CM5A-LR, MIROC-ESM-CHEM, NorESM1-M) and for four RCPs (RCP 2.6, 4.5, 6.0 and 8.5) – totaling 20 combinations of, respectively, RCPs and climate models – were used for generating climate input data in NAEZ-Afghanistan covering the period of 2011 to 2099 and were used to compile results for three future 30-year periods, the 2020s (period 2011–2040), 2050s (period 2041–2070) and the 2080s (period 2070–2099).

1 WATCH was a large integrated project funded by the European Commission under the sixth Framework Programme, global change and ecosystems thematic priority area (contract number: 036946). The WATCH project started in 2007 and continued to 2011.

3. Agro-climatic indicators

Mean annual temperature

Temperature is a major determinant of crop growth and development. In AEZ, the effect of temperature on crops is characterized in each grid-cell by thermal regimes. Thermal regimes are represented by six types of indicators: (i) thermal climates; (ii) thermal zones; (iii) length of temperature growing periods; (iv) accumulated temperature sums; (v) temperature profiles; and (vi) permafrost zones.

Mean annual temperature is used to give a very general characterization of thermal conditions. The foremost influence on the mean annual temperature of a location is its latitudinal position and altitude. The spatial pattern of mean annual temperature in Afghanistan for historical 1981–2010 conditions is shown in Figure 1. The ensemble means of projected future annual temperatures for period 2041–2070 are presented in Figure 2, for future climate under RCP 4.5 (left) and RCP 8.5 (right), respectively.

Some details of changes of mean annual temperatures by eight regions are listed in Table 1. For instance, in the 2050s (period 2041–2070), the ensemble mean of the projected annual temperature increases by region under RCP 4.5 ranges between 2.0°C to 2.8 °C. Under RCP 8.5, expected temperature changes relative to period 1981–2010 are between 2.9 °C to 4.0 °C.

Figure 3 shows the delineation of eight regions used for presenting regional results and changes of agro-climatic indicators under current and future climate.

Mean annual temperature (°C)

Period 1981–2010

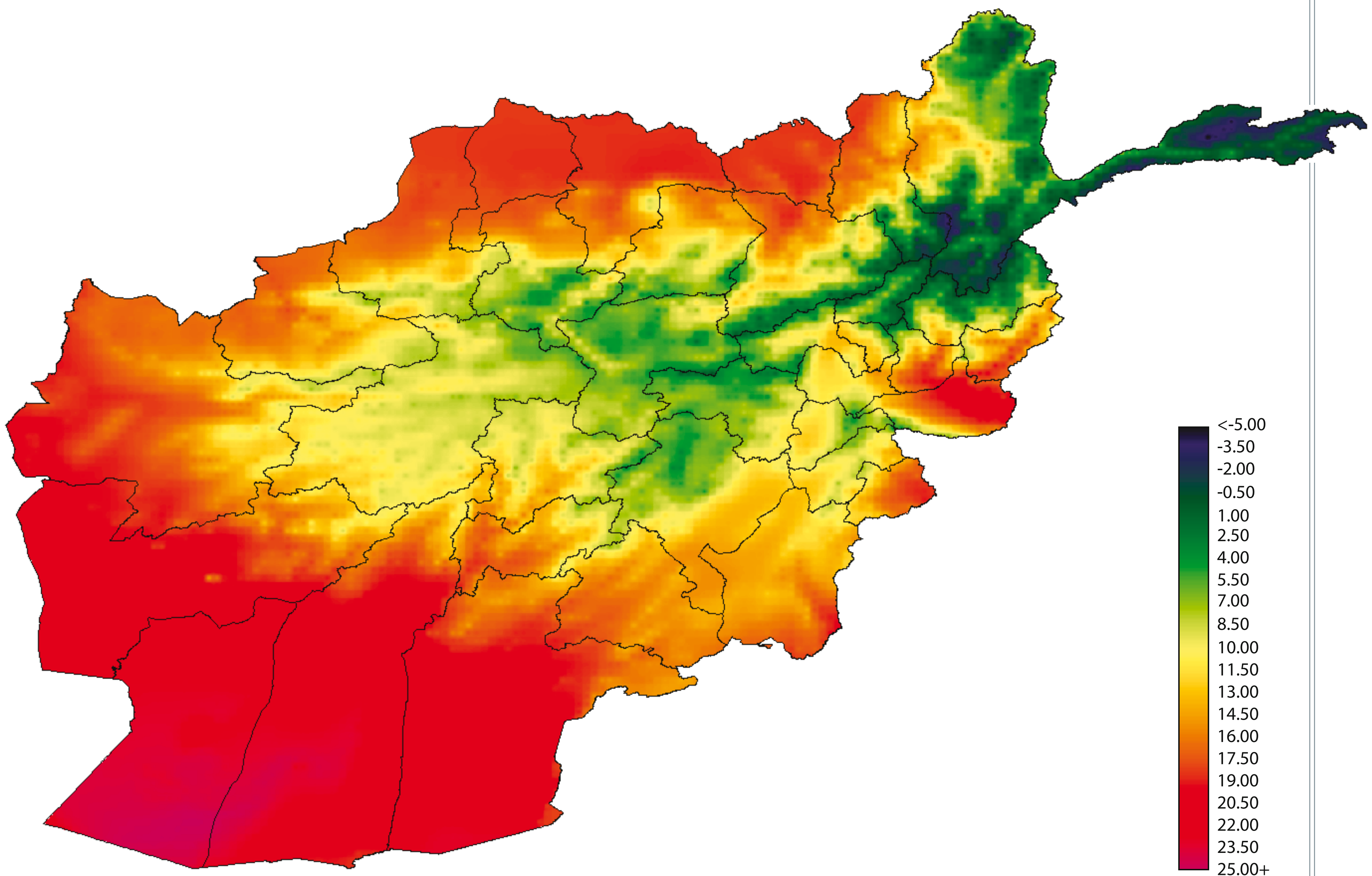

Source: IIASA, 2019

Figure 1

Ensemble mean
Period 2041–2070

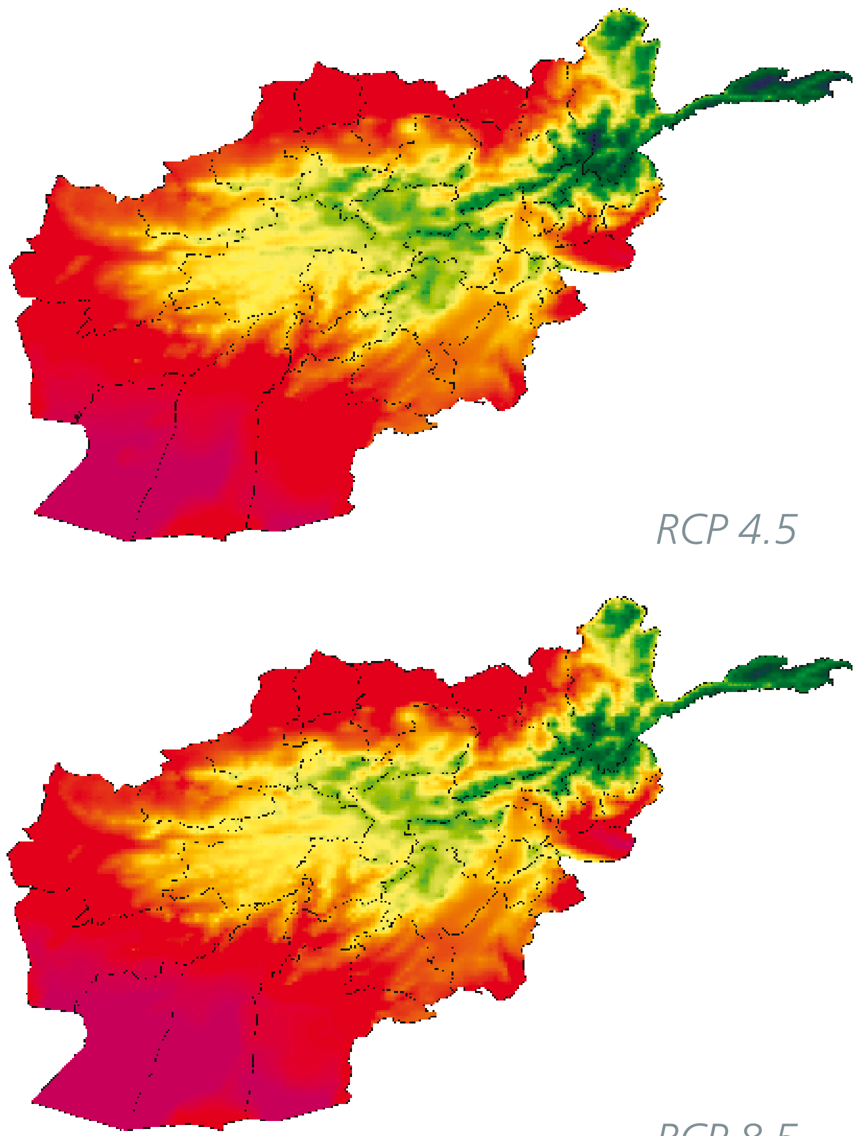

Source: IIASA, 2019

Figure 2

Major regions used for reporting the results of agro-climatic analysis

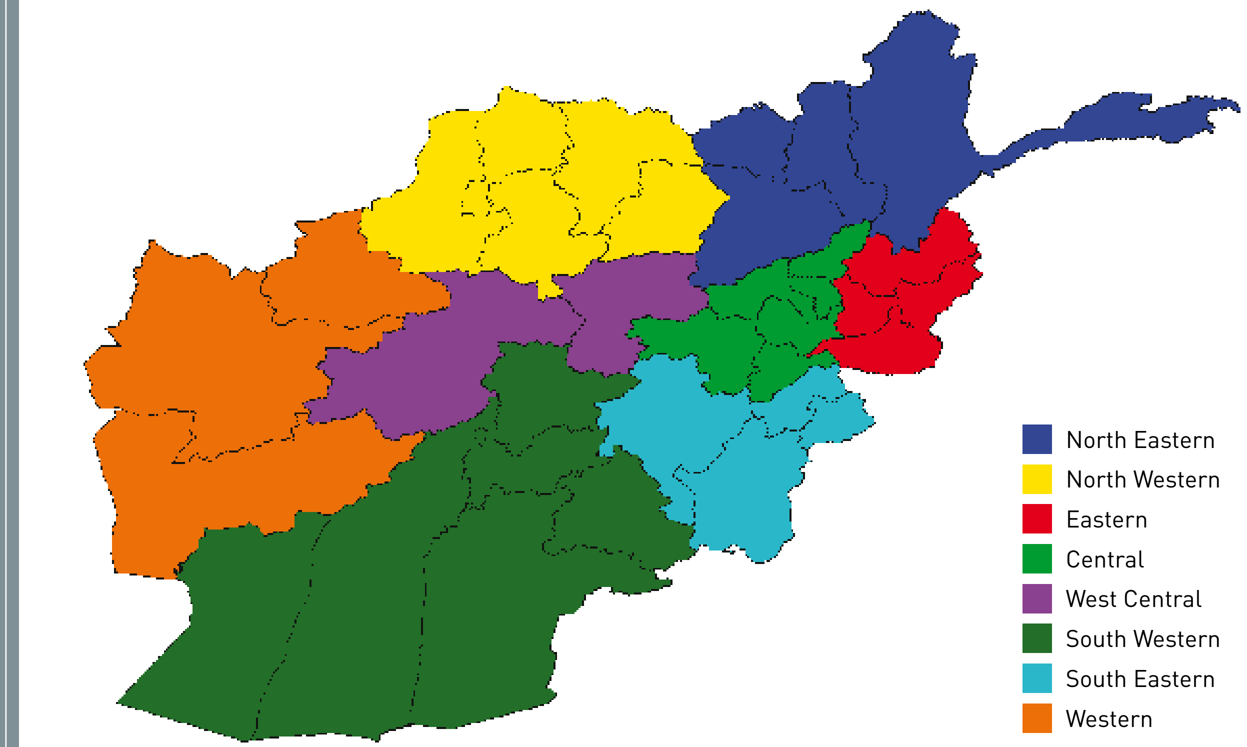

Figure 3

Source: IIASA, 2019

Table 1 - Changes of mean annual temperature (°C), period 2020s, 2050s and 2080s vs historical

Regions	Area (km²)	Historical		Ensemble mean RCP 4.5						Ensemble mean RCP 8.5					
		1961–1990	1981–2010	2020s	2050s	2080s	Difference with 1981–2010 2020s	Difference with 1981–2010 2050s	Difference with 1981–2010 2080s	2020s	2050s	2080s	Difference with 1981–2010 2020s	Difference with 1981–2010 2050s	Difference with 1981–2010 2080s
North Eastern	80 718	6.0	6.3	7.7	9.1	9.9	1.4	2.8	3.6	8.1	10.2	12.6	1.8	3.9	6.3
North Western	77 271	12.8	13.3	14.4	15.6	16.2	1.1	2.3	2.9	14.7	16.4	18.5	1.4	3.1	5.2
Eastern	25 059	10.5	10.5	12.0	13.3	14.1	1.5	2.8	3.6	12.4	14.5	16.7	1.9	4.0	6.2
Central	31 072	6.4	6.5	7.9	9.2	9.9	1.4	2.7	3.4	8.2	10.2	12.4	1.7	3.7	5.9
West Central	55 719	7.2	7.8	8.9	10.2	10.9	1.1	2.4	3.1	9.2	11.1	13.4	1.4	3.3	5.6
Western	160 581	13.7	14.6	15.5	16.6	17.3	0.9	2.0	2.7	15.8	17.5	19.7	1.2	2.9	5.1
South Eastern	28 472	12.9	13.0	14.3	15.5	16.2	1.3	2.5	3.2	14.6	16.5	18.7	1.6	3.5	5.7
South Western	183 421	18.7	19.7	20.6	21.7	22.3	0.9	2.0	2.6	20.9	22.6	24.9	1.2	2.9	5.2

Source: Calculations based on 30 arc-second NAEZ Afghanistan climate inventory.

Temperature seasonality

Due to the geographical position of Afghanistan at latitudes between 29.3 °N and 38.5 °N, the country falls within the temperate and sub-tropical latitudinal climate zones.

It experiences a pronounced temperature seasonality, as can be seen in Figure 4 which shows for historical 1981–2010 climate, the mean monthly temperatures in January, April, July and October, respectively.

The difference between warmest and coolest month, in the range of 20 °C to 30 °C, is shown in Figure 5.

Mean monthly temperature (°C)

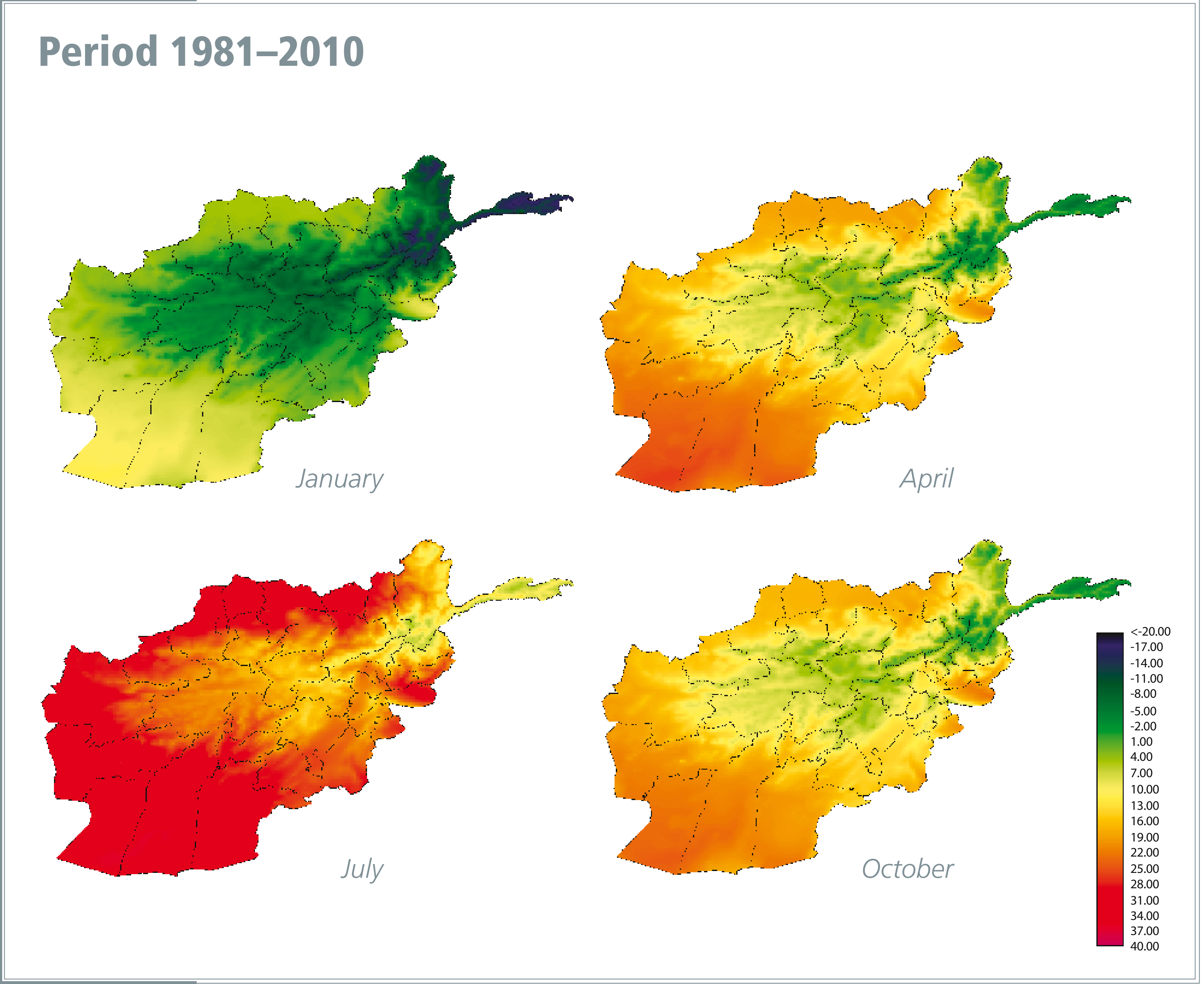

Source: IIASA, 2019

Figure 4

Seasonal amplitude monthly temperature (°C)

Period 1981–2010

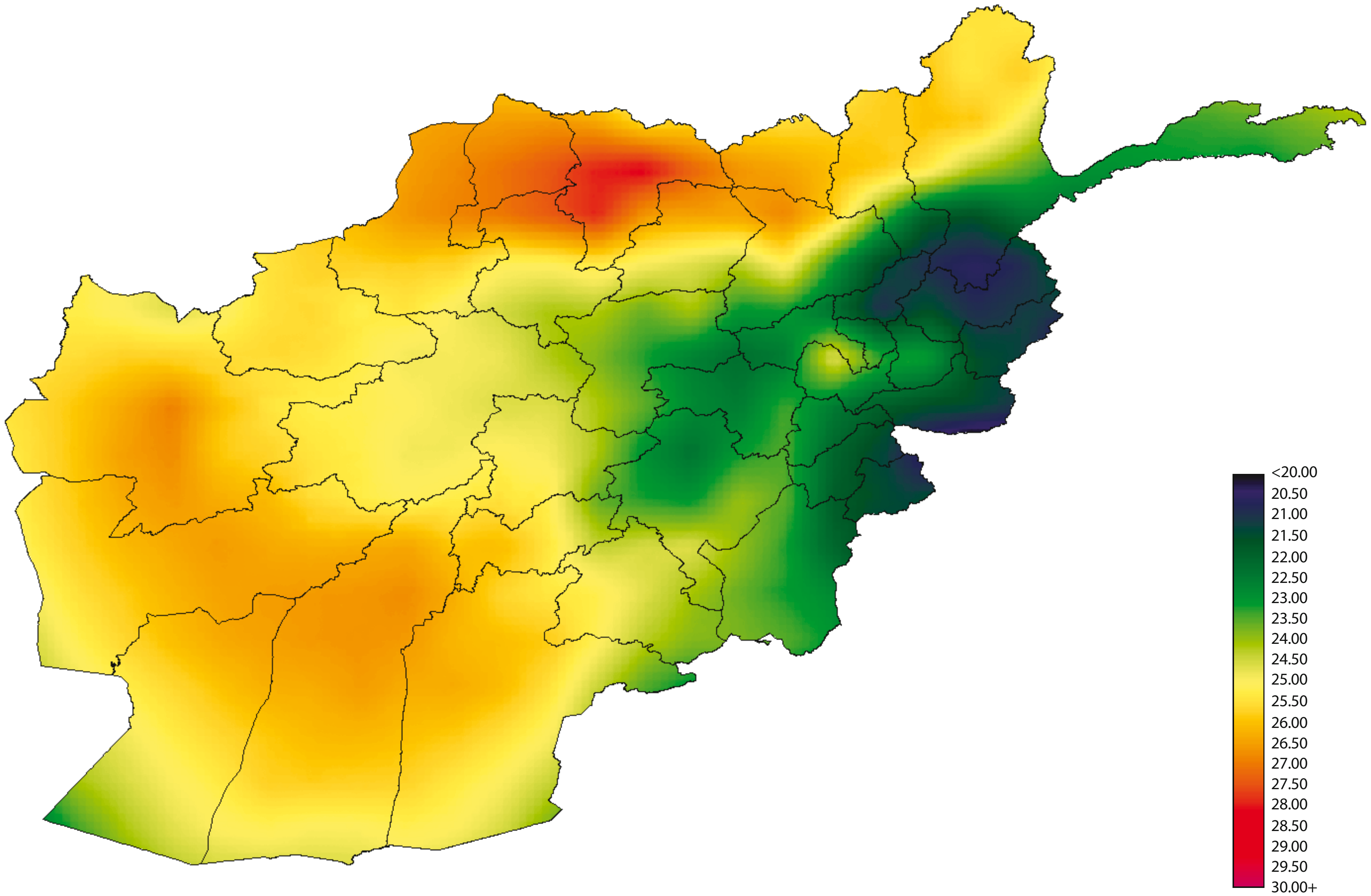

Source: IIASA, 2019

Figure 5

Annual precipitation

Besides temperature, annual precipitation – both its total amount and distribution within the year – is of critical importance for plant growth in general; and in particular, for the cultivation of rain-fed crops. Figure 6 shows the spatial distribution of historical average annual precipitation of period 1981–2010, indicating fairly modest amounts overall and a decreasing pattern of precipitation along a transsect from north-east to south-west Afghanistan. Projected future precipitation shows a similar spatial pattern, but annual precipitation amounts may slightly decrease in the future, as shown in Figure 7.

Table 2 gives an account of projected annual precipitation changes by region. It indicates that precipitation amounts will change little compared to 1981–2010 in the north-eastern and north-western region, whereas changes will be more substantial in the other regions. Decreases of precipitation will be most pronounced in west-central and southern regions.

Year-by-year results simulated in NAEZ for 1961 to 2099 were used to calculate geospatial rasters with indicator statistics for 30-year periods of 1961–1990, 1971–2000 and 1981–2010. Statistics of agro-climatic indicators include:

avg giving the mean of the time series of the respective period;

cvr giving the coefficient of variation (i.e. 100 times standard deviation over mean);

std giving the standard deviation of the observed or simulated values in the indicated period;

p10 giving the 10-percent quantile of the time series;

p50 giving the median of the respective time series; and

p90 giving the 90-percent quantile of the indicator values in the period.

Mean annual precipitation (mm)

Period 1981–2010

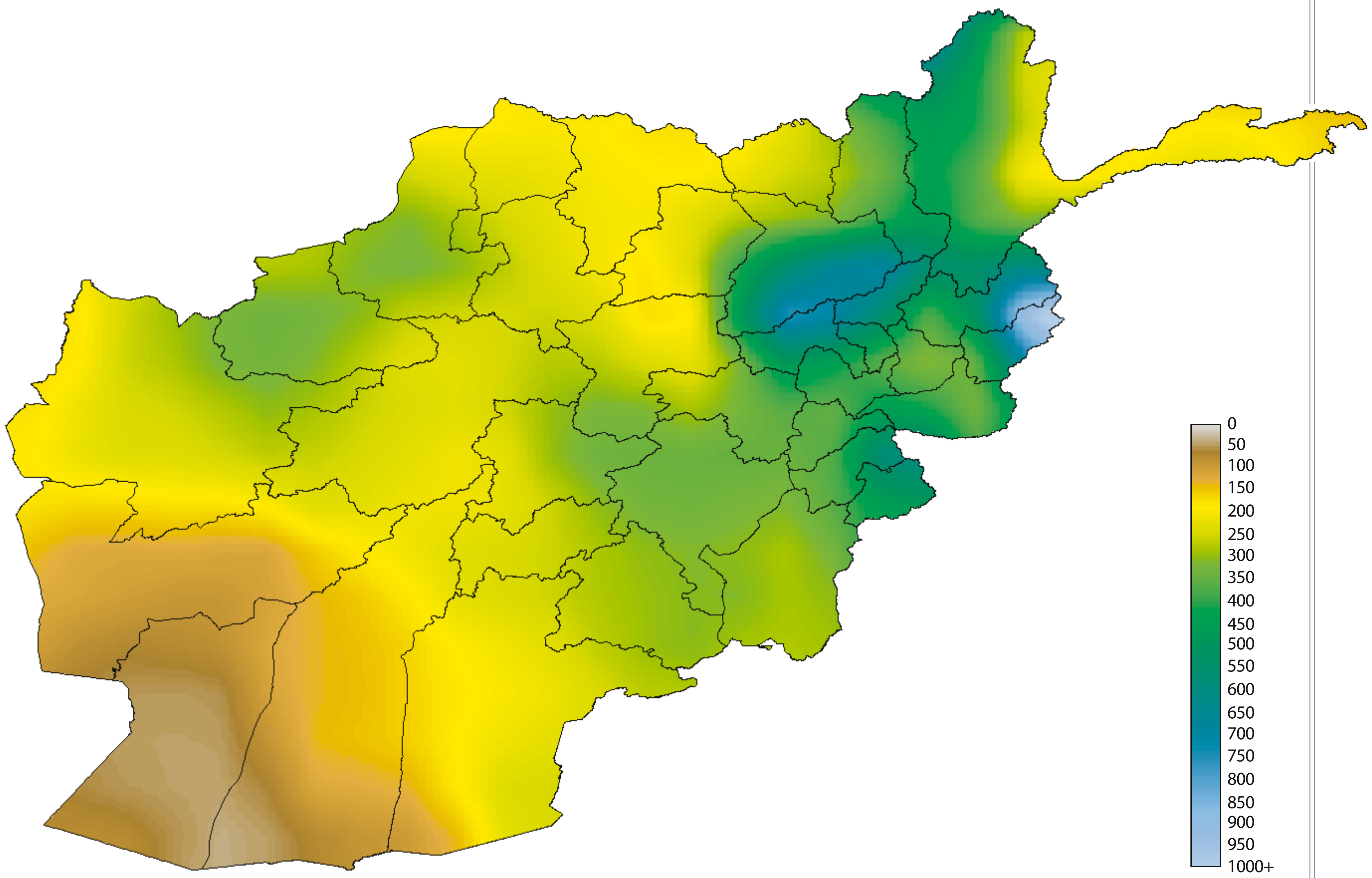

Source: IIASA, 2019

Figure 6

Ensemble mean
Period 2041–2070

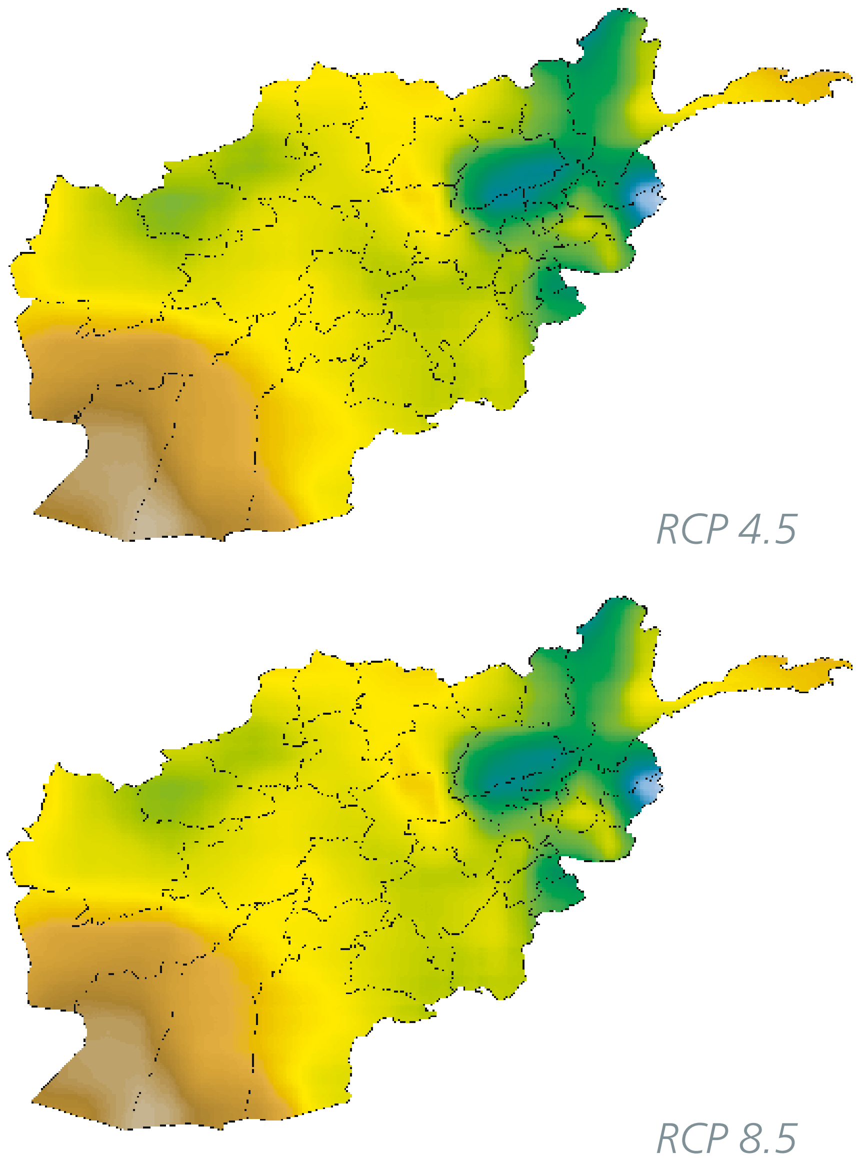

Source: IIASA, 2019

Figure 7

Variability of annual precipitation (CVR %), period 1981–2010

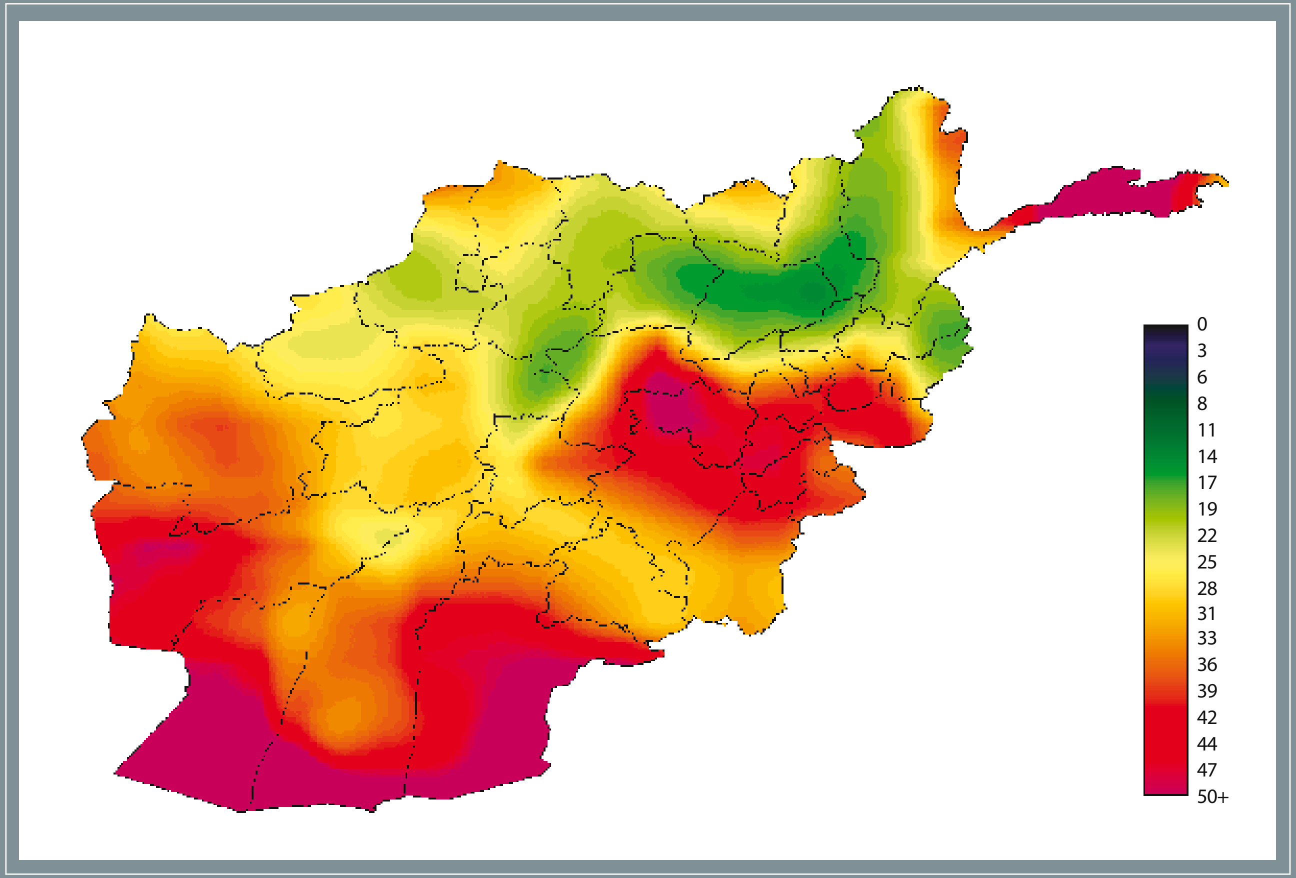

Source: IIASA, 2019

Figure 8

For instance, Figure 8 presents a measure of the variability of historical precipitation in terms of a coefficient of variation (CVR percent) obtained by comparing, for the historical period 1981–2010, the calculated standard deviation to the mean values.

For locations mapped in green, the standard deviation during the 30-year period was less than 20 percent of its mean value.

A red color indicates a CVR of 40 percent and more.

Table 2 - Changes of mean annual precipitation (mm), period 2020s, 2050s and 2080s vs historical

Regions	Area (km²)	Historical		Ensemble mean RCP 4.5						Ensemble mean RCP 8.5					
		1961–1990	1981–2010	2020s	2050s	2080s	% Difference with 1981–2010			2020s	2050s	2080s	% Difference with 1981–2010		
							2020s	2050s	2080s				2020s	2050s	2080s
North Eastern	80 718	376	375	374	371	366	0	-1	-2	346	356	347	-8	-5	-7
North Western	77 271	243	239	236	227	220	-1	-5	-8	212	220	209	-11	-8	-13
Eastern	25 059	466	502	457	454	442	-9	-10	-12	436	431	433	-13	-14	-14
Central	31 072	393	428	379	370	355	-11	-14	-17	341	349	328	-20	-18	-23
West Central	55 719	270	290	258	245	236	-11	-15	-18	234	237	215	-19	-18	-26
Western	160 581	220	215	219	201	197	2	-7	-9	194	199	184	-10	-7	-15
South Eastern	28 472	332	355	314	310	298	-11	-13	-16	307	305	285	-13	-14	-20
South Western	183 421	153	161	155	138	136	-3	-14	-15	147	143	124	-9	-11	-23

Source: Calculations based on 30 arc-second NAEZ Afghanistan climate inventory.

Precipitation seasonality

Besides temperature seasonality, the climate of Afghanistan also depicts a pronounced seasonality of precipitation, as illustrated in Figure 9, presenting average historical precipitation of selected months, i.e. January, April, July and October of period 1981–2010.

The major part of annual precipitation in Afghanistan falls in winter and early spring, whereas the summer and early autumn are dry and hot, notably in the north-western, western and south-western regions.

By implication, where rain-fed crop cultivation is possible at the available low precipitation, cropping needs to occur in winter and spring, cultivating a suitable winter or spring type such as wheat and barley or other cool-weather crops.

Cropping in summer or perennial crops largely depend on the availability of water for irrigation.

Mean monthly precipitation (°C)

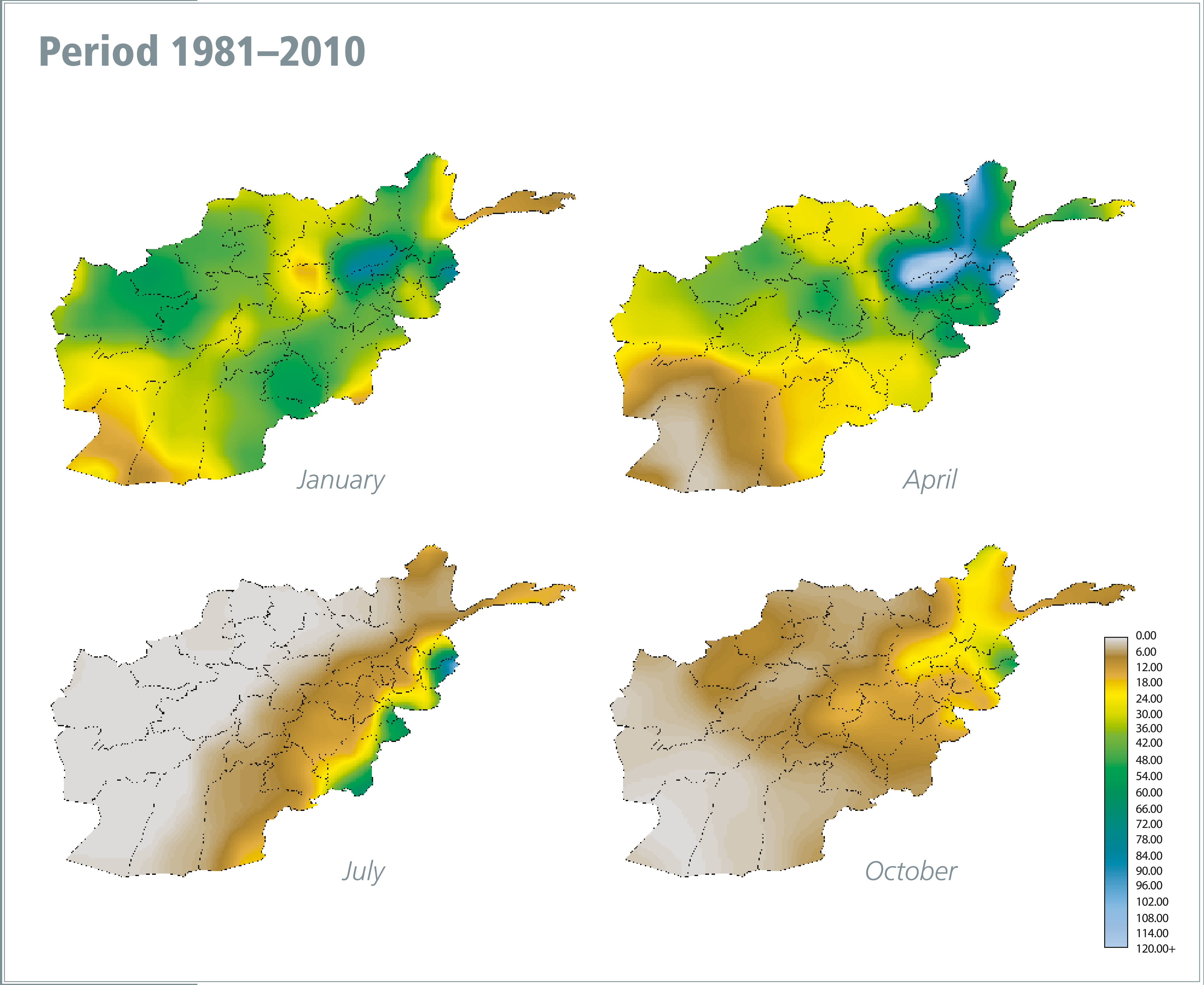

Source: IIASA, 2019

Figure 9

Ensemble mean, RCP 8.5
Period 2041–2070

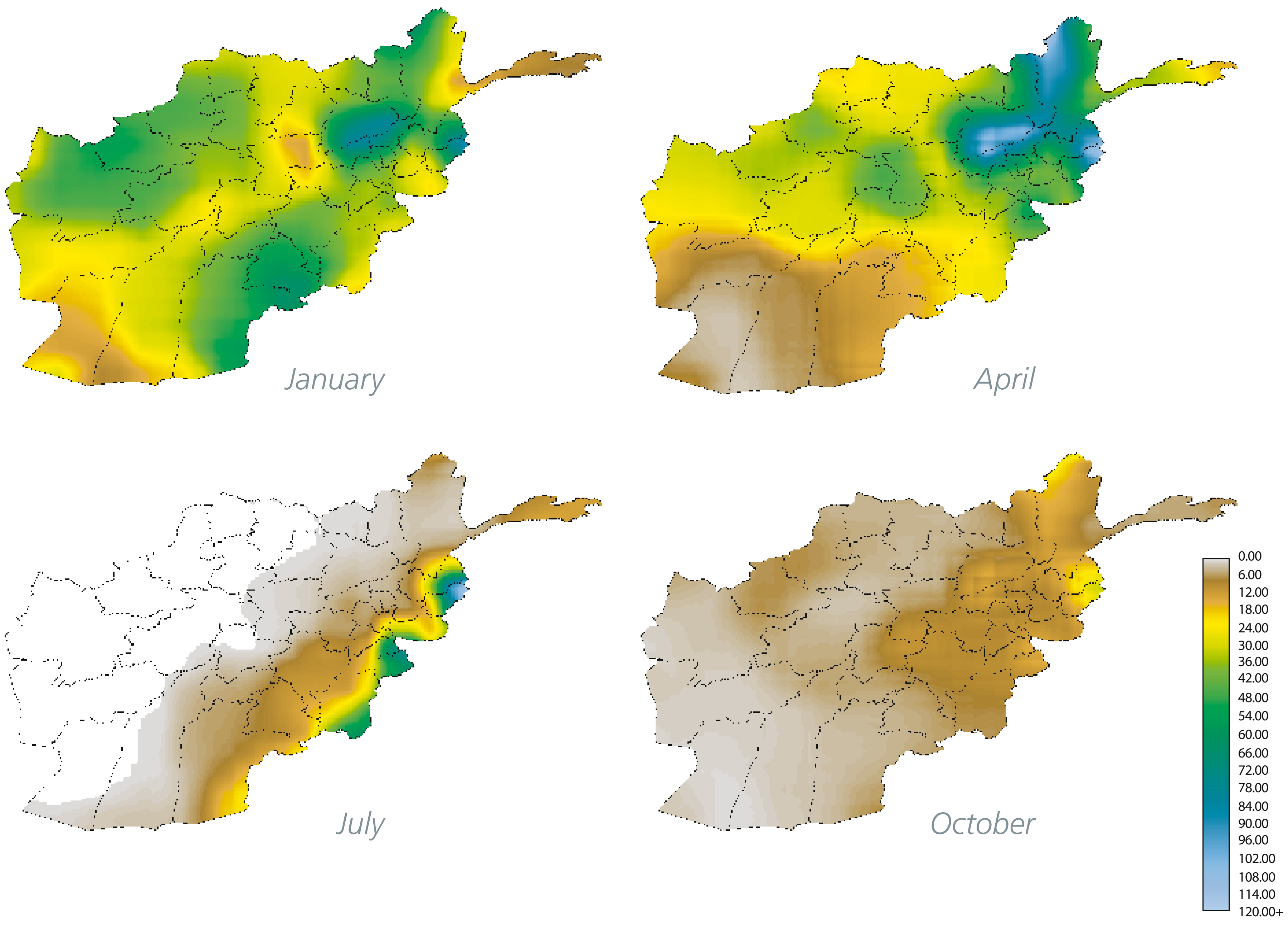

Source: IIASA, 2019

Figure 10

For comparison, Figure 10 shows ensemble means of average monthly precipitation of selected months projected under RCP 8.5 concentration pathway assumptions for years of the period 2041–2070.

While spatial patterns resemble those of the historical period, amounts in the 2050s are slightly reduced compared to precipitation during the period of 1981–2010.

Temperature growing periods (LGPt)

The period during the year when temperatures are conducive to crop growth and development is represented in AEZ by the 'temperature growing periods'.

The length of the 'temperature growing period' (LGPt) is calculated as the number of days in the year when average daily temperature (Ta) is above a temperature threshold "t". In AEZ, three standard temperature thresholds for temperature growing periods are used: (i) periods with Ta > 0 °C (LGPt0); (ii) periods with Ta > 5 °C (LGPt5), which is considered as the period conducive to plant growth and development; and (iii) periods with Ta > 10 °C (LGPt10), which is used as a proxy for the period of low risks for late and early frost occurrences.

The spatial pattern of LGPt5 during 1981–2010 is presented in Figure 11. It shows the temperature growing period was less than 100 days in higher-altitude areas of northeast Afghanistan, less than 200 days in parts of central Afghanistan, and indicates potentially year-round growing conditions (where water is available) in the south-west region.

Temperature growing period (LGPt>5 °C days)

Period 1981–2010

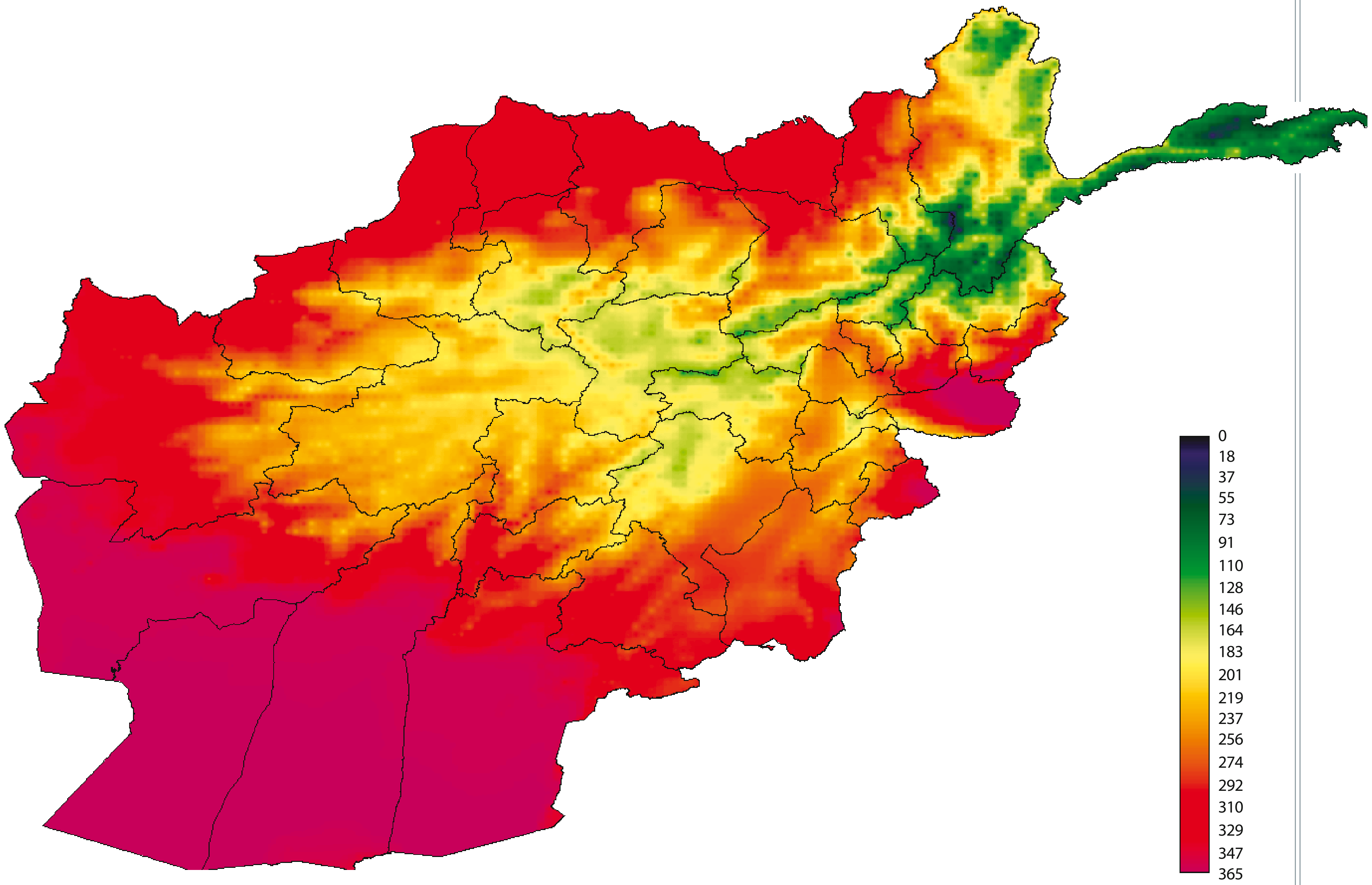

Source: IIASA, 2019

Figure 11

Ensemble mean
Period 2041–2070

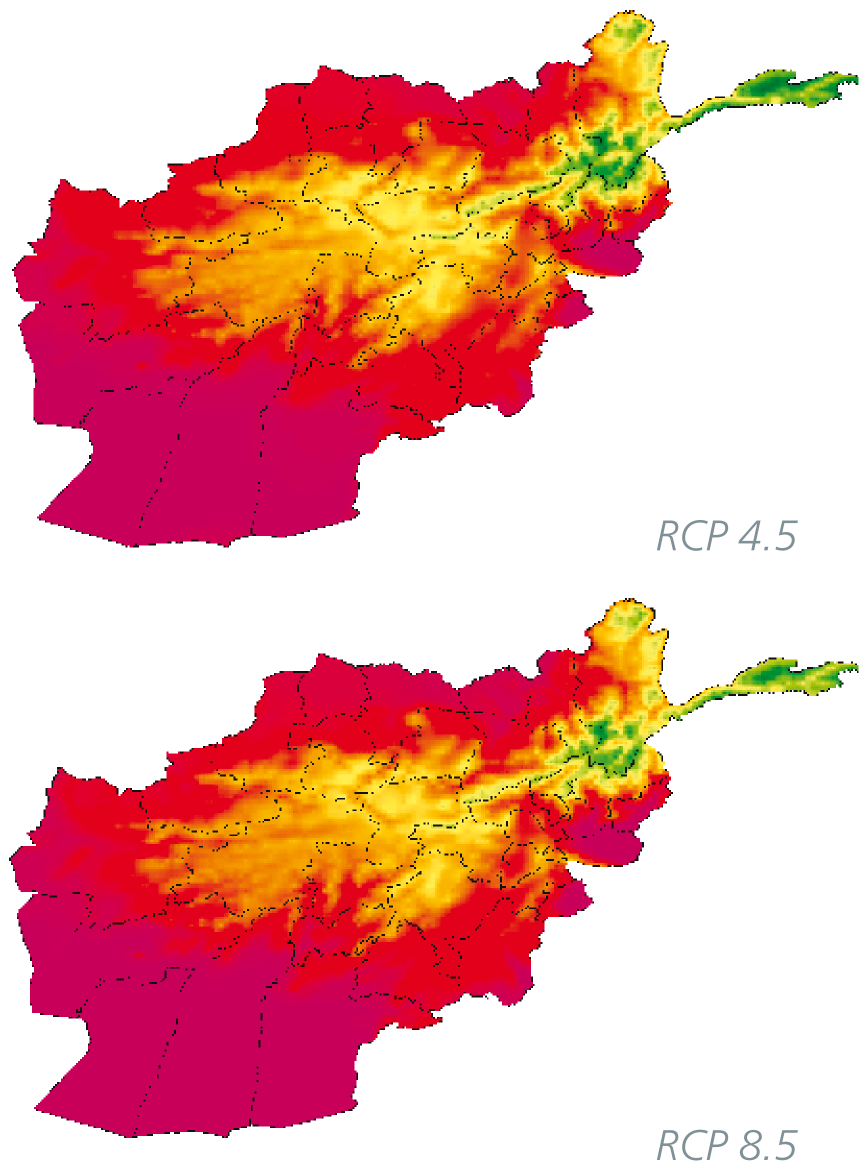

Source: IIASA, 2019

Figure 12

With climate change, additional temperature growing period days will be gained, especially in central and north-eastern Afghanistan (see Figure 12).

Table 3 lists the average number of temperature growing period days (LGPt5) for historical and projected future climate. Regional averages for 1981–2010 range from 195 days (north-eastern region) to 342 days (south-western region). By the 2050s the temperature growing period LGPt5 will increase by some 10 to 40 days, depending on region and RCP assumptions.

Table 3 - Changes of temperature growing periods (LGPt>5 °C days), period 2020s, 2050s and 2080s vs historical

Regions	Area (km²)	Historical		Ensemble mean RCP 4.5						Ensemble mean RCP 8.5					
		1961–1990	1981–2010	2020s	2050s	2080s	% Difference with 1981–2010			2020s	2050s	2080s	% Difference with 1981–2010		
							2020s	2050s	2080s				2020s	2050s	2080s
North Eastern	80 718	193	195	213	228	237	9	17	21	218	241	265	11	23	36
North Western	77 271	268	274	282	293	301	3	7	10	288	303	319	5	11	17
Eastern	25 059	253	254	270	284	292	6	12	15	276	295	314	8	16	23
Central	31 072	201	203	218	233	240	8	15	19	222	245	273	10	21	35
West Central	55 719	207	212	225	239	247	6	13	17	229	251	278	8	18	31
Western	160 581	281	291	296	305	312	2	5	7	300	313	328	3	8	13
South Eastern	28 472	279	279	295	309	319	6	11	14	300	323	343	8	16	23
South Western	183 421	335	342	345	350	354	1	2	4	347	354	359	2	4	5

Source: Calculations based on 30 arc-second NAEZ Afghanistan climate inventory.

Difference in sensitivity of crops for early and late frost is accounted for through the matching of crop/LUT growth cycles with prevailing frost-free periods.

The frost-free period is approximated by the period during the year when mean daily temperatures are above 10 °C (LGPt=10).

Depending on the sensitivity of a specific crop/LUT the matching of growth-cycle length with the available frost-free period provides optimum match, sub-optimum match or not suitable conditions.

The geospatial pattern of the length of the 'frost-free' period of the historical period 1981–2010 and of projected future climate in 2041–2070 is shown in Figure 13 and Figure 14, respectively.

"Frost-free" period (LGPt>10 °C days)

Period 1981–2010

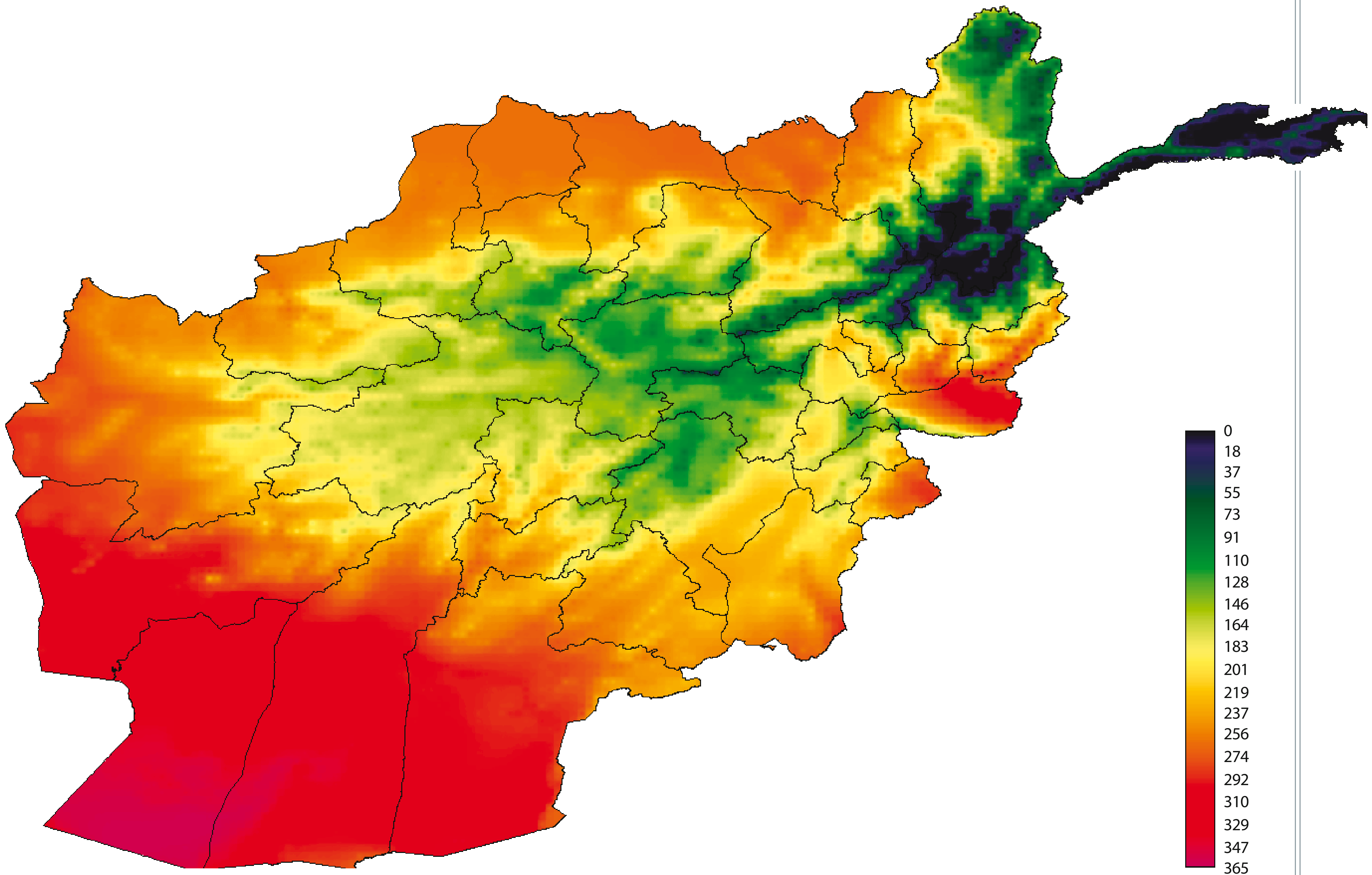

Source: IIASA, 2019

Figure 13

Ensemble mean Period 2041–2070

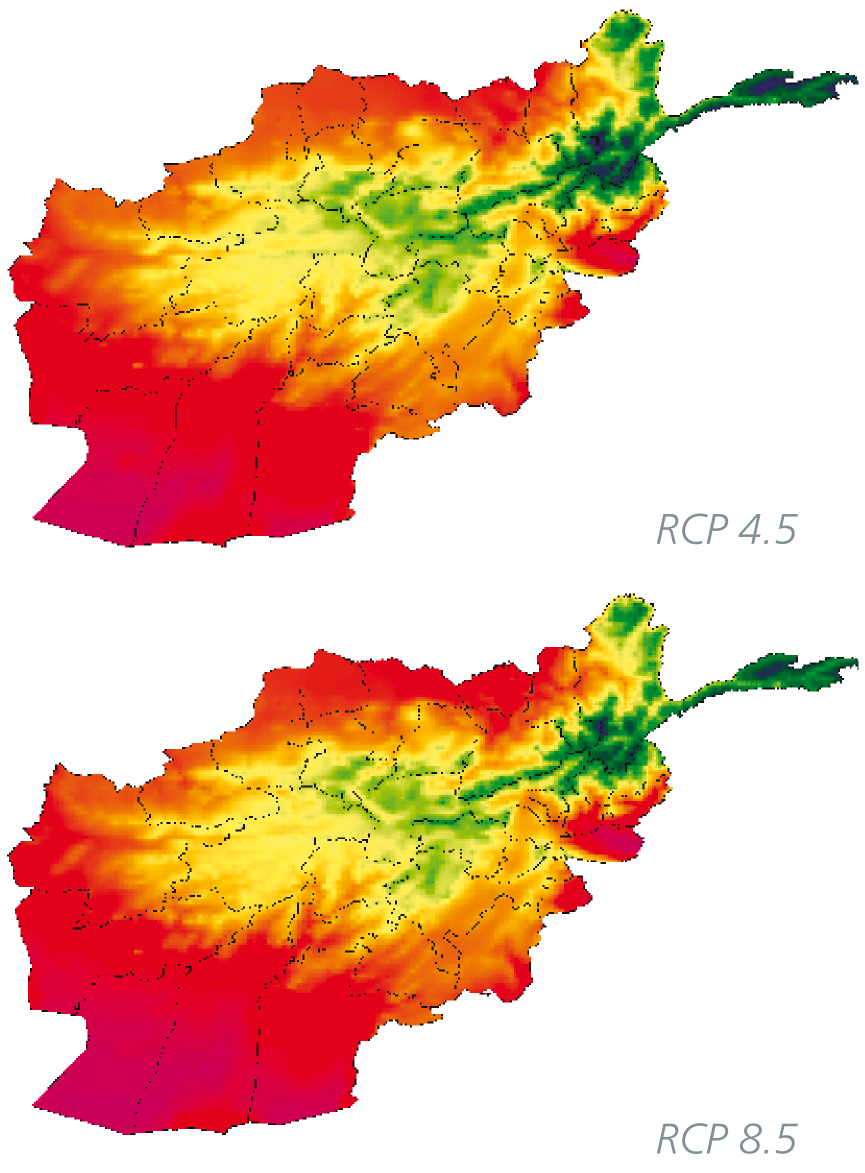

Source: IIASA, 2019

Figure 14

As with LGPt5, the 'frost-free' period indicator LGPt10 will increase noticeably with global warming. Region averages shown in Table 4 increase under RCP 4.5 in the 2050s by 7 percent to 27 percent and under RCP 8.5, by 11 percent to 37 percent, with most pronounced changes materializing in the central and north-eastern regions due to strong impacts at prevailing high altitudes.

In the latter case, under climate-change projections assuming RCP 8.5 radiative forcing, the regional averages of the LGPt10 indicator for the 2080s compare well to the LGPt5 indicator during 1981–2010.

Table 4 - Changes of "frost-free" temperature growing periods (LGPt>10 °C days) period 2020s, 2050s and 2080s vs historical

Regions	Area (km²)	Historical		Ensemble mean RCP 4.5						Ensemble mean RCP 8.5					
		1961–1990	1981–2010	2020s	2050s	2080s	% Difference with 1981–2010			2020s	2050s	2080s	% Difference with 1981–2010		
							2020s	2050s	2080s				2020s	2050s	2080s
North Eastern	80 718	131	132	152	169	177	15	27	34	155	182	210	17	37	59
North Western	77 271	210	213	223	235	241	5	10	13	227	244	267	6	14	25
Eastern	25 059	187	188	210	229	237	11	21	26	215	241	267	15	28	42
Central	31 072	141	142	160	175	181	12	23	27	163	185	210	15	30	48
West Central	55 719	150	157	169	183	189	8	16	20	172	192	217	9	22	38
Western	160 581	223	231	240	251	258	4	9	12	244	261	282	6	13	22
South Eastern	28 472	220	221	235	248	255	6	12	15	239	259	286	8	17	29
South Western	183 421	281	292	301	312	320	3	7	10	305	323	338	5	11	16

Source: Calculations based on 30 arc-second NAEZ Afghanistan climate inventory.

Accumulated temperature (Tsum)

For crop suitability assessments, individual crop/LUT heat unit requirements are matched with temperature sums during the crop/LUT growth cycle duration, defined as the sum of mean daily temperatures calculated from a base temperature of 0°C, resulting in optimum, sub-optimum or non-suitable ranges.

Heat requirements of crops are expressed in accumulated temperatures. Reference temperature sums (Tsum) are calculated for each grid-cell by accumulating daily average temperatures (Ta) for days when Ta is above the respective threshold temperatures "t" as follows: (i) 0°C ($Tsum_0$), (ii) 5 °C ($Tsum_5$), and (iii) 10 °C ($Tsum_{10}$).

For example, a map of historical 1981–2010 $Tsum_5$ (i.e. accumulated temperature sum on days with average daily temperature exceeding 5 °C) is shown in Figure 15. Future patterns of $Tsum_5$ in the 2050s are presented in Figure 16.

Accumulated temperature for LGPt>5 °C

Period 1981–2010

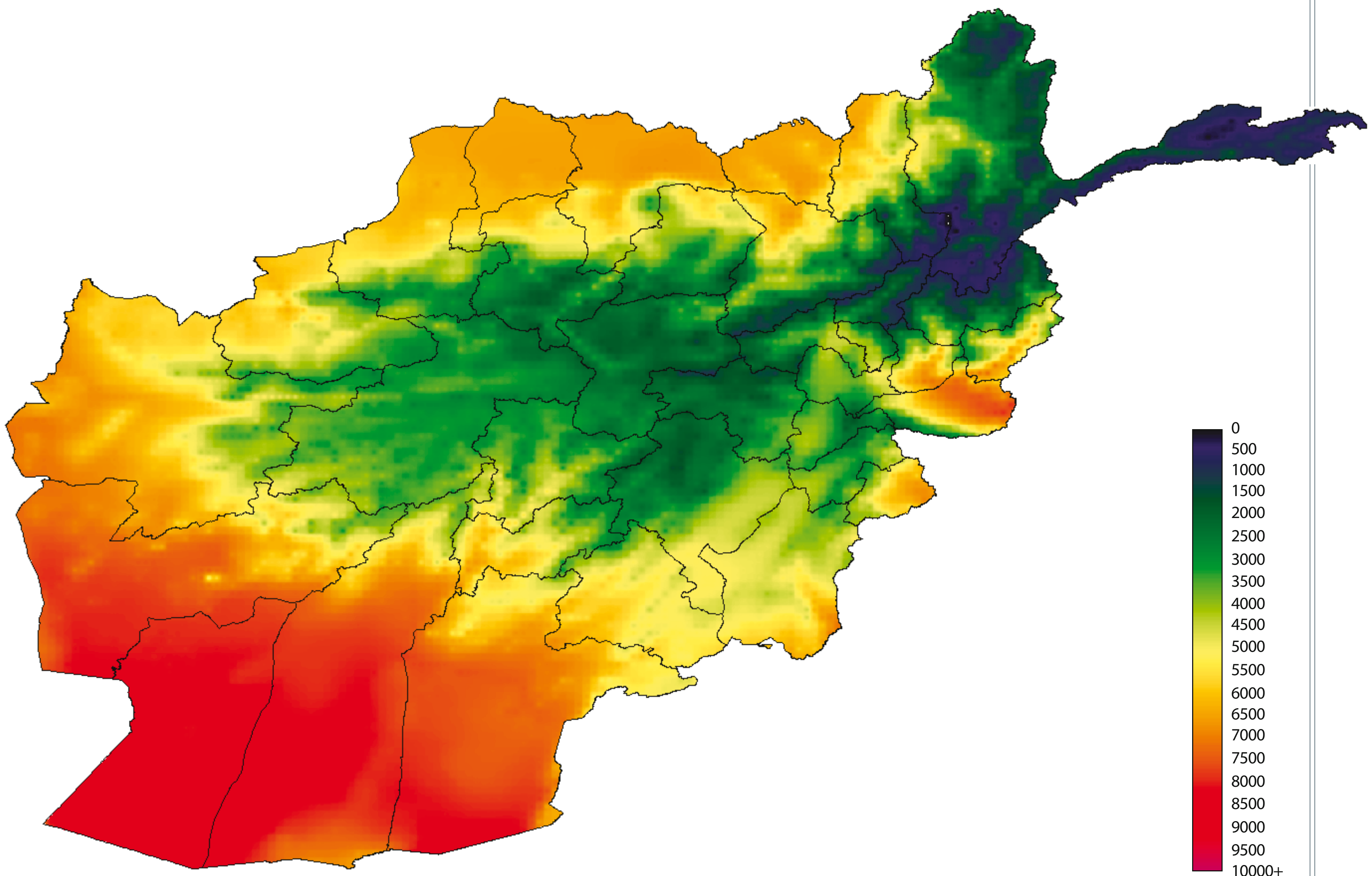

Source: IIASA, 2019

Figure 15

Ensemble mean
Period 2041–2070

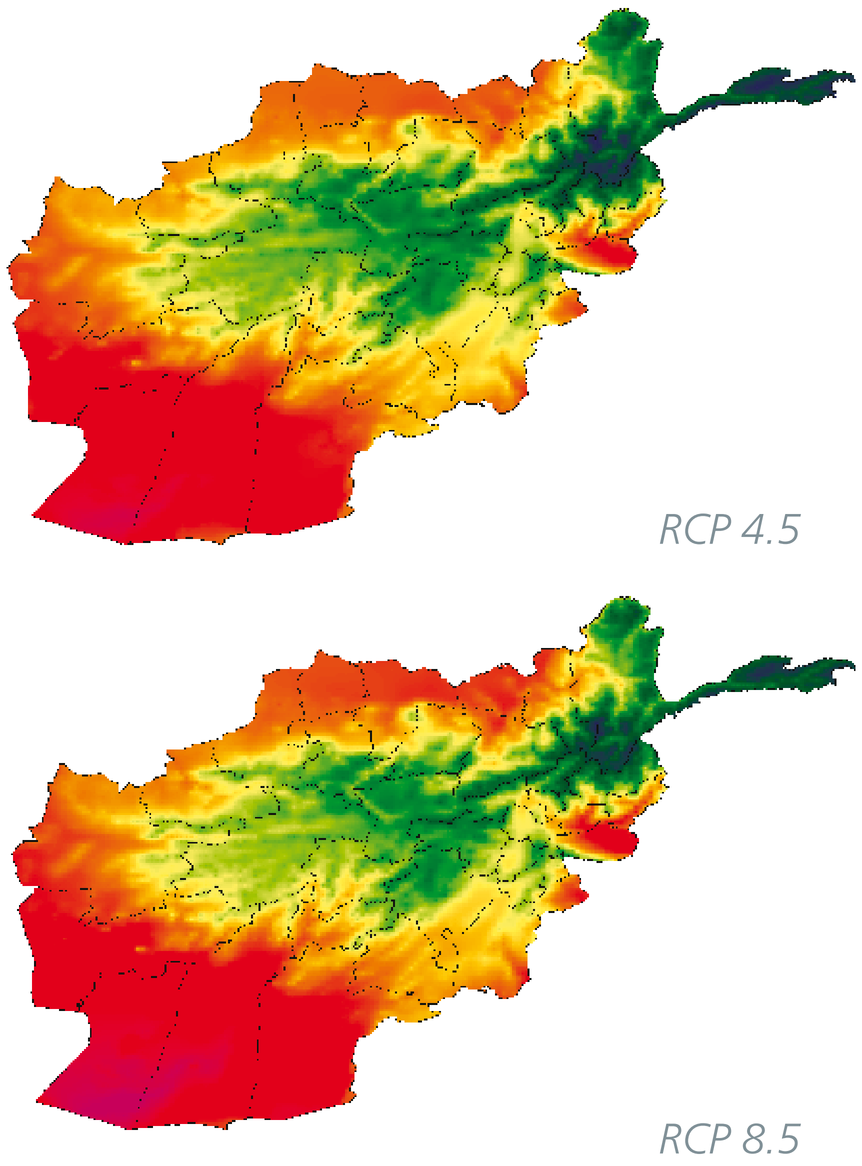

Source: IIASA, 2019

Figure 16

Table 5 lists the historical and future average regional values of the $Tsum_5$ indicator, which will increase significantly in all cases.

It is worth noting that these increases in heat provision are due to a dual impact: namely, increases of daily temperatures as well as an increase of the number of days in a year when the threshold temperature (5°C in the case of $Tsum_5$) is exceeded.

Table 5 - Changes of accumulated temperature for LGPt>5 °C period 2020s, 2050s and 2080s vs historical

Regions	Area (km²)	Historical		Ensemble mean RCP 4.5						Ensemble mean RCP 8.5					
		1961–1990	1981–2010	2020s	2050s	2080s	% Difference with 1981–2010: 2020s	2050s	2080s	2020s	2050s	2080s	% Difference with 1981–2010: 2020s	2050s	2080s
North Eastern	80 718	2841	2878	3286	3685	3892	14	28	35	3371	3995	4722	17	39	64
North Western	77 271	4719	4856	5240	5659	5877	8	17	21	5334	5944	6741	10	22	38
Eastern	25 059	4002	4011	4504	4932	5183	12	23	29	4618	5293	6086	15	32	52
Central	31 072	2672	2692	3087	3462	3648	15	29	35	3153	3722	4462	17	38	66
West Central	55 719	2902	3046	3391	3777	3961	11	24	30	3453	4022	4792	13	32	57
Western	160 581	4986	5299	5622	6014	6230	6	13	18	5712	6316	7126	8	19	34
South Eastern	28 472	4606	4626	5104	5547	5799	10	20	25	5214	5901	6765	13	28	46
South Western	183 421	6785	7149	7465	7883	8131	4	10	14	7579	8227	9065	6	15	27

Source: Calculations based on 30 arc-second NAEZ Afghanistan climate inventory.

Reference evapotranspiration (ETo)

Reference evapotranspiration (ETo) represents evapotranspiration from a defined reference surface, which closely resembles an extensive surface of green, well-watered grass of uniform height (12 cm), actively growing and completely shading the ground. AEZ calculates ETo from the attributes in the climate database for each grid-cell according to the Penman-Monteith equation.

References and a detailed description of the implementation of the Penman-Monteith equations in AEZ is provided in Appendix 1.

A key factor in the calculation of ETo is temperature, but radiation, relative humidity and wind speed at a location also affect the outcomes.

Annual reference evapotranspiration for historical climate of 1981–2010 is shown in Figure 17.

Note that the value of ETo increases more than linearly with temperature. Hence, it comes as no surprise that warming will increase the evaporative demand of vegetation in the 2050s (see Figure 18), under RCP 8.5 by some 4 percent to 12 percent, depending on region. Outcomes by region are listed in Table 6.

Mean annual reference evapotranspiration (ETo, mm)

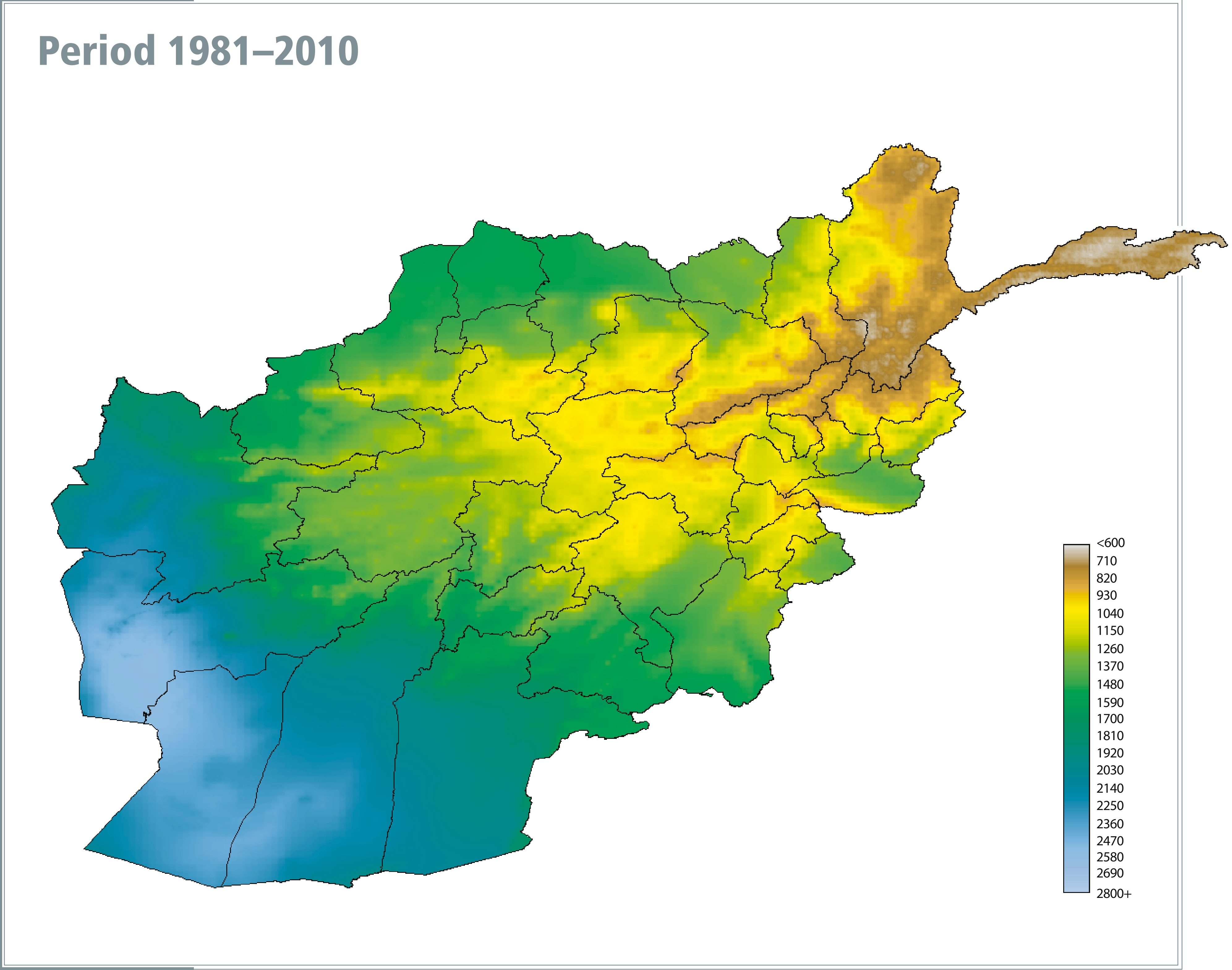

Source: IIASA, 2019

Figure 17

Ensemble mean
Period 2041–2070

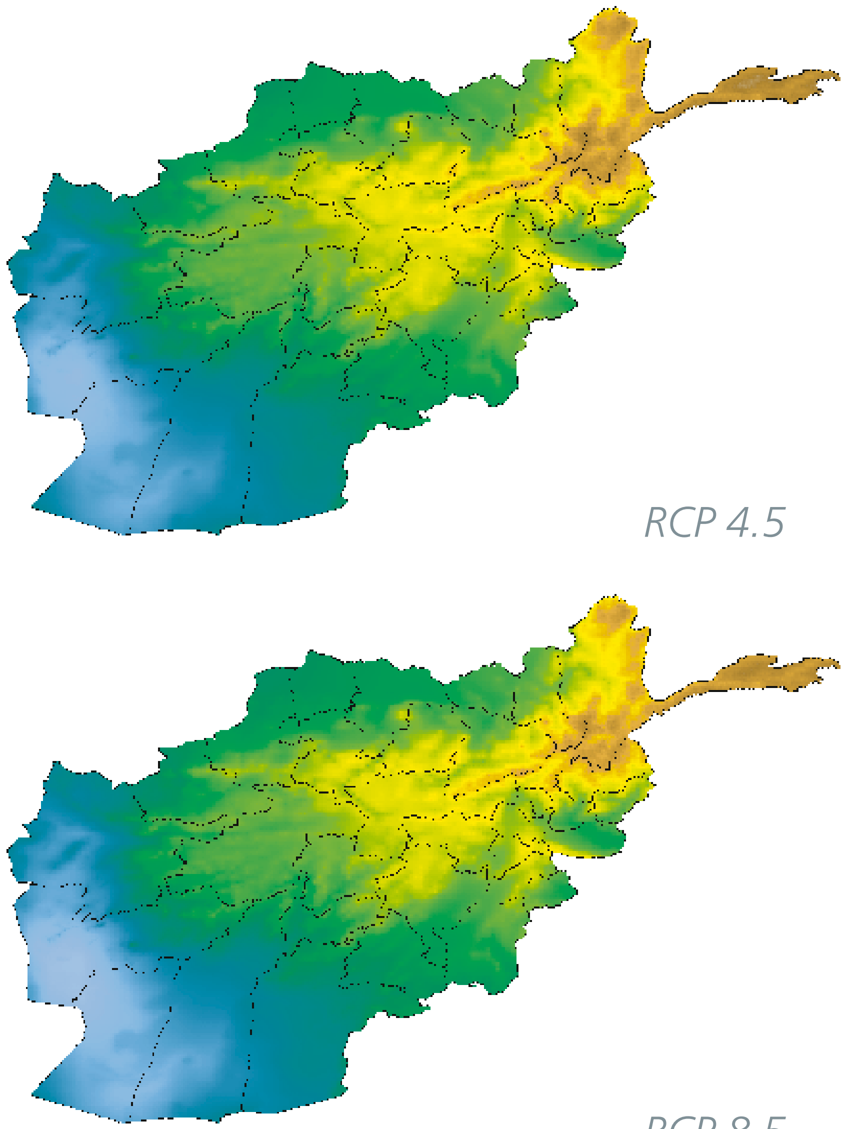

Source: IIASA, 2019

Figure 18

As shown in Table 6, percent increases of average regional annual reference evapotranspiration are most pronounced in north-eastern, central and eastern Afghanistan due to their geographical location and higher altitudes. In the long term, by the 2080s (period 2070–2099), average regional ETo will increase by more than 10 percent under RCP 4.5 projections and nearly 20 percent under RCP 8.5 projections.

This can enhance vegetation growth where water is available but is likely to further enhance water stress where water is already a limiting factor.

For assessing future crop suitability and plant growth, it is important to know whether the increased evaporative demand can be met by future precipitation (or irrigation); or whether prevailing water stress will curtail land productivity in future even more than now.

Table 6 - Changes of mean annual reference evapotranspiration (ETo, mm) period 2020s, 2050s and 2080s vs historical

Regions	Area (km²)	Historical		Ensemble mean RCP 4.5						Ensemble mean RCP 8.5					
		1961–1990	1981–2010	2020s	2050s	2080s	% Difference with 1981–2010			2020s	2050s	2080s	% Difference with 1981–2010		
							2020s	2050s	2080s				2020s	2050s	2080s
North Eastern	80 718	899	953	988	1031	1063	4	8	11	1003	1068	1136	5	12	19
North Western	77 271	1215	1329	1347	1405	1441	1	6	8	1369	1445	1527	3	9	15
Eastern	25 059	1048	1088	1131	1172	1208	4	8	11	1144	1208	1280	5	11	18
Central	31 072	957	1031	1065	1112	1146	3	8	11	1079	1144	1219	5	11	18
West Central	55 719	1062	1185	1198	1250	1283	1	6	8	1212	1279	1362	2	8	15
Western	160 581	1559	1756	1753	1823	1870	0	4	6	1780	1883	1995	1	7	14
South Eastern	28 472	1239	1333	1359	1406	1447	2	5	9	1372	1441	1529	3	8	15
South Western	183 421	1770	1986	1955	2018	2069	-2	2	4	1979	2072	2184	0	4	10

Source: Calculations based on 30 arc-second NAEZ Afghanistan climate inventory.

Annual moisture availability index (P/ETo)

The Moisture Availability Index compares the amount of incoming precipitation to the evaporative demand of the FAO reference crop. An index value of 100 means that precipitation equals reference potential evapotranspiration.

Values below 100 indicate the occurrence of some water deficit during part of the year; values above 100 mean that precipitation exceeds evaporative demand on an annual basis.

In the NAEZ analysis, a moisture availability index is calculated for year-round conditions, for six-month periods and for three-month periods to provide a general understanding of soil moisture conditions and water stress occurring overall and within certain periods of a year.

For annual conditions, Figure 19 presents the mean annual moisture availability index for the historical period 1981–2010. Figure 20 shows the annual moisture availability index in the 2050s for projected climate under RCP 4.5 (top) and RCP 8.5 (bottom), indicating a worsening of the annual vertical water balance.

Mean annual moisture availability index (100xP/ETo)

Period 1981–2010

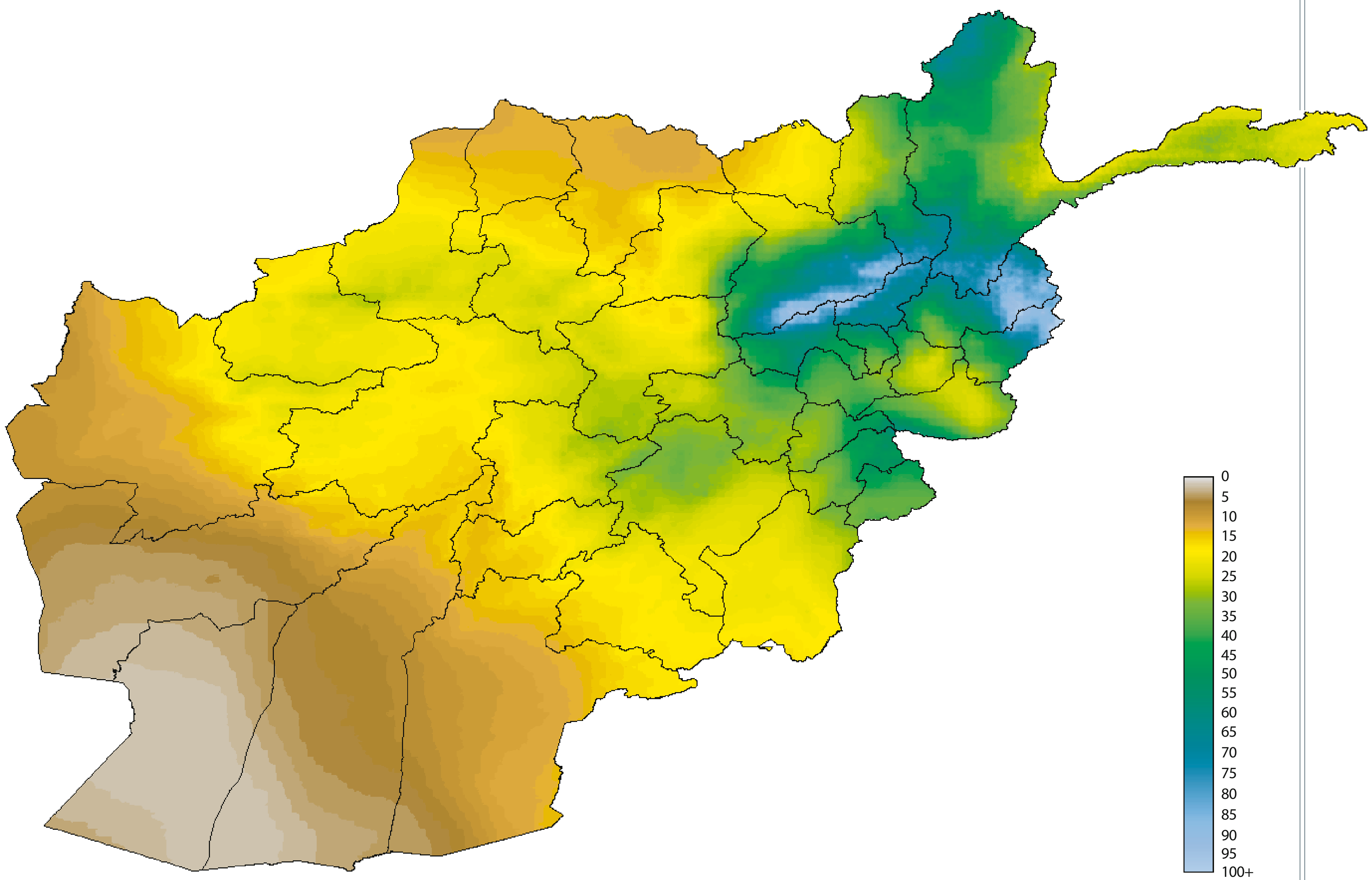

Source: IIASA, 2019

Figure 19

Ensemble mean
Period 2041–2070

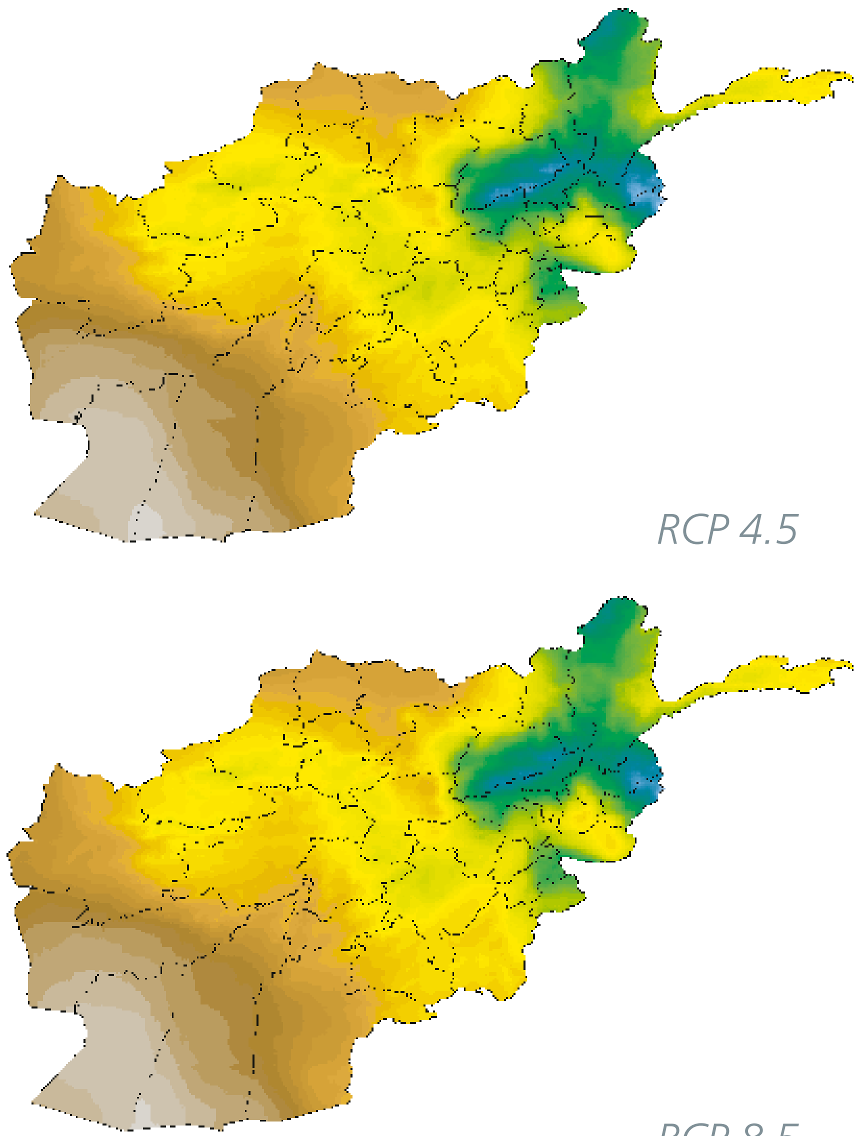

Source: IIASA, 2019

Figure 20

Table 7 provides some regional details of the level of mean annual moisture availability index and changes under future climate conditions.

It shows that in all regions the average annual moisture availability index values have been below 50 percent in the historical periods and it illustrates that the decrease of the annual index will progress in the future with the intensity of climate change, i.e. with RCP and time.

The projected decline of the P/ETo ratio, which is closely related to runoff, suggests that in the long-term, water resources will be negatively affected as well, a trend that will partly be mitigated by the retreat and melting of glaciers.

Table 7 - Changes of annual moisture availability index (Annual P/ETo) period 2020s, 2050s and 2080s vs historical

Regions	Area (km²)	Historical		Ensemble mean RCP 4.5						Ensemble mean RCP 8.5					
		1961–1990	1981–2010	2020s	2050s	2080s	% Difference with 1981–2010			2020s	2050s	2080s	% Difference with 1981–2010		
							2020s	2050s	2080s				2020s	2050s	2080s
North Eastern	72 204	43	41	40	37	36	-4	-9	-13	36	35	32	-13	-16	-23
North Western	187 310	21	19	18	17	16	-1	-9	-14	16	16	14	-13	-14	-23
Eastern	116 244	48	49	44	42	40	-11	-15	-20	41	38	36	-17	-22	-26
Central	148 467	43	43	37	35	33	-13	-19	-24	33	32	28	-23	-26	-35
West Central	88 929	26	25	22	20	19	-11	-19	-24	20	19	16	-20	-24	-35
Western	89 645	16	14	14	12	12	2	-9	14	12	12	10	-11	-13	-25
South Eastern	75 883	28	28	24	23	21	-13	-17	-22	23	22	19	-16	-21	-30
South Western	778 682	10	9	9	8	8	-1	-16	-17	8	8	6	-8	-14	-30

Source: Calculations based on 30 arc-second NAEZ Afghanistan climate inventory.

Winter moisture availability index (P/ETo)

As previously noted, the territory of Afghanistan is characterized by considerable seasonality of precipitation and monthly temperatures.

While precipitation is mostly received during October to March, this coincides with the cool period and hence, lower seasonal evaporative demand ETo.

As a consequence, the seasonal (six-month) moisture availability index is much higher during winter and early spring compared to summer.

As shown in Figure 21, precipitation received during October to March can meet a large fraction or even exceed potential evapotranspiration in all regions except the south-west region. As observed and noted in the previous analysis, precipitation will likely decrease somewhat and temperatures (and hence ETo) will increase in a future climate.

Mean winter moisture availability index (100xP/ETo)

Period 1981–2010 (Oct/Mar)

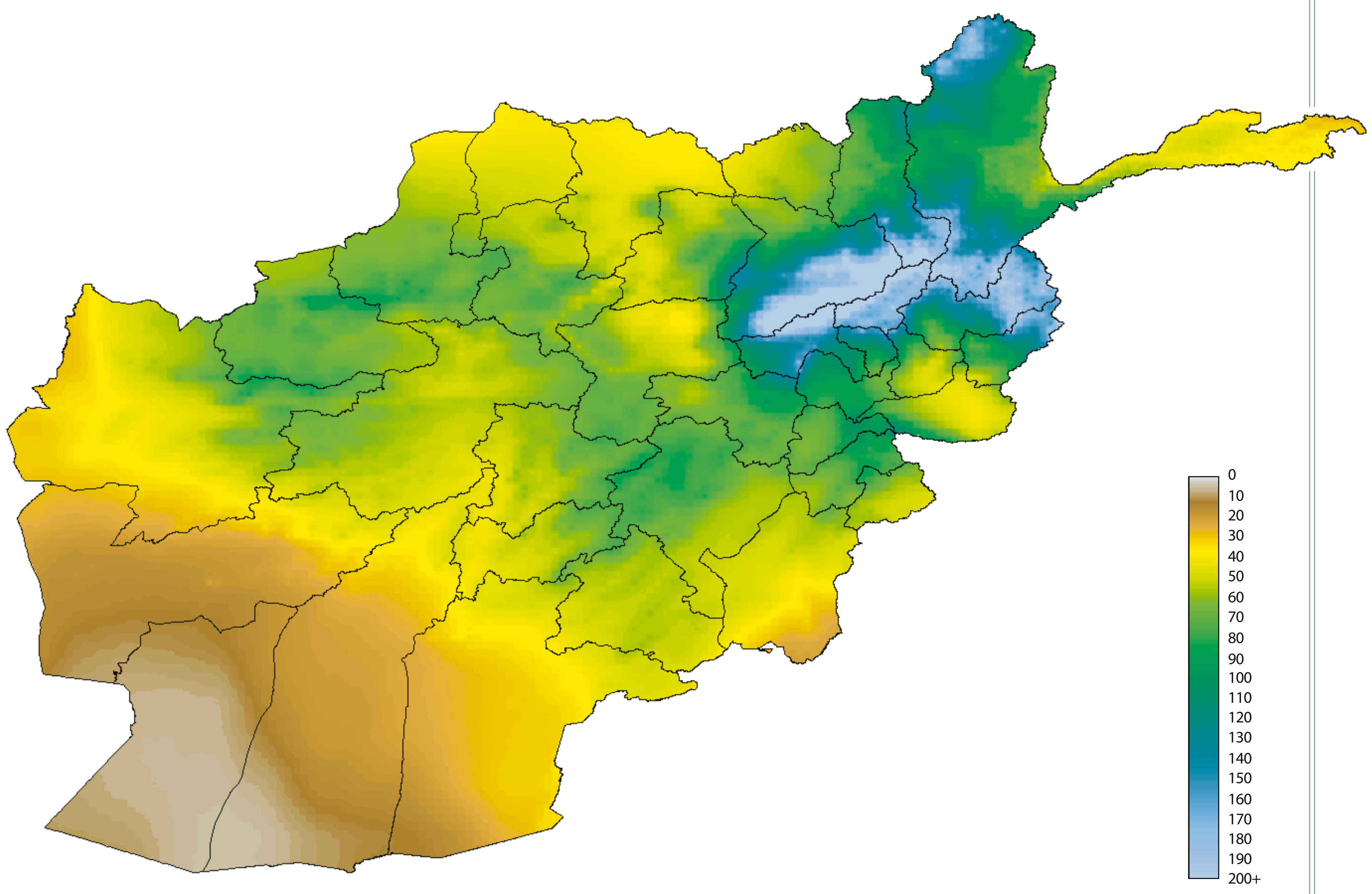

Source: IIASA, 2019

Figure 21

Ensemble mean
Period 2041–2070 (Oct/Mar)

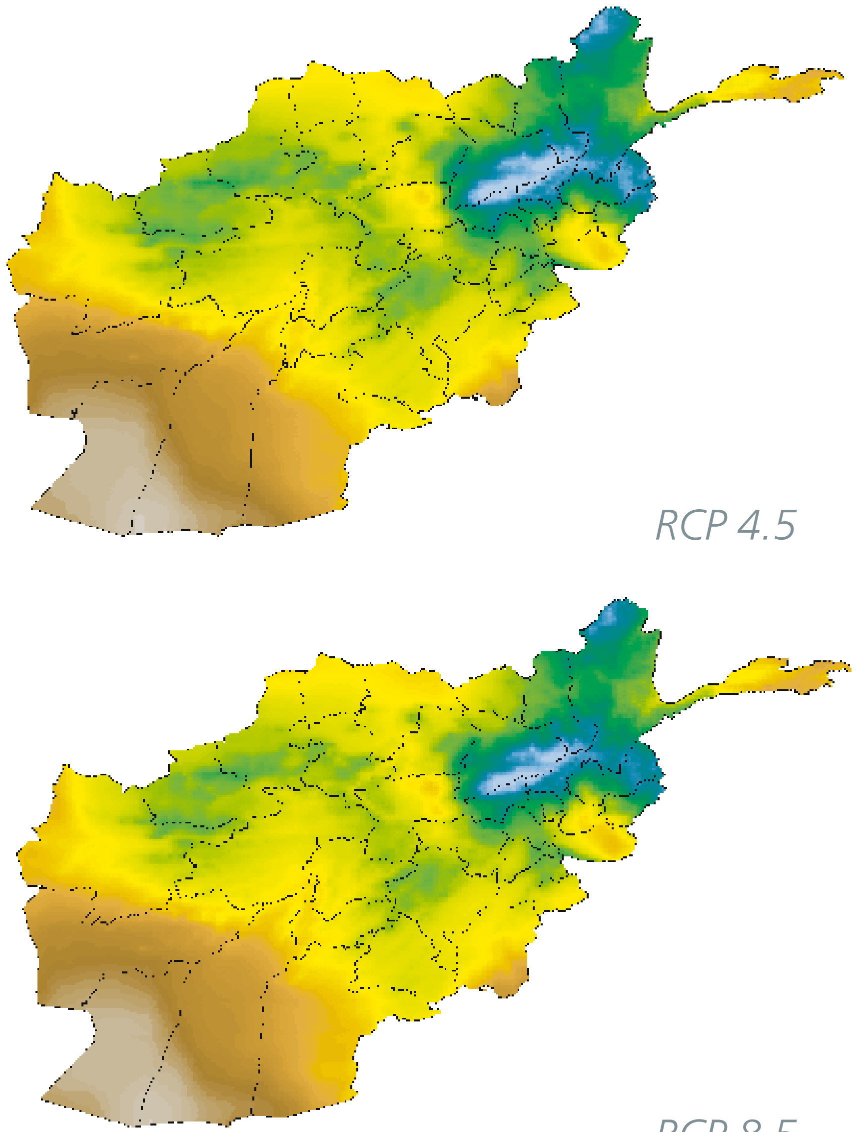

Source: IIASA, 2019

Figure 22

Figure 22 indicates for the 2050s a worsening of the seasonal winter moisture balance in all regions.

For the regions of Afghanistan, Table 8 indicates that seasonal precipitation has exceeded seasonal potential evapotranspiration during October to March in north-eastern, eastern and central Afghanistan and was lowest (less than 30 percent) in the south-western region.

By the 2050s, the ensemble mean of projected regional winter moisture availability index values will decrease by -8 percent to -17 percent for climate projected assuming radiative forcing according to RCP 4.5; under RCP 8.5 projections changes are in the range of -13 percent to -24 percent.

Note that the winter moisture availability index is indicative of conditions for rain-fed cropping, suggesting that some current rain-fed areas may no longer be viable for cropping in a future climate.

Table 8 - Changes of winter moisture availability index (Winter P/ETo) period 2020s, 2050s and 2080s vs historical

Regions	Area (km²)	Historical		Ensemble mean RCP 4.5						Ensemble mean RCP 8.5					
		1961–1990	1981–2010	2020s	2050s	2080s	% Difference with 1981–2010			2020s	2050s	2080s	% Difference with 1981–2010		
							2020s	2050s	2080s				2020s	2050s	2080s
North Eastern	72 204	114	106	105	96	90	-1	-9	-14	92	91	83	-13	-14	-22
North Western	187 310	63	57	59	52	48	3	-8	-16	50	50	45	-12	-13	-21
Eastern	116 244	96	101	90	84	77	-11	-17	-24	78	77	69	-22	-24	-32
Central	148 467	109	107	99	89	82	-7	-17	-23	85	83	72	-21	-22	-33
West Central	88 929	69	63	60	52	48	-5	-17	-24	52	50	42	-17	-21	-34
Western	89 645	49	44	46	39	36	5	-10	-17	39	38	33	-12	-13	-25
South Eastern	75 883	53	52	47	43	39	-9	-17	-24	42	41	33	-19	-21	-36
South Western	778 682	29	36	27	22	21	2	-16	-21	24	22	18	-7	-15	-32

Source: Calculations based on 30 arc-second NAEZ Afghanistan climate inventory.

Summer moisture availability index (P/ETo)

The seasonal balance between water available from precipitation and evaporative demand (potential evapo-transpiration) in summer is much inferior to winter.

Figure 23 and Figure 24 show the average seasonal six-month moisture availability index for April to September, respectively, for the historical period 1981–2010 and for future ensemble means of period 2041–2070 under RCP 4.5 (top) and RCP 8.5 (bottom).

Mean summer moisture availability index (100xP/ETo)

Period 1981–2010 (Apr/Sep)

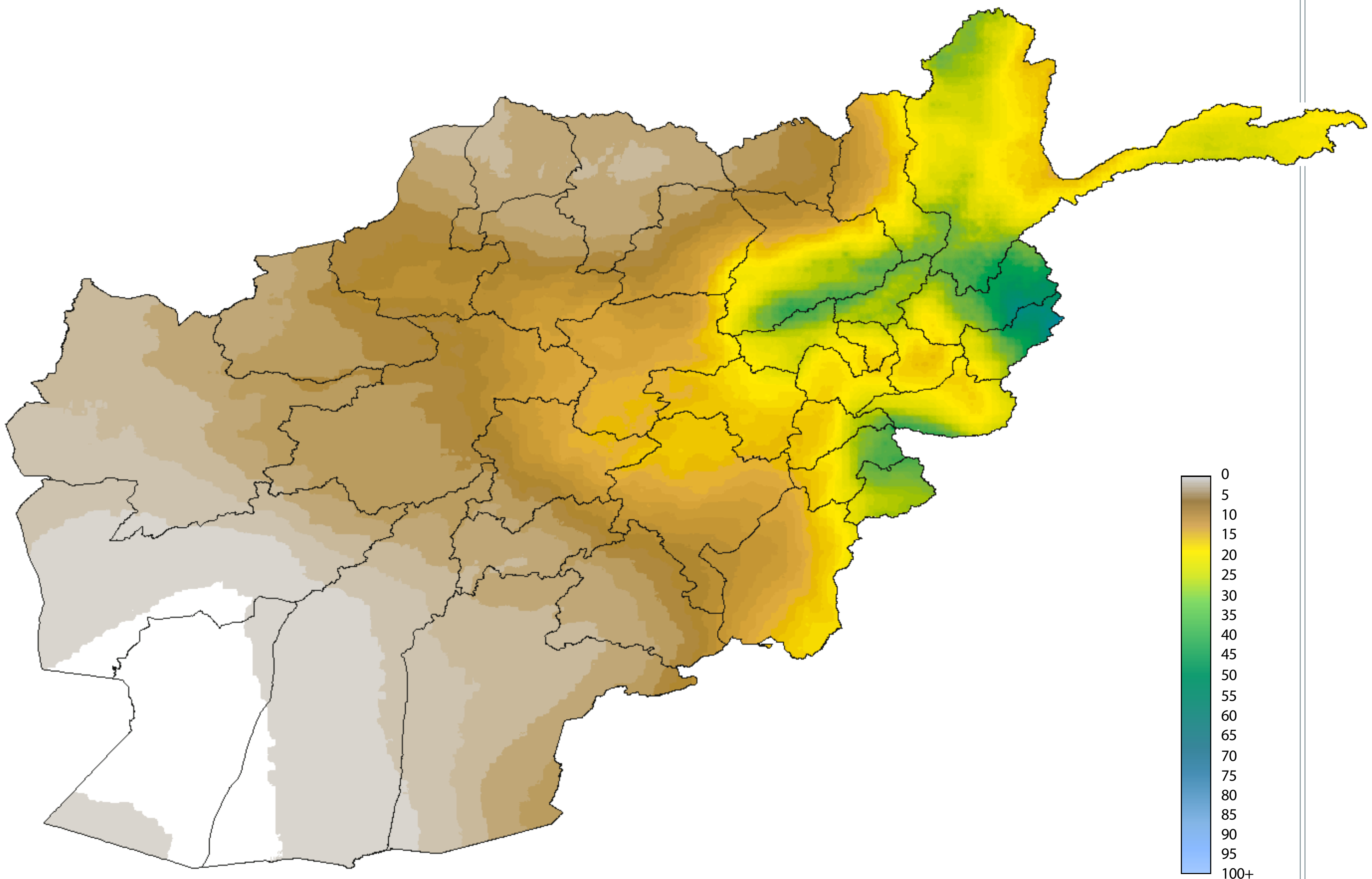

Source: IIASA, 2019

Figure 23

Ensemble mean
Period 2041–2070 (Apr/Sep)

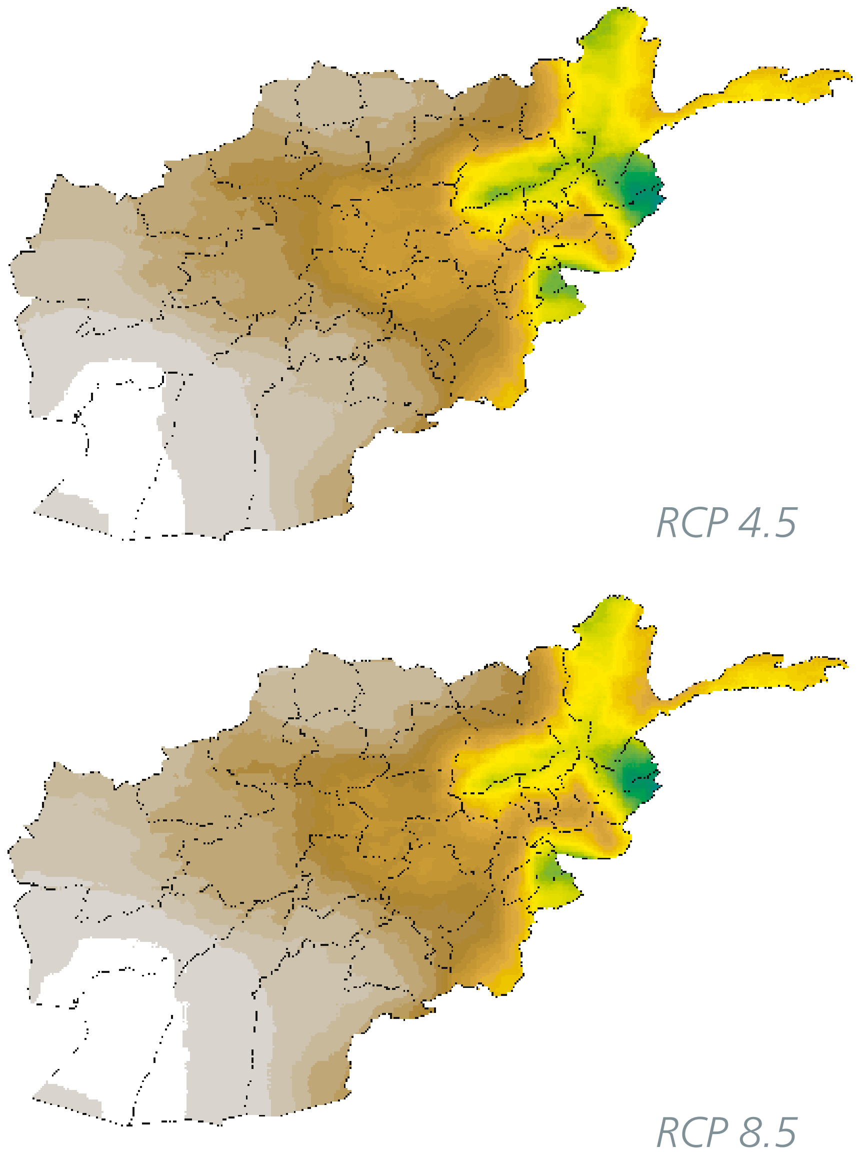

Source: IIASA, 2019

Figure 24

Table 9 present a summary of regional summer moisture availability index values showing that average values during 1981–2010 were mostly below 20 percent (except for about 30 percent in the eastern region), which indicates a significant moisture deficit during summer.

According to projected climate in the 2050s, the regional summer moisture availability index will further decrease from already low values, by -11 percent to -25 percent under the RCP 4.5 concentration pathway; and by -18 percent to -36 percent under RCP 8.5.

This will increase irrigation water demand per unit area where irrigated cropping is possible in summer.

Table 9 - Changes of summer moisture availability index (Summer P/ETo) period 2020s, 2050s and 2080s vs historical

Regions	Area (km²)	Historical		Ensemble mean RCP 4.5						Ensemble mean RCP 8.5					
		1961–1990	1981–2010	2020s	2050s	2080s	% Difference with 1981–2010			2020s	2050s	2080s	% Difference with 1981–2010		
							2020s	2050s	2080s				2020s	2050s	2080s
North Eastern	72 204	21	20	19	18	18	-8	-11	-13	14	16	17	-29	-21	-14
North Western	187 310	7	6	5	5	5	-8	-12	-10	4	5	5	-34	-22	-17
Eastern	116 244	30	30	27	26	25	-11	-13	-16	24	24	27	-21	-20	-10
Central	148 467	20	20	16	15	15	-22	-25	-28	12	13	15	-42	-36	-28
West Central	88 929	11	11	9	9	8	-19	-23	-25	6	7	8	-42	-33	-27
Western	89 645	5	4	4	3	3	-3	-11	-6	2	3	3	-36	-22	-11
South Eastern	75 883	17	18	15	15	14	-15	-16	-21	14	14	16	-23	-20	-12
South Western	778 682	2	2	2	2	2	-9	-14	-9	2	2	2	-32	-18	-14

Source: Calculations based on 30 arc-second NAEZ Afghanistan climate inventory.

Quarterly moisture availability index

Figure 25 presents average quarterly (three-month) moisture availability index values for the historical period 1981–2010.

It confirms an apparent geographical moisture availability gradient with highest index values in north-eastern and eastern Afghanistan; to very low values in the south-western region. While the north-eastern region receives substantial precipitation in all quarters, except July to September, the south-western region falls short of precipitation in all quarters.

This spatial pattern will persist also in the projected future climate, albeit with generally decreasing index values in all seasons, as portrayed in Figure 26.

Quarterly moisture availability index (100xP/ETo)

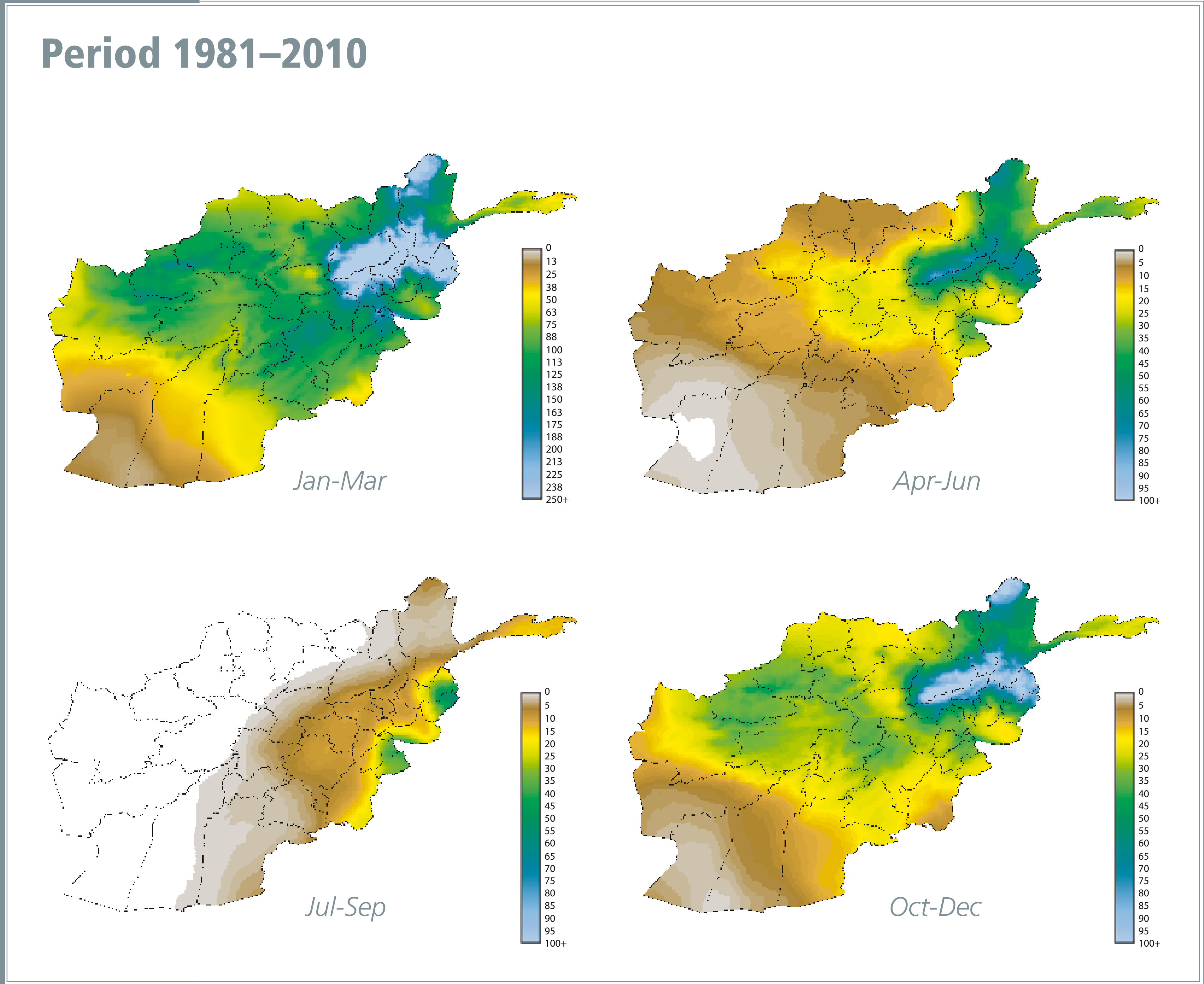

Source: IIASA, 2019

Figure 25

Ensemble mean, RCP 8.5
Period 2041–2070

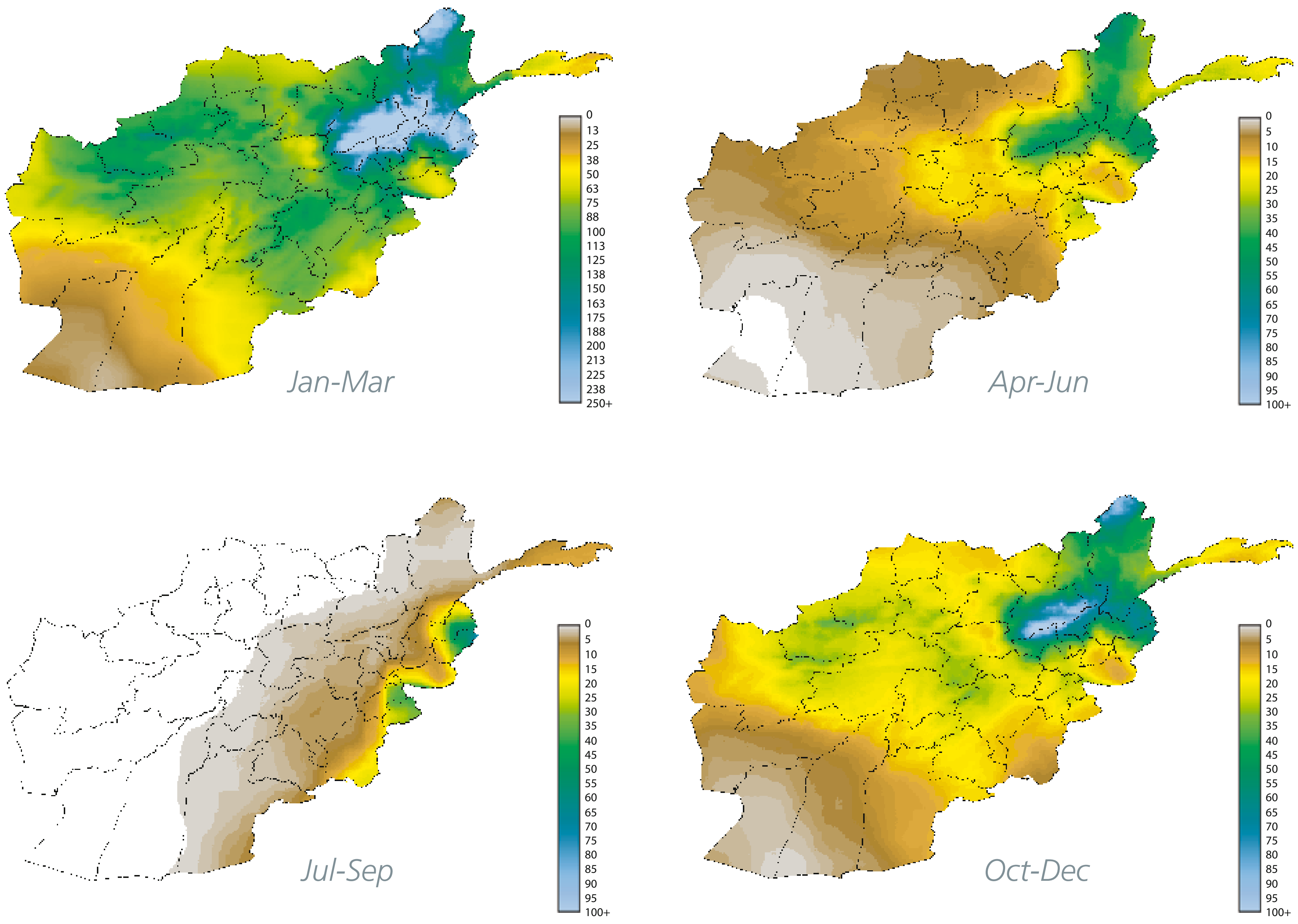

Source: IIASA, 2019

Figure 26

Actual evapotranspiration of reference crop (ETa)

NAEZ calculates a daily reference soil-water balance for each grid-cell and estimates actual evapotranspiration for a reference crop. Daily soil moisture balance calculation procedures follow the methodologies outlined in "Crop Evapotranspiration".

The quantification of a reference water balance determines annual "actual" evapotranspiration (ETa) and reference water deficit (WDe). References and details of the NAEZ reference water balance are given in Appendix 2.

The volume of water available for plant uptake accounts for accumulated daily water inflow from precipitation or snowmelt and subtracts outflow from actual evapotranspiration and excess water lost due to runoff or deep percolation.

The actual evapotranspiration (ETa) of the FAO reference crop simulated in the daily water balance of NAEZ Afghanistan is well below the reference potential evapotranspiration (ETo), indicating very significant seasonal or year-round soil moisture deficits of the land in Afghanistan.

The spatial distribution of average ETa during 1981–2010 is shown in Figure 27.

Mean actual evapotranspiration (ETa, mm)

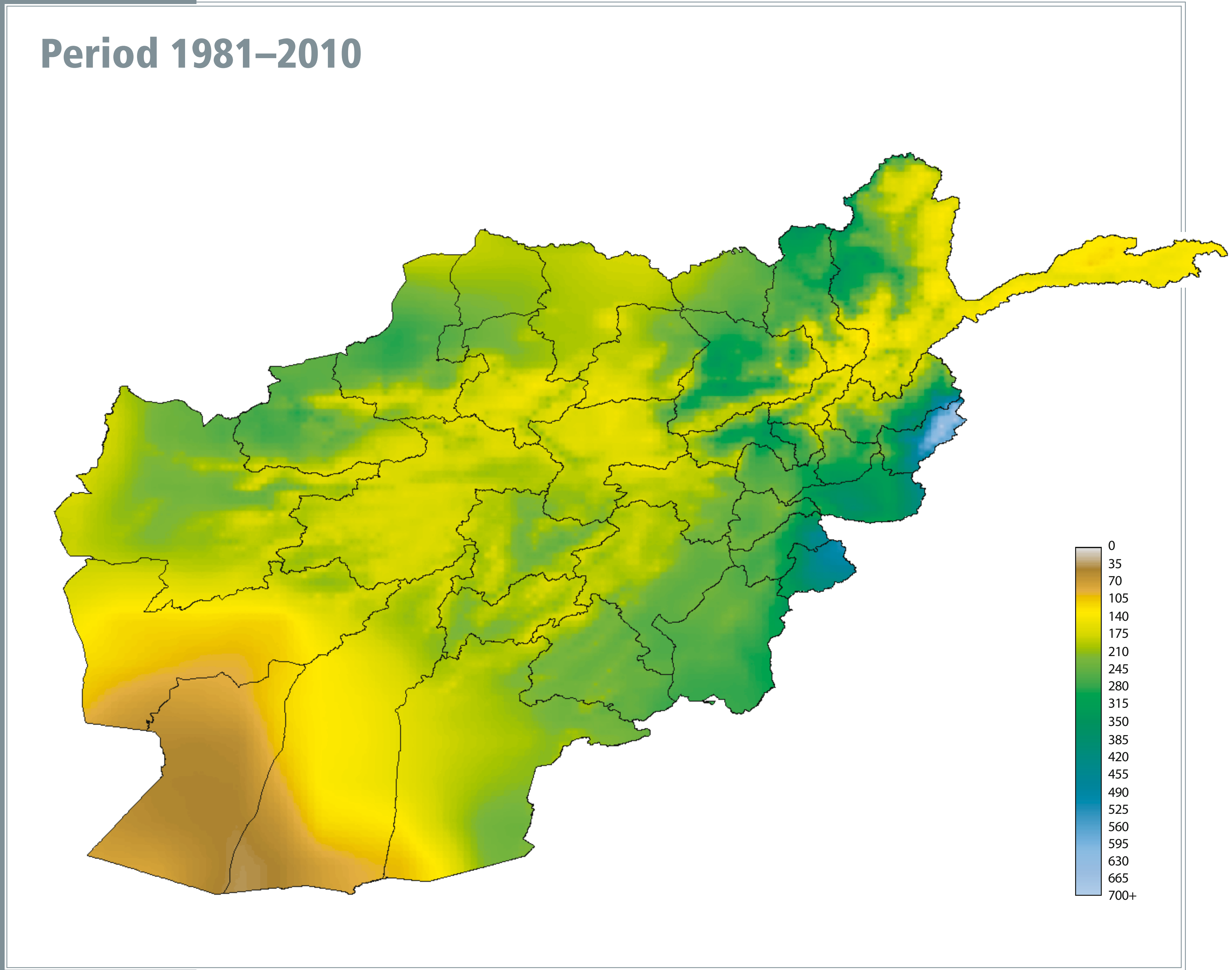

Source: IIASA, 2019

Figure 27

Ensemble mean
Period 2041–2070

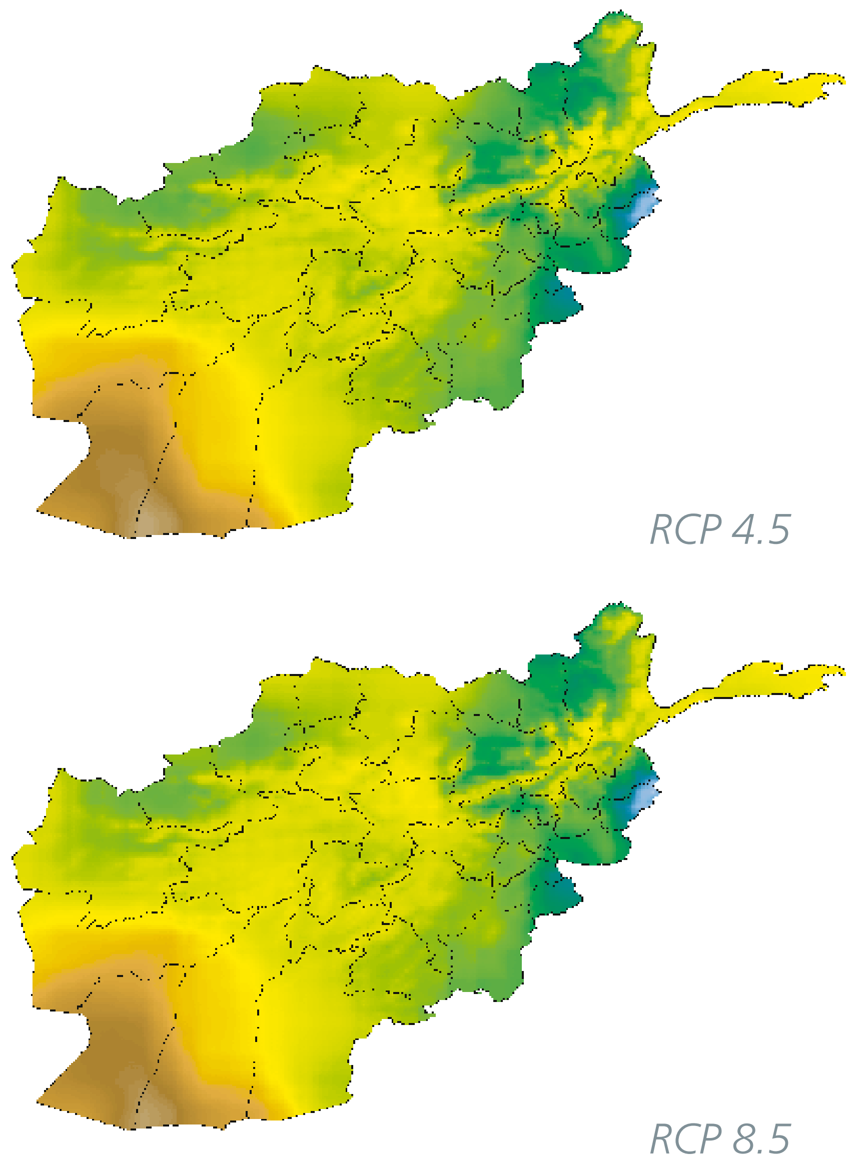

Source: IIASA, 2019

Figure 28

Future ETa in the 2050s is given in Figure 28 for projections under RCP 4.5 (top) and RCP 8.5 (bottom).

Table 10 summarizes results of simulated actual evapotranspiration (ETa) by region. Note that ETa depends on potential evapotranspiration (ETo) of a location; hence, on temperature as well as on soil moisture supply, resulting in highest average ETa values in eastern and south-eastern regions.

Under climate change, most regions record some decrease of ETa, except in the north-eastern region where the increased ETo and seasonal availability of soil water results in a modest increase of ETa, despite of an overall worsening of the annual P/ETo ratio.

Table 10 - Changes of annual actual evapotranspiration of FAO reference crop (ETa, mm) period 2020s, 2050s and 2080s vs historical

Regions	Area (km²)	Historical		Ensemble mean RCP 4.5						Ensemble mean RCP 8.5					
		1961–1990	1981–2010	2020s	2050s	2080s	% Difference with 1981–2010			2020s	2050s	2080s	% Difference with 1981–2010		
							2020s	2050s	2080s				2020s	2050s	2080s
North Eastern	80 718	204	215	215	226	227	0	5	6	213	227	239	-1	6	11
North Western	77 271	197	204	188	193	188	-8	-5	-8	180	186	183	-12	-9	-10
Eastern	25 059	309	329	309	322	317	-6	-2	-4	312	316	335	-5	-4	2
Central	31 072	202	228	206	217	212	-10	-5	-7	204	213	225	-11	-7	-1
West Central	55 719	182	203	177	184	178	-12	-9	-12	171	179	179	-15	-12	-11
Western	160 581	174	178	166	166	160	-6	-7	-10	158	162	158	-11	-9	-11
South Eastern	28 472	280	297	259	271	255	-13	-9	-14	261	262	260	-12	-12	-12
South Western	183 421	137	146	131	125	120	-11	-15	-18	126	124	115	-14	-15	-21

Source: Calculations based on 30 arc-second NAEZ Afghanistan climate inventory.

Reference annual water deficit (WDe)

The difference between potential and actual uptake of water simulated for the FAO reference crop (i.e. the reference annual water deficit WDe = ETo-ETa) is used as an indicator of the discrepancy between evaporative demand of a well-watered vegetation and soil moisture supply under rain-fed conditions (WDe, mm), as shown for historical conditions in Figure 29.

In Figure 30 – showing the mean annual reference water deficit in the period 2041–2070 projected under RCM 4.5 (left) and RCM 8.5 (right) assumptions – the spatial pattern of the historical period is maintained but the annual discrepancy between potential evapotranspiration and simulated actual evapotranspiration of the FAO reference crop is widening somewhat, due to warming.

It suggests that permanent crops and natural vegetation are especially likely to face increased water stress under future conditions.

Mean reference annual water deficit (WDe, mm)

Period 1981–2010

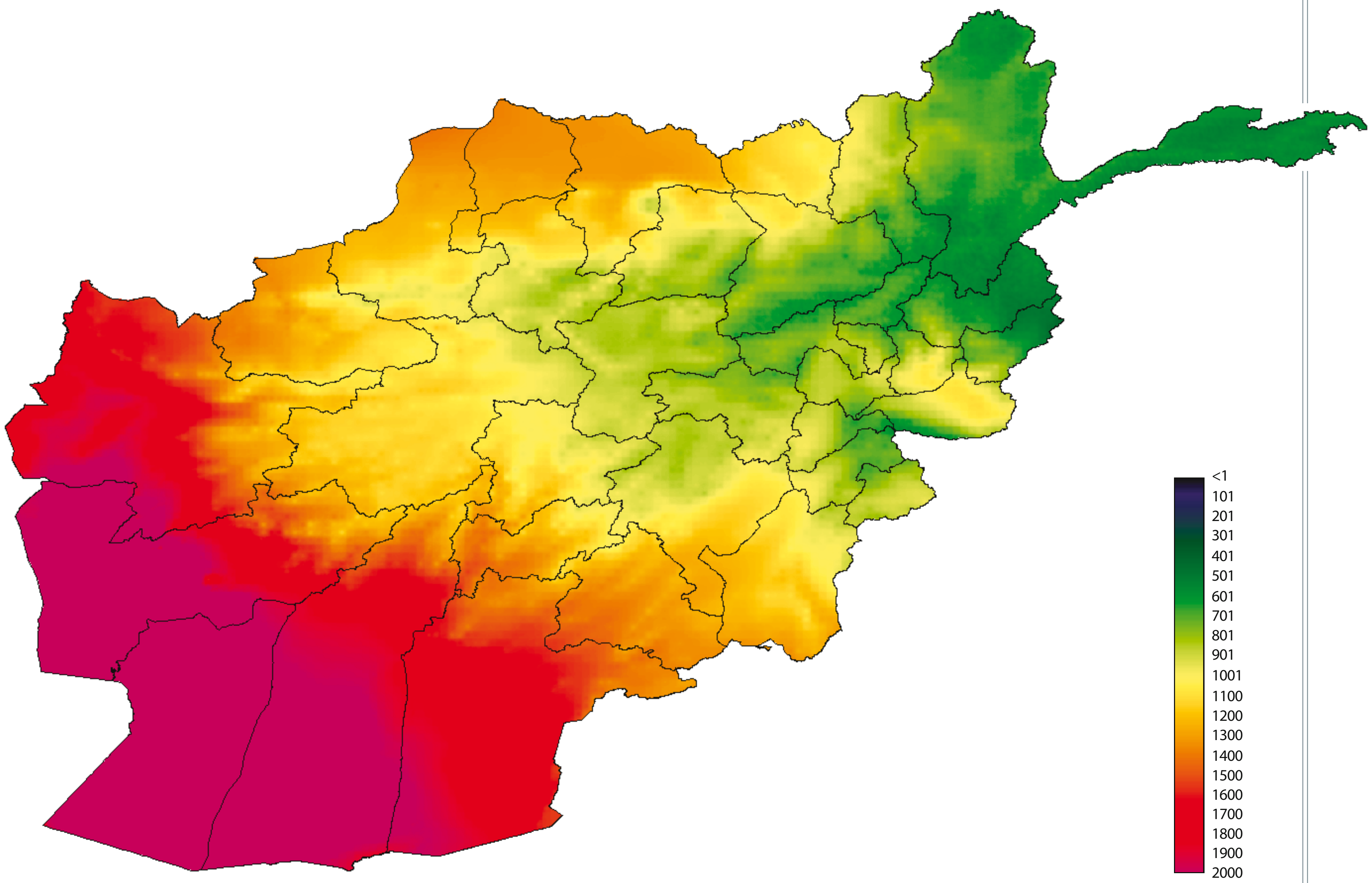

Source: IIASA, 2019

Figure 29

Ensemble mean
Period 2041–2070

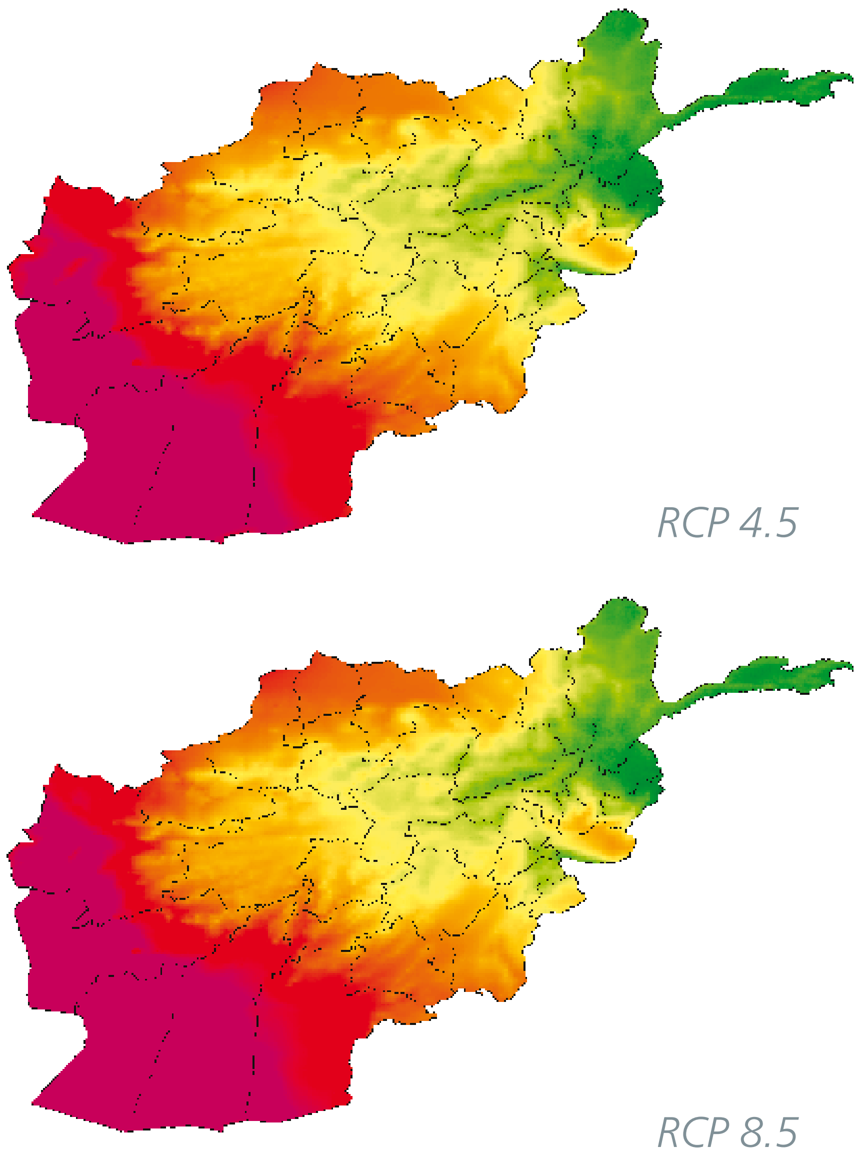

Source: IIASA, 2019

Figure 30

©FAO/ Giulio Napolitano

Reference length of growing period (LGP days)

The agro-climatic potential productivity of land depends largely on the number of days during the year when temperature regime and moisture supply are conducive to crop growth and development.

The number of days in this period is termed the reference length of growing period (LGP). The LGP is determined based on prevailing temperatures and grid-cell specific water balance calculations for a reference crop. In a formal sense, LGP refers to the number of days when average daily temperature is above 5°C (i.e. within LGPt5) and ETa is above a specific fraction of ETo.

In the current AEZ parameterization, LGP days are considered when ETa ≥ 0.5 x ETo, which aims to capture periods when temperature and soil moisture conditions are conducive to rain-fed crop cultivation (FAO reference crop).

Figure 31 presents a map of reference length of growing period for Afghanistan, which is based on a reference soil moisture holding capacity of 100 mm.

Reference lenght of growing period (days)

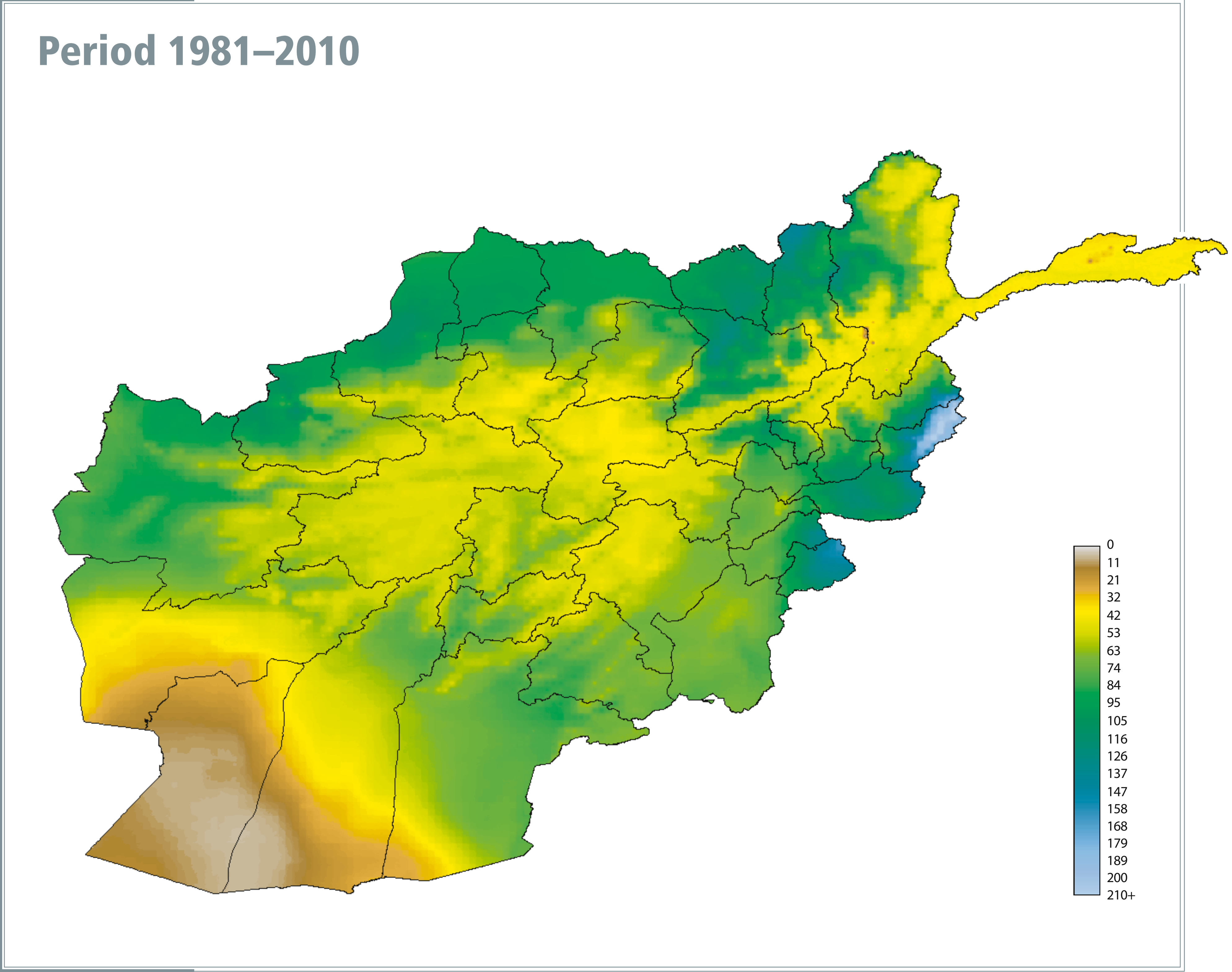

Source: IIASA, 2019

Figure 31

Ensemble mean Period 2041–2070

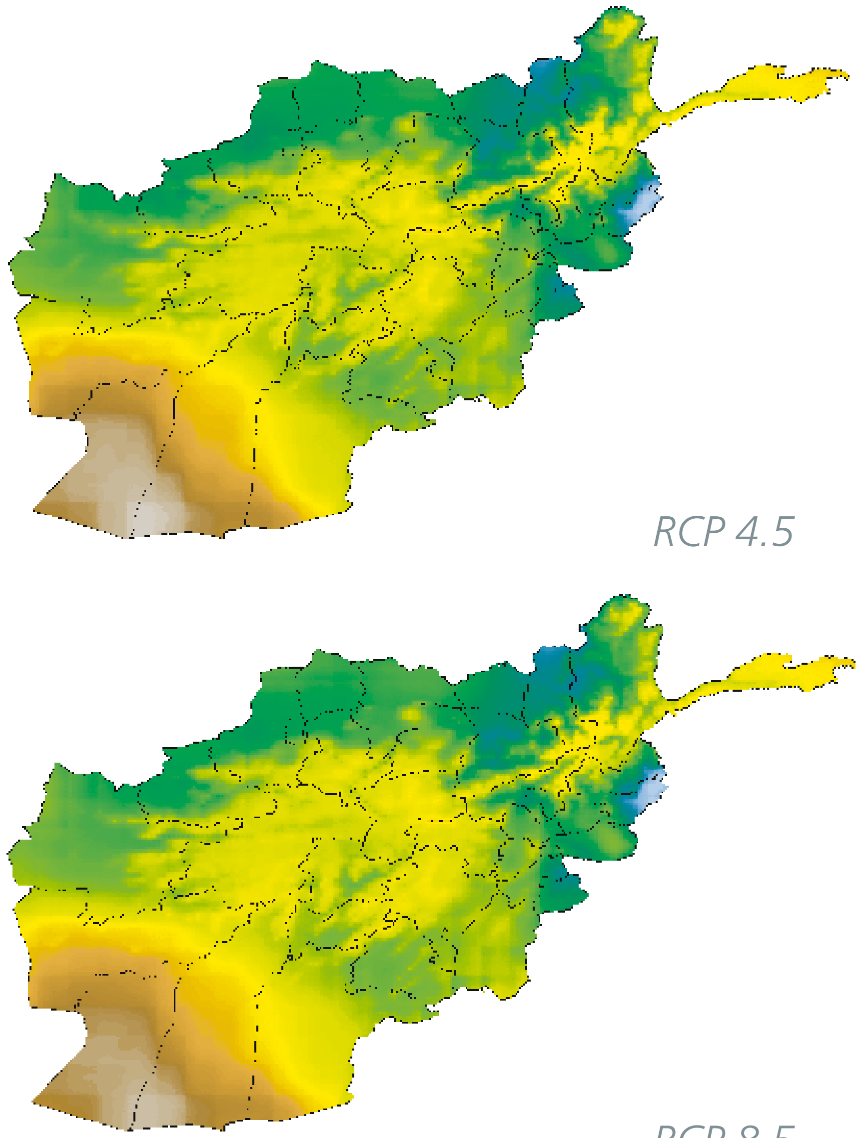

Source: IIASA, 2019

Figure 32

Figure 32 shows ensemble means of LGP days for future climate in the period 2041–2070. It indicates that the spatial pattern of LGP observed in the historical period will generally persist into the future.

Table 11 lists average number of LGP days by region, with highest average values of more than 100 days occurring in eastern and north-eastern regions.

Simulations for future climate suggest that the number of annual LGP days may increase somewhat in north-eastern and central Afghanistan, whereas decreases are recorded in all other regions. The magnitude of these changes will depend on the intensity of climate change but generally conclusions will hold also for the 2080s.

Table 11 - Changes of lenght of growing period (LGP, days) for current cropland period 2020s, 2050s and 2080s vs historical

Regions	Area (km²)	Historical		Ensemble mean RCP 4.5						Ensemble mean RCP 8.5					
		1961–1990	1981–2010	2020s	2050s	2080s	% Difference with 1981–2010			2020s	2050s	2080s	% Difference with 1981–2010		
							2020s	2050s	2080s				2020s	2050s	2080s
North Eastern	13 909	104	101	107	116	117	6	14	15	107	116	121	5	15	20
North Western	21 296	80	80	75	80	78	-7	0	-3	74	78	79	-8	-2	-2
Eastern	1726	111	116	101	105	96	-13	-9	-17	98	95	92	-15	-18	-20
Central	3 489	70	74	69	76	73	-7	3	-1	68	74	82	-7	1	11
West Central	4 812	61	60	54	58	56	-10	-3	-7	53	57	59	-11	-5	-2
Western	16 439	70	72	68	69	66	-6	-4	-9	65	67	66	-11	-7	-9
South Eastern	2 908	86	85	73	78	73	-14	-7	-14	74	75	74	-13	-12	-12
South Western	10 524	64	63	53	48	46	-15	-23	-27	49	47	41	-22	-25	-35

Source: Calculations based on 30 arc-second NAEZ Afghanistan climate inventory.

Length of growing period zones (LGP zones)

The length of growing period data is used for the classification of general moisture regime classes, LGP zones, defined in terms of 30-day ranges of number of growing period days (see Figure 33 for historical climate and Figure 34 for LGP zones in the 2050s).

The moisture regime within an LGP is characterized by different water supply conditions as follows: Growing period days without water stress (ETa = ETo): when reference crop water requirements are fully met (i.e. no water stress occurs). These LGP days can further be differentiated as follows:

1. Daily rainfall is higher than crop water requirements (P > ETo). In this case, excess rainfall can add to replenish the soil moisture storage until field capacity is reached.
2. Days when rainfall falls short of crop water requirements (P < ETo) but easily available soil moisture exceeds crop water requirements. In this case, ETa still equals ETo and the soil moisture content in the soil profile is decreasing.

Growing period days with water stress (ETa < ETo): ETa falls short of ETo. The crop experiences water stress as not enough readily available water can be obtained from rainfall or moisture stored in the soil profile. Water stress implies that crop growth and yield formation are reduced.

Lenght of growing period zones

Period 1981–2010

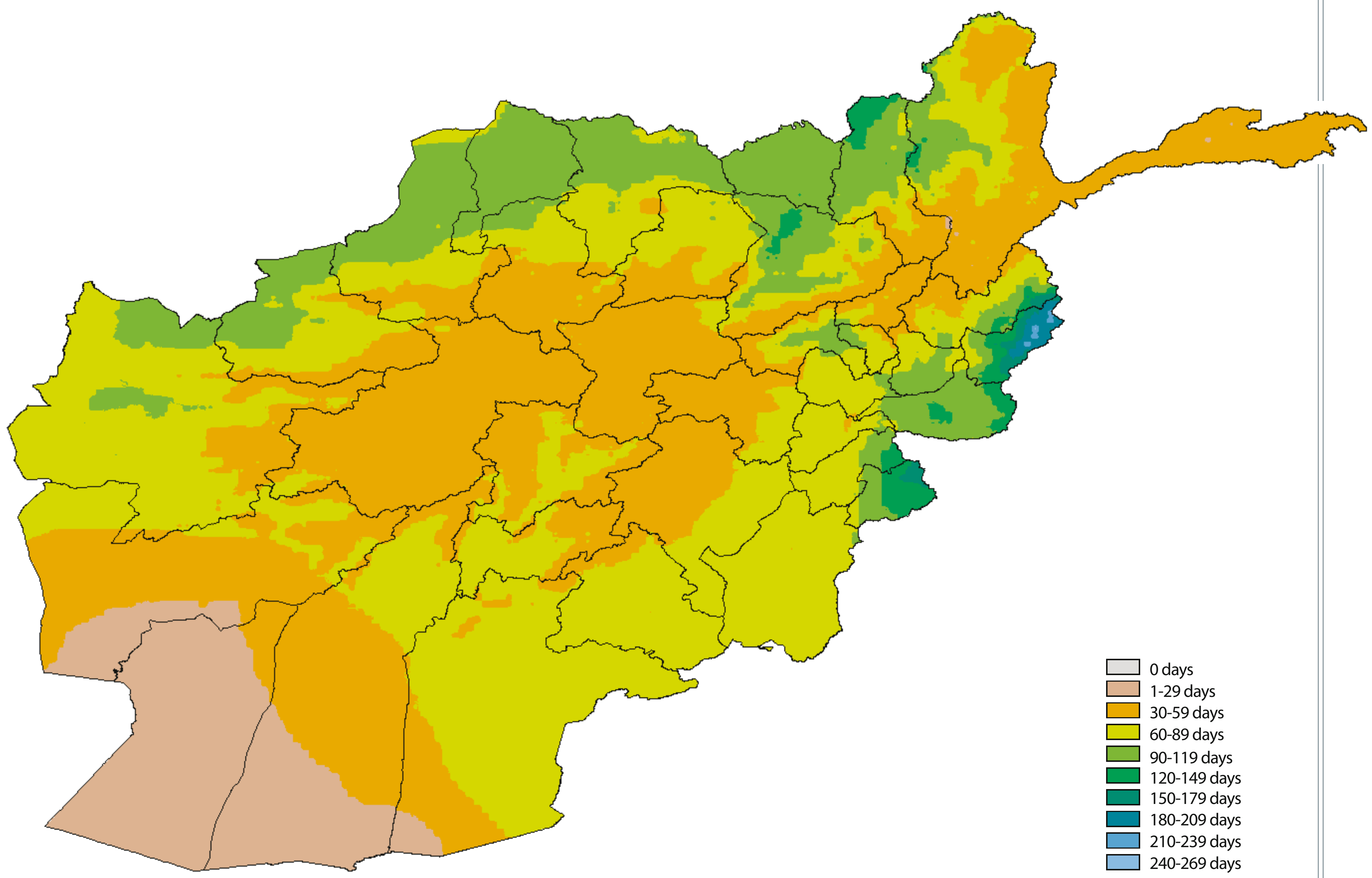

Source: IIASA, 2019

Figure 33

Ensemble mean
Period 2041–2070

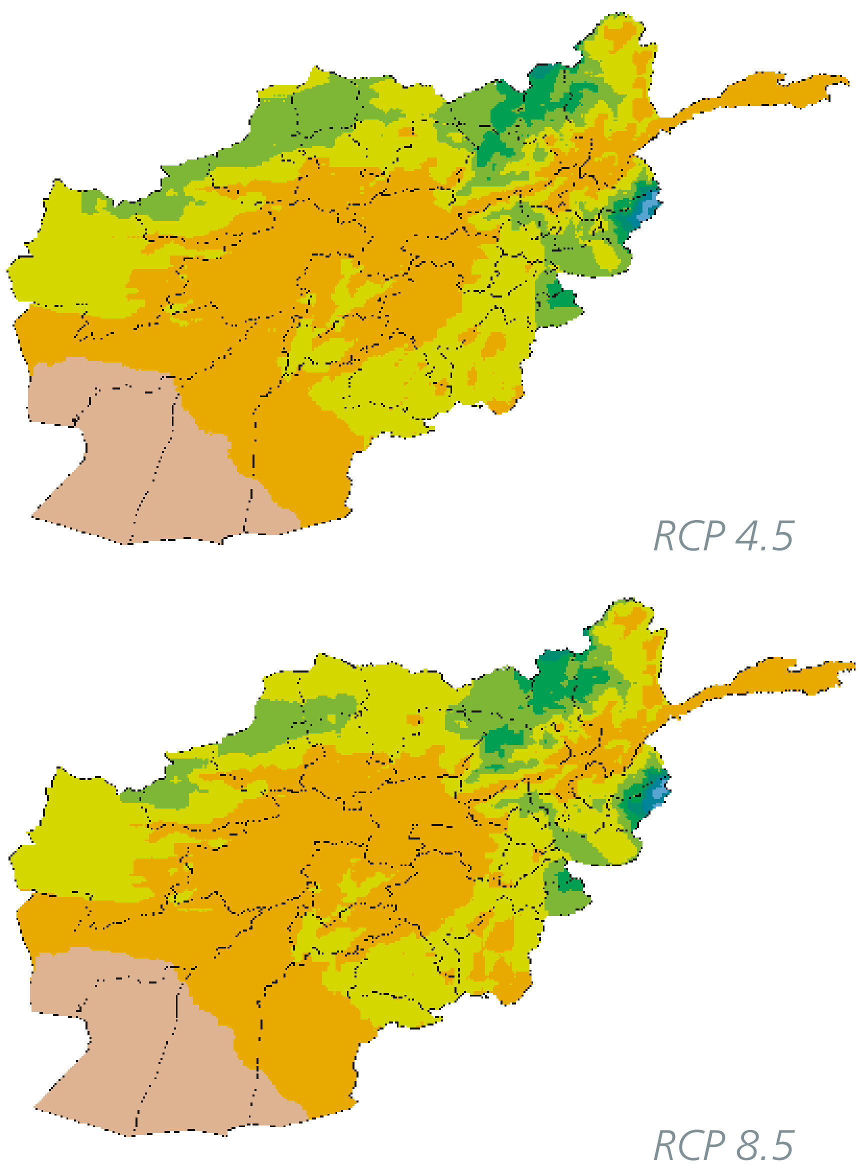

Source: IIASA, 2019

Figure 34

Net primary productivity (NPP)

Net primary production (NPP) is estimated in AEZ as a function of incoming solar radiation and soil moisture at the rhizosphere.

Actual crop evapotranspiration (ETa) has a close relationship with NPP of natural vegetation as it is quantitatively related to plant photosynthetic activity which is also driven by radiation and water availability.

NPP is computed based on daily values of estimated actual evapotranspiration (ETa) in the reference water balance (see Appendix 2) and serves as a climate-related indicator of rain-fed biological activity.

Separate evaluations of the NPP potential are performed, for moisture supply under natural conditions and an estimate applicable when adequate water is supplied (e.g. by irrigation) to ensure daily ETa matches ETo. Details of the NPP calculation procedure are given in Appendix 3.

Figure 35 shows the spatial pattern of average reference NPP potential under rain-fed conditions for historical climate of the period 1981–2010; future rain-fed NPP potential is presented in Figure 36. NPP values are given in kg carbon per hectare (kg C/ha).

Net primary production potential for rain-fed conditions (kg C/ha)

Period 1981–2010

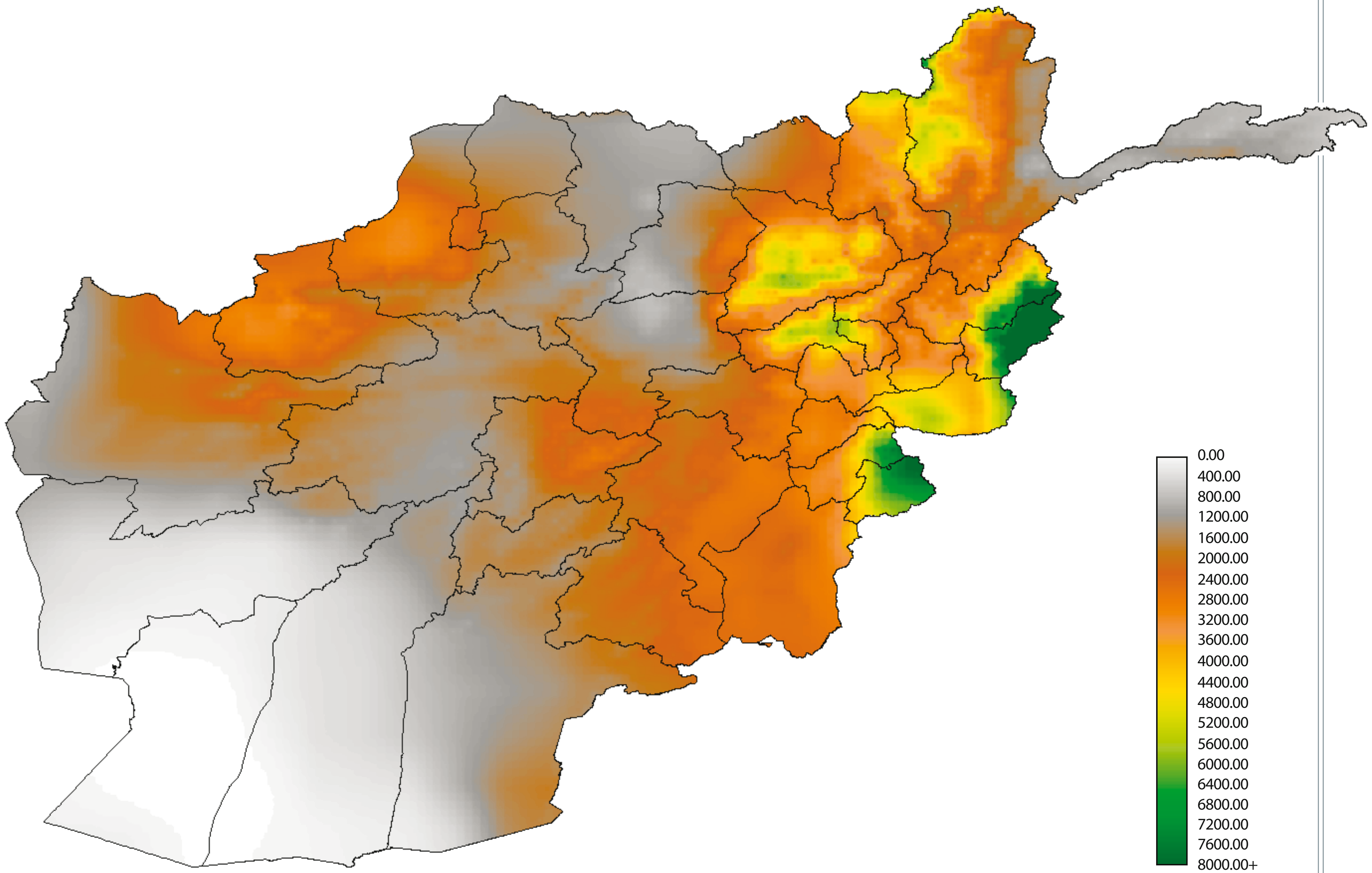

Source: IIASA, 2019

Figure 35

Ensemble mean Period 2041–2070

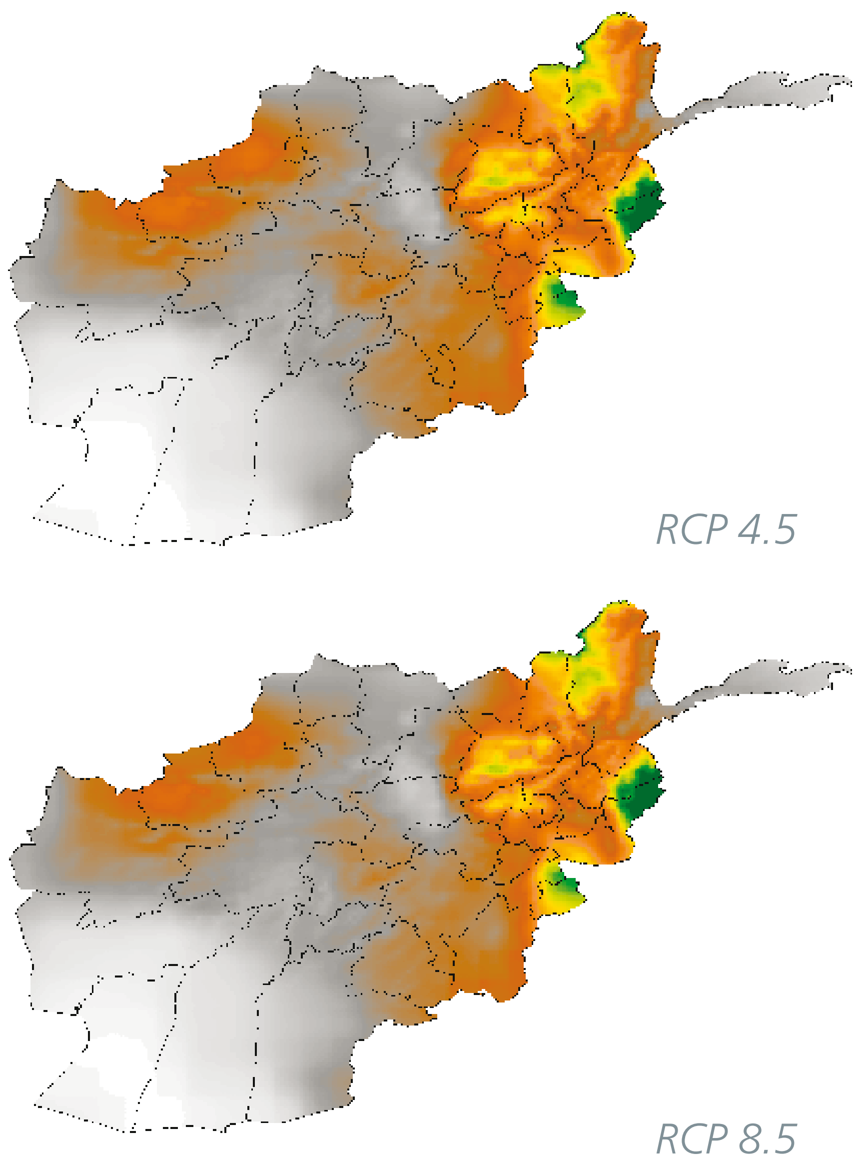

Source: IIASA, 2019

Figure 36

Average reference NPP potential for rain-fed conditions by region is listed in Table 12.

The highest average regional rain-fed potential of nearly five tonnes of carbon per hectare during 1981-2010 was achieved in the comparatively wet eastern region, followed by south-eastern region (3.4 tons C/ha), central region (3.1 tons C/ha), and north-eastern region (2.8 tons C/ha).

Under climate change, the rain-fed NPP potential is expected to decline by -10 percent to -30 percent depending on region and RCP, with the exception of the north-eastern region where a small increase of the rain-fed NPP potential may materialize due to warming.

Table 12 - Changes of Net Primary Production potential for rain-fed conditions (kg C/ha) period 2020s, 2050s and 2080s vs historical

Regions	Area (km²)	Historical		Ensemble mean RCP 4.5						Ensemble mean RCP 8.5					
		1961–1990	1981–2010	2020s	2050s	2080s	% Difference with 1981–2010			2020s	2050s	2080s	% Difference with 1981–2010		
							2020s	2050s	2080s				2020s	2050s	2080s
North Eastern	80 718	2643	2786	2708	2869	2868	-3	3	3	2553	2803	2944	-8	1	6
North Western	77 271	1610	1635	1465	1443	1385	-10	-12	-15	1246	1351	1331	-24	-17	-19
Eastern	25 059	4382	4958	4301	4485	4344	-13	-10	-12	4241	4298	4589	-14	-13	-7
Central	31 072	2498	3081	2415	2527	2397	-22	-18	-22	2217	2354	2467	-28	-24	-20
West Central	55 719	1589	2000	1504	1477	1393	-25	-26	-30	1318	1372	1342	-34	-31	-33
Western	160 581	1315	1310	1244	1124	1091	-5	-14	-17	1053	1090	1038	-20	-17	-21
South Eastern	28 472	3090	3492	2730	2846	2576	-22	-19	-26	2714	2671	2620	-22	-24	-25
South Western	183 421	679	794	685	570	563	-14	-28	-29	655	593	496	-18	-25	-38

Source: Calculations based on 30 arc-second NAEZ Afghanistan climate inventory.

Net primary production potential for irrigated conditions (kg C/ha)

As noted previously for ETa, NPP also depends on the temperature regime, radiation and soil moisture supply at a location.

For the land of Afghanistan, often either temperature (high altitude) and/or soil moisture supply (especially in western and southern areas) are limiting factors resulting in rather low rain-fed NPP potential estimates compared to potential NPP when assuming no moisture limitations (see Figure 37).

For assumed irrigation conditions, some increases of potential NPP can be expected under climate change due to elevated ETo as a consequence of warming, especially at mid- and high-altitude zones.

See Figure 38 for results in the 2050s under RCP 4.5 (top) and RCP 8.5 (bottom) respectively.

Period 1981–2010

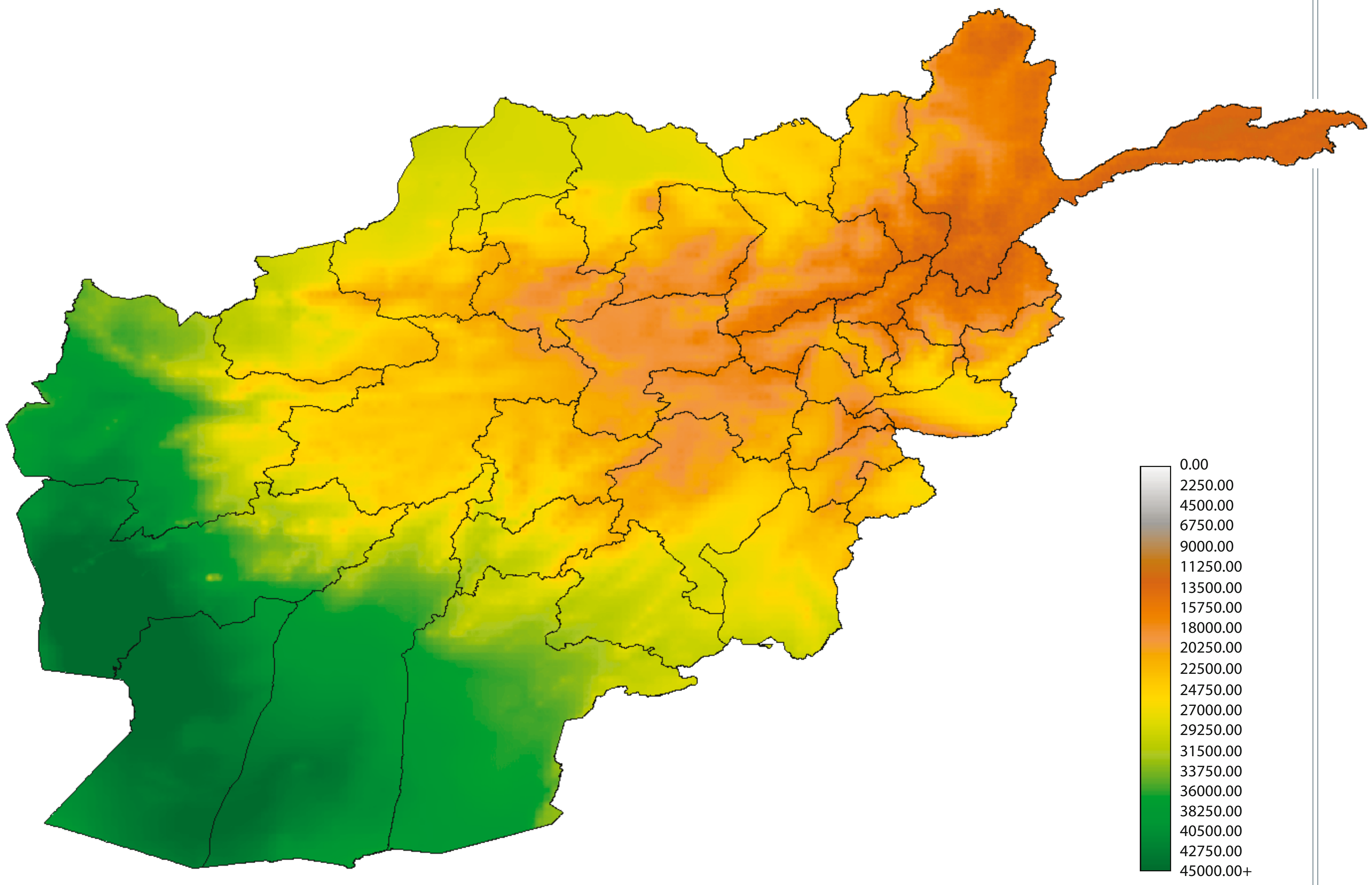

Source: IIASA, 2019

Figure 37

Ensemble mean
Period 2041–2070

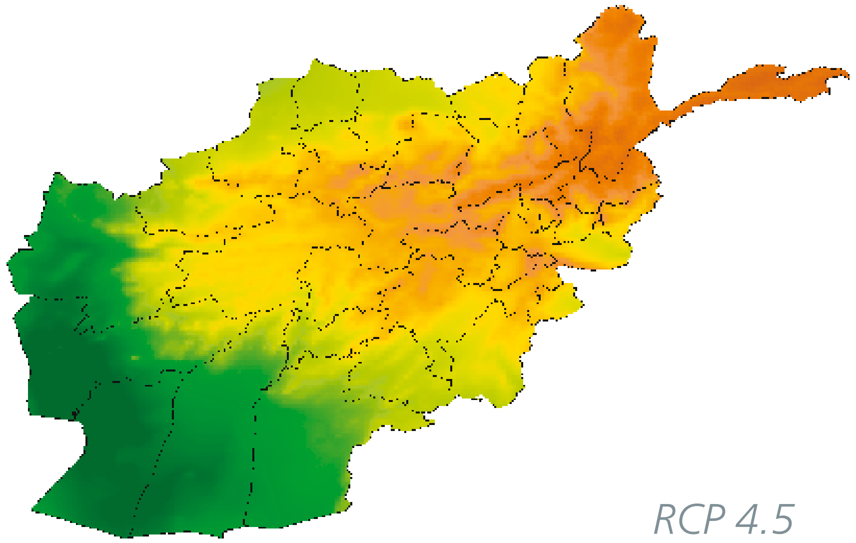

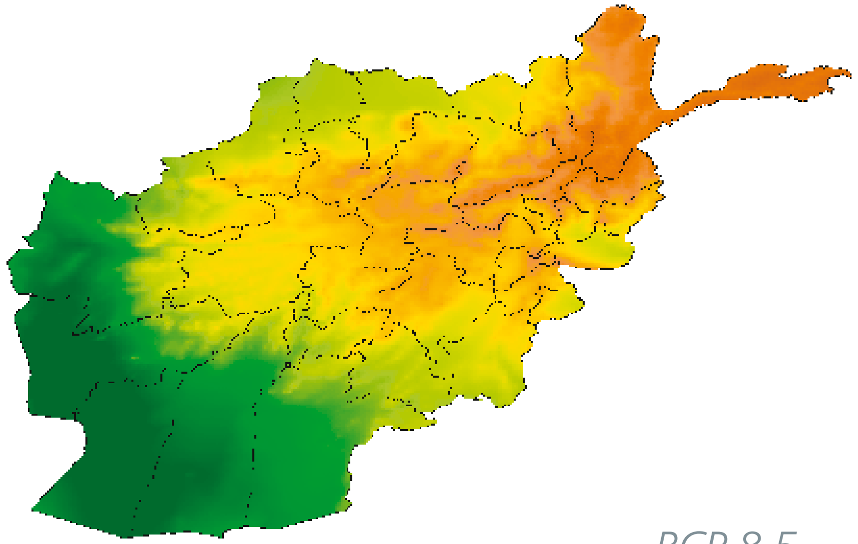

Source: IIASA, 2019

Figure 38

Multiple cropping zones

In areas where the growing period is sufficiently long to allow more than one crop to be grown in the same year or season, single crop yields do not reflect the full potential of total time available.

To assess the multiple cropping potential, a number of multiple cropping zones have been defined in AEZ through matching both growth cycle and temperature requirements of suitable crops with time available for crop growth. For rain-fed conditions, this period is approximated by the number of LGP days; and for irrigated conditions, the temperature growing period LGPt5 is used.

Delineation of multiple cropping zones is also based on several other agro-climatic attributes calculated during AEZ analysis.

For the definition of multiple cropping zones, four types of crops are distinguished: thermophilic crops requiring warm temperatures (e.g. maize); cryophilic crops (e.g. potato) performing best under cool and moderately cool conditions; hibernating crops (e.g. winter wheat); and wetland crops (e.g. paddy rice) with specific water requirements.

Furthermore, the crops are subdivided according to growth cycle length, namely of less or more than 120 days duration, respectively. The following eight zones are classified and mapped in AEZ:

A. Zone of no cropping (too cold or too dry for rain-fed crops)
B. Zone of single cropping
C. Zone of limited double cropping (relay cropping; single wetland rice may be possible)
D. Zone of double cropping (sequential cropping; double cropping with wetland rice not possible)
E. Zone of double cropping (sequential cropping; wetland rice crop possible)
F. Zone of double rice or limited triple cropping (partly relay cropping; no third crop possible in case of two wetland rice crops)
G. Zone of triple cropping (sequential cropping of three short-cycle crops; two wetland rice crops possible)
H. Zone of triple rice cropping (sequential cropping of three wetland rice crops possible)

Multiple cropping zones for rain-fed conditions

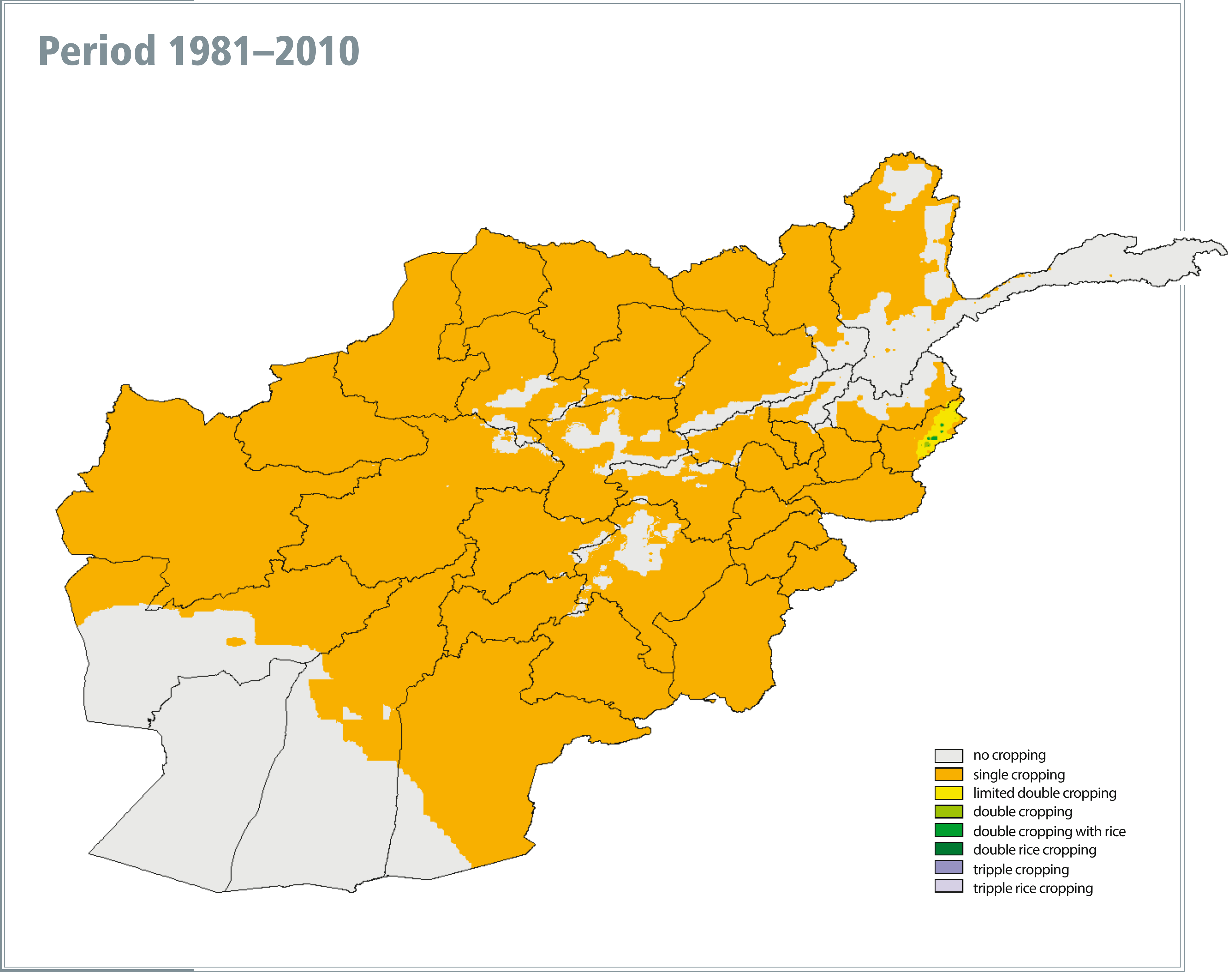

Source: IIASA, 2019

Figure 39

Ensemble mean
Period 2041–2070

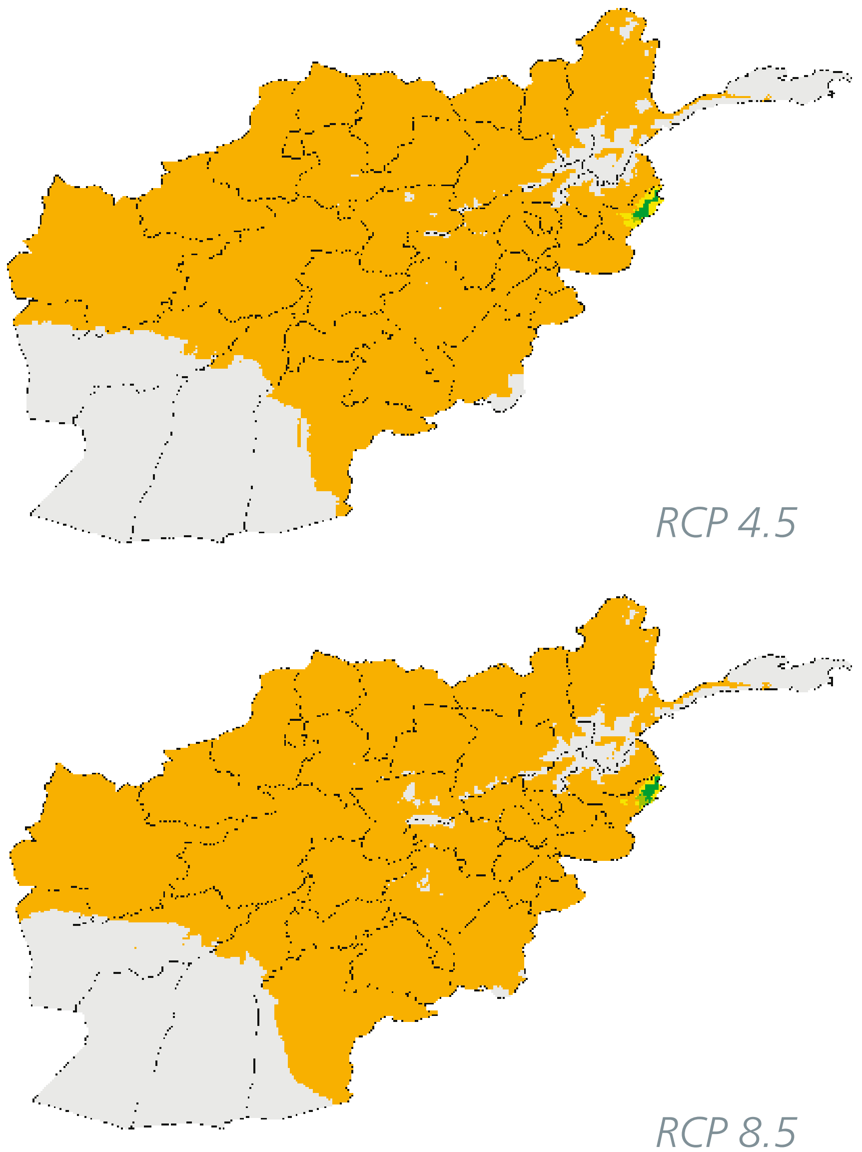

Source: IIASA, 2019

Figure 40

A map of multiple cropping zones for rain-fed conditions during historical period 1981–2010 is presented in Figure 39. Impacts of climate change on rain-fed, multiple cropping zones are shown in Figure 40 for climate in period 2041–2070 under RCP 4.5 assumptions (top) and RCP 8.5 (bottom).

Note that for historical periods under rain-fed conditions, only single cropping (or no cropping) was viable in almost all territory of Afghanistan, due to temperature limitations (mostly north-eastern, eastern and central region) and/or severe moisture limitations (western, south-western and south-eastern regions). While moisture limitations will continue (and somewhat worsen) into the future and result in some expansion of the no-cropping zone in the south-western region, minor improvements (from no cropping to single cropping; or, from single cropping to limited double-cropping) may occur in the north-eastern, eastern and central regions due to global warming (see Figure 40).

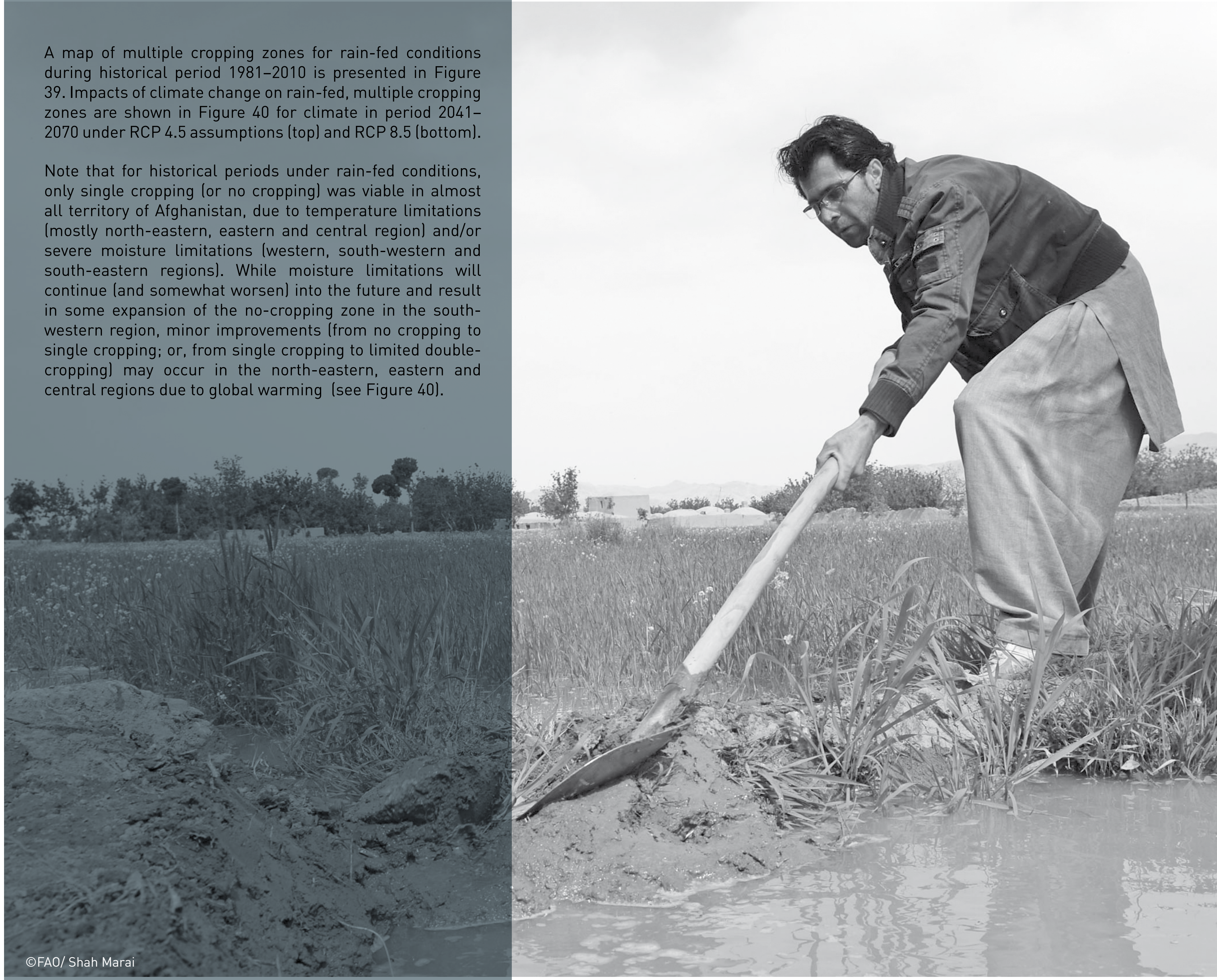

Historical results of multiple cropping zones in Afghanistan for assumed irrigation conditions are shown in Figure 41.

When moisture limitations can be overcome with irrigation, the prevailing temperature regime allows for triple cropping in south-western Afghanistan and in pockets of eastern and south-eastern Afghanistan.

In most of the central region and part of the north-eastern region, only one sequential or no crop is possible due to limited heat provision. In the north-western, western and south-eastern regions dominantly double cropping can be practiced where water is available.

With climate change, and if water can be supplied, the irrigated multiple cropping potential is expected to increase in all regions due to warming. This will be very distinct in the north-eastern, north-western, central and eastern regions.

The impacts by the 2080s are shown in Figure 42 for climate change under RCP 4.5 (top) and RCP 8.5 (bottom).

Multiple cropping zones for irrigated conditions

Period 1981–2010

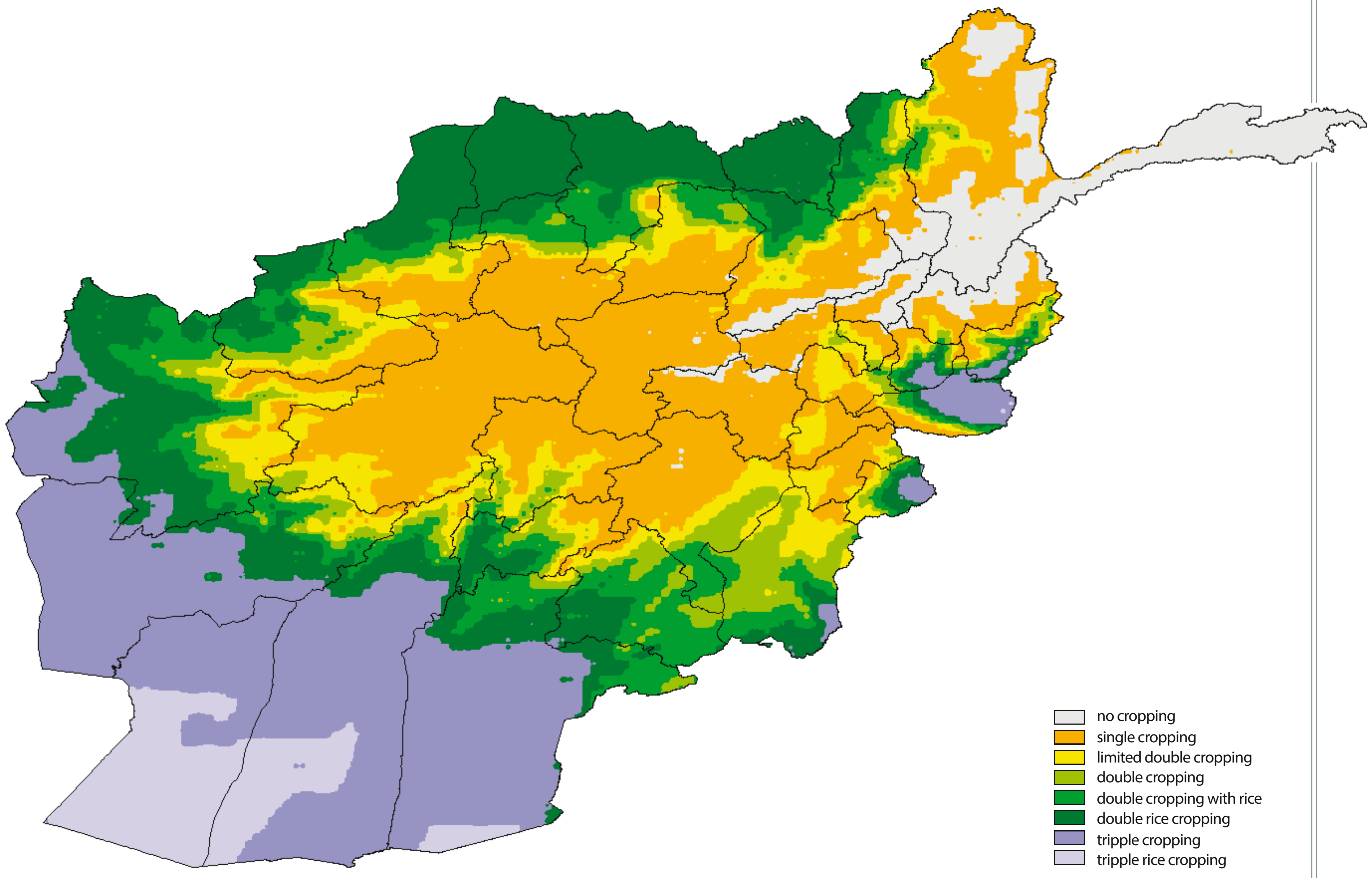

Source: IIASA, 2019

Figure 41

Ensemble mean
Period 2070–2099

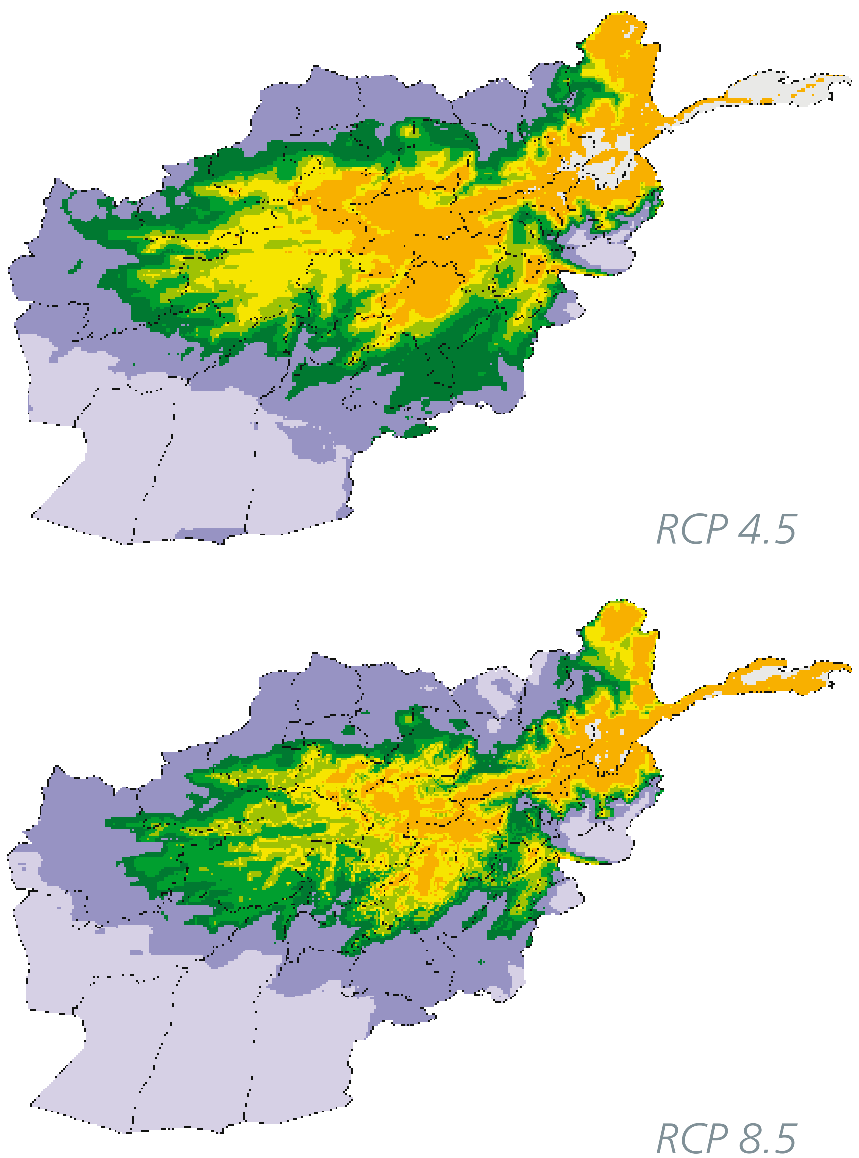

Source: IIASA, 2019

Figure 42

Köppen climate classification (KG2)

Köppen climate classification is a widely used, vegetation-based, empirical climate classification system developed by Wladimir Köppen in the early 20th century. His aim was to devise formulas that would define climatic boundaries in such a way as to correspond to different observed vegetation zones (biomes).

Köppen's classification is based on a subdivision of terrestrial climates into five major types, which are represented by the capital letters A (tropical), B (dry), C (temperate), D (cold), and E (polar). Each of these climate types, except for B, is defined by temperature criteria. Type B designates climates in which the controlling factor on vegetation is dryness (rather than coldness).

Dry climates are divided into arid (BW) and semi-arid (BS) subtypes. Other climate types are sub-divided according to seasonal precipitation characteristics.

A map of level-2 Köppen climate classes for Afghanistan, based on the climate attributes of period 1981–2010, is shown in Figure 43. It shows large areas dominated by arid and semi-arid climates in the south-western, western and north-western regions and also indicates the areas in the central and north-eastern regions which are characterized by temperate and cold climate conditions with dry summers.

Figure 44 provides estimates of Köppen climate classes for future climate in the period 2041–2070 simulated under respectively RCP 4.5 (left) and RCP 8.5 (right) conditions. The maps show the dominant class from the respective ensemble of NAEZ simulations and time period. Changes compared to the historical pattern in the 2050s are most visible in central and north-eastern Afghanistan where large areas, which are currently classified as temperate or cold climates, change class to BS (semi-arid steppe climate). Such changes reflect the expected trends of warming and drying as noted previously, which will mitigate coldness in these areas but will also exacerbate dryness.

Note also that stretches of class BW (arid desert climate) will expand in the south-western and north-western regions.

Köppen climate classification (level-2)

Period 1981–2010

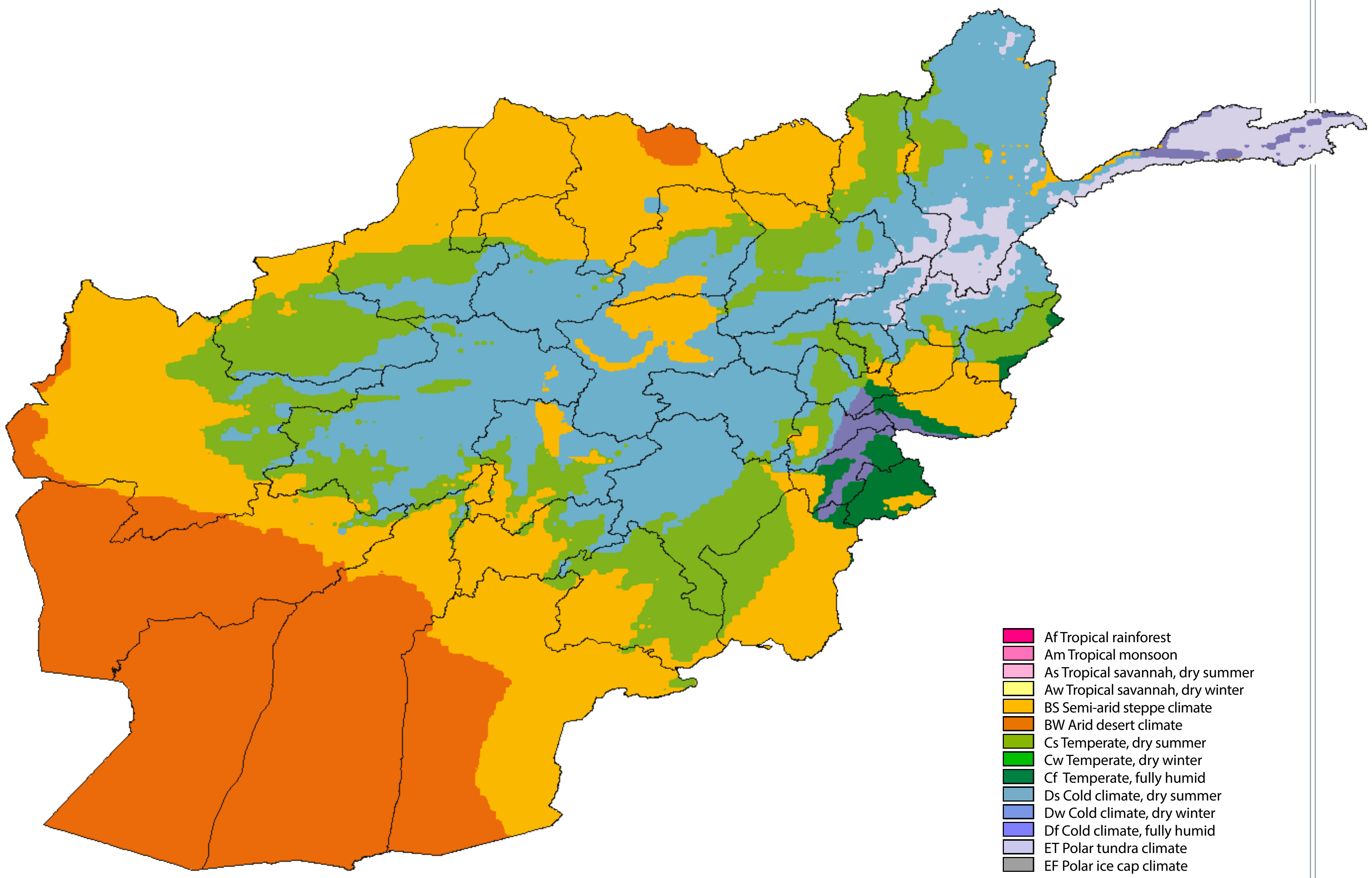

Source: IIASA, 2019

Figure 43

Period 2041–2070

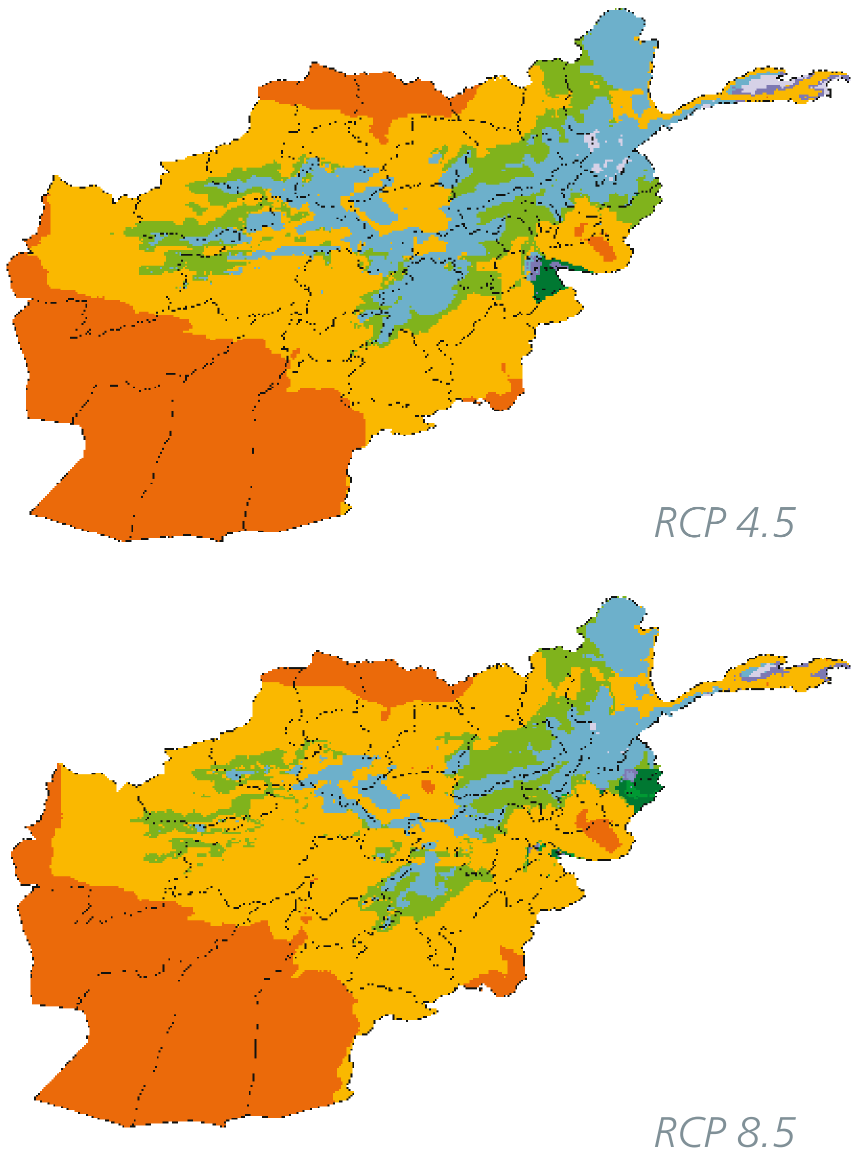

Source: IIASA, 2019

Figure 44

Annual number of rain-days (NDR)

The NAEZ analysis uses daily data of temperature (minimum and maximum) and precipitation. This allows the computation of various statistics, including the number of rain-days in a year, here defined as days with precipitation P ≥ 1 mm.

Figure 45 presents a map of average number of rain-days during 1981–2010 ranging between less than 10 rain-days in parts of the south-western region, to about 150 days in some parts of the eastern region.

The level and spatial pattern of number of rain-days in a future climate are shown in Figure 46, which also highlights the geographical downward gradient of days from north-east to south-west, and which indicates some reduction of number of rain-days by the 2050s compared to 1981–2010.

Annual number of rain-days (days)

Period 1981–2010

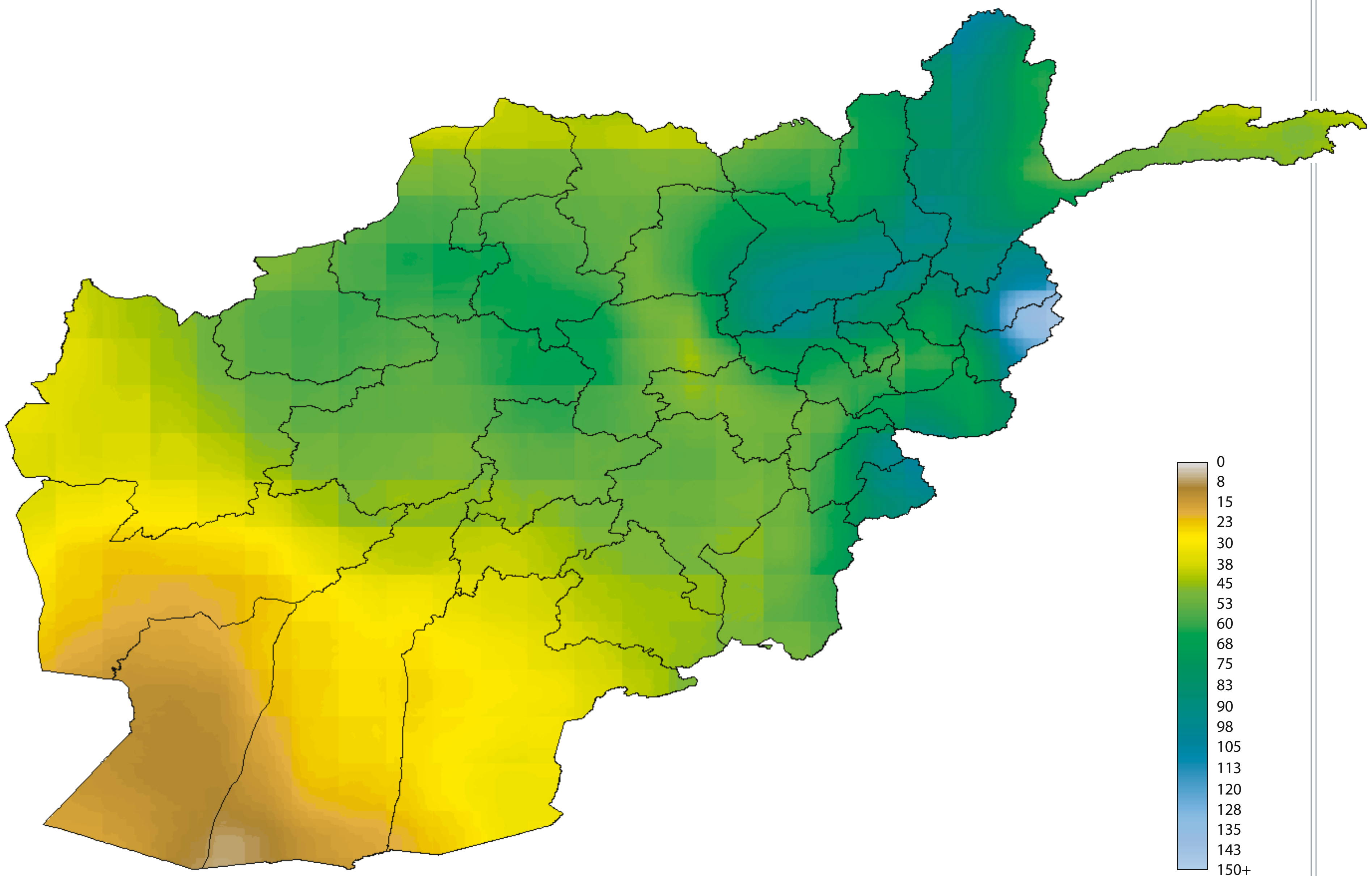

Source: IIASA, 2019

Figure 45

Ensemble mean
Period 2041–2070

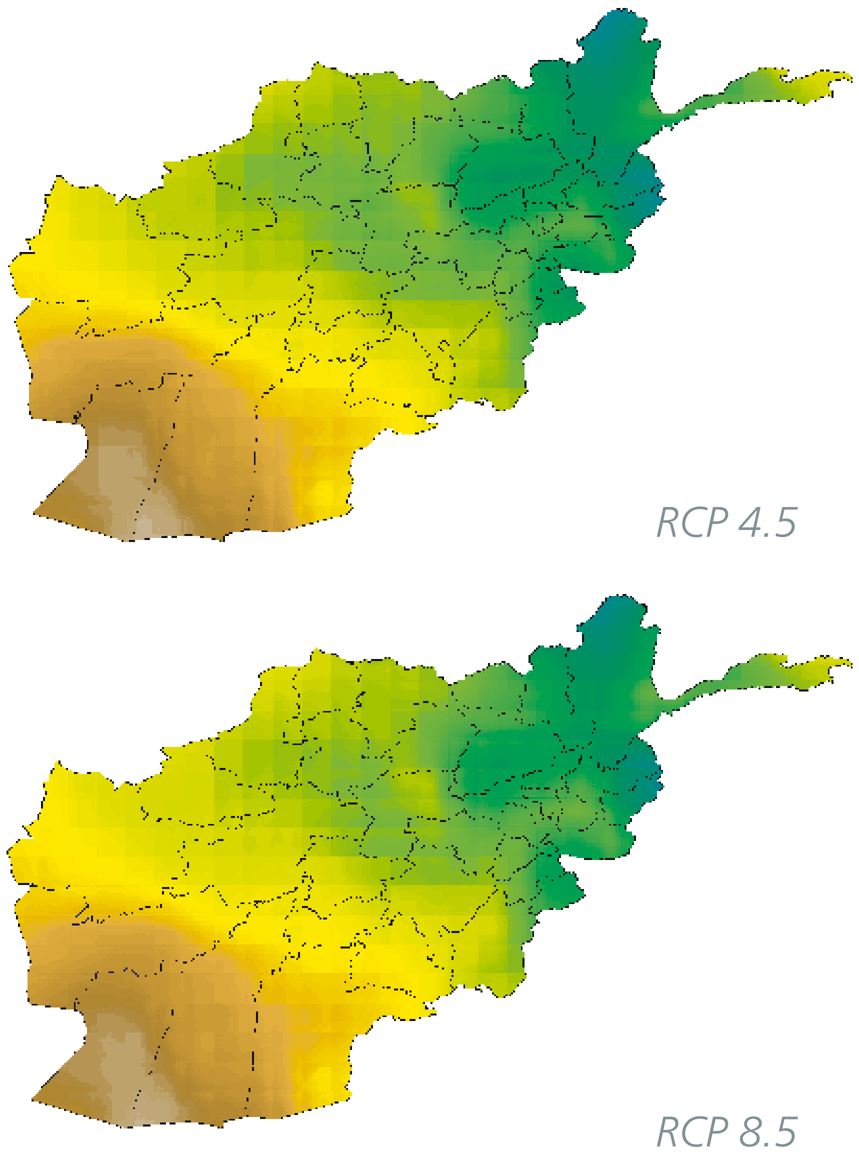

Source: IIASA, 2019

Figure 46

Some regional details are listed in Table 13. It shows that regional average number of rain-days during 1981–2010 was in the range of 27 rain-days (south-western region) to 85 rain-days (eastern region).

Projected decreases of rain-days in 2041–2070 are -5 to -14 days under RCP 4.5; and -8 to -17 days under RCP 8.5.

Table 13 - Changes of annual number of rain-days (days) period 2020s, 2050s and 2080s vs historical

Regions	Area (km²)	Historical		Ensemble mean RCP 4.5						Ensemble mean RCP 8.5					
		1961–1990	1981–2010	2020s	2050s	2080s	Days difference with 1981–2010			2020s	2050s	2080s	Days difference with 1981–2010		
							2020s	2050s	2080s				2020s	2050s	2080s
North Eastern	80 718	67	74	70	69	67	-4	-5	-7	67	66	61	-7	-9	-13
North Western	77 271	50	55	49	47	44	-6	-8	-11	45	44	40	-10	-11	-15
Eastern	25 059	73	85	71	71	67	-13	-14	-17	69	67	64	-15	-17	-21
Central	31 072	59	63	60	58	55	-3	-5	-8	57	55	50	-7	-8	-13
West Central	55 719	49	53	47	45	42	-6	-8	-11	43	42	37	-9	-11	-15
Western	160 581	38	41	34	32	29	-7	-10	-12	31	30	26	-11	-12	-15
South Eastern	28 472	52	62	51	51	47	-11	-11	-15	49	48	45	-12	-14	-17
South Western	183 421	22	27	21	19	18	-6	-8	-9	19	19	17	-8	-9	-10

Source: Calculations based on 30 arc-second NAEZ Afghanistan climate inventory.

Number of humid months (NHUM)

A further aspect of the vertical water balance is provided in NAEZ by an index counting the number of months in a year when precipitation (P) exceeds potential evapotranspiration (ETo), termed number of humid months (NHUM).

During historical years, most land in Afghanistan experienced predominantly zero, one or two humid months. In some parts of central, eastern and north-eastern regions, up to six humid months have occurred (see Figure 47).

Monthly precipitation exceeding potential evapotranspiration will become less frequent in a future climate, as shown in Figure 48 for the 2050s.

By implication, the periods in a year when the replenishment of soil moisture is possible due to P > ETo will occur less frequently with global warming, compared to period 1981–2010.

Number of humid months (NHUM with P>ETo)

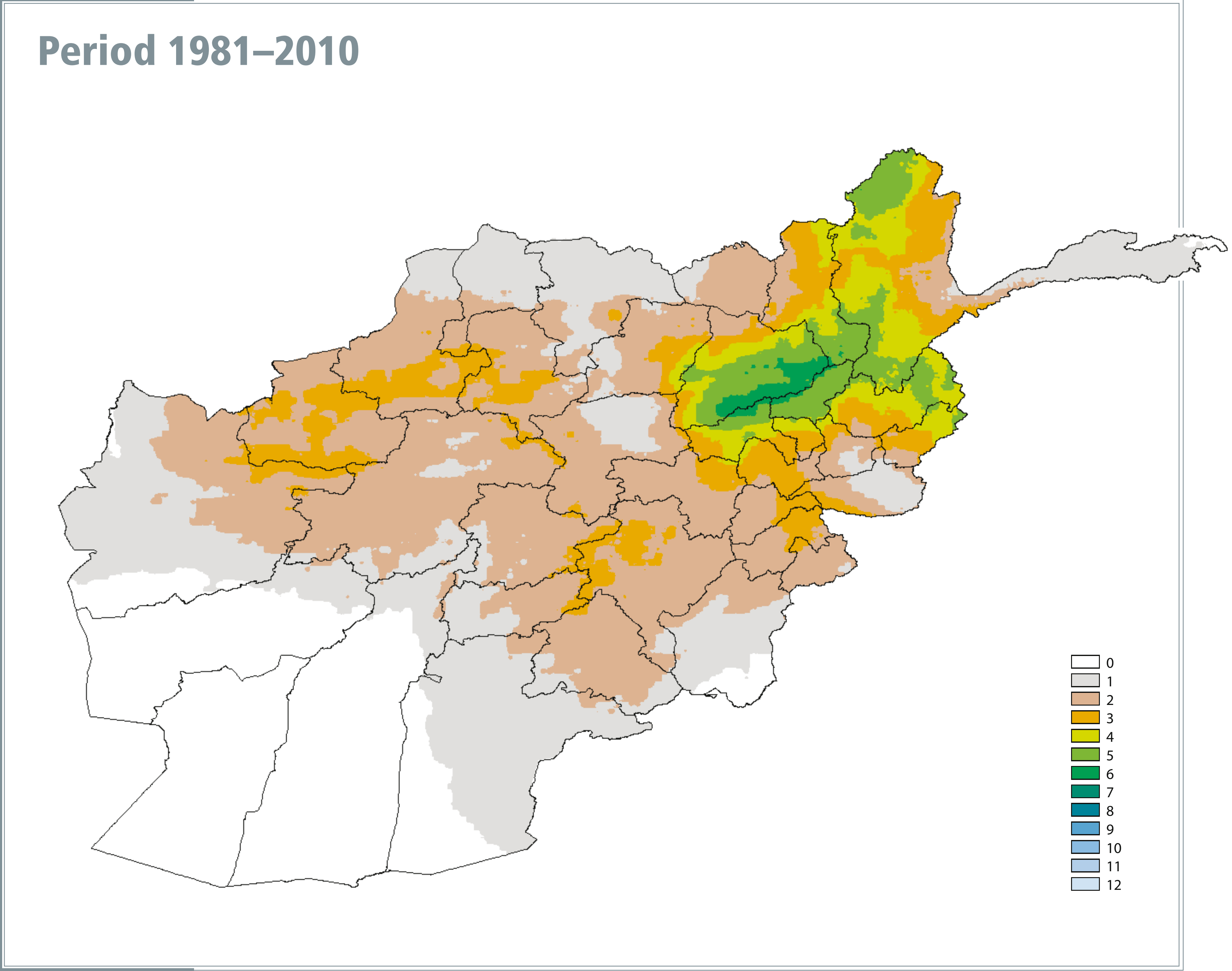

Source: IIASA, 2019

Figure 47

Ensemble mean
Period 2041–2070

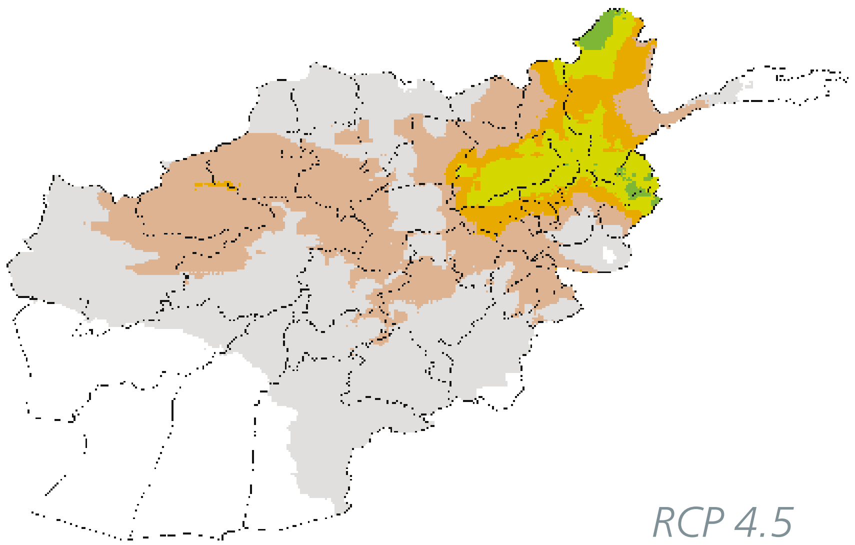

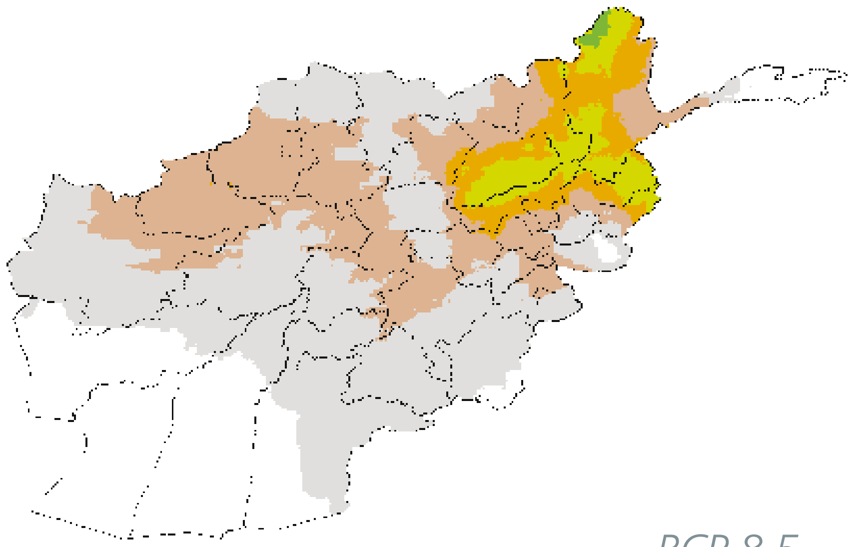

Source: IIASA, 2019

Figure 48

Number of "frost" days (with Tmin < 0 °C)

Daily data of minimum and maximum temperatures are used in NAEZ to compute various statistics of extreme temperature events.

One such index counts the number of 'frost' days in a year, defined as days when minimum daily temperature falls below 0°C. Under historical conditions, such days occurred everywhere in Afghanistan, with rather short frost periods in south-western Afghanistan and in pockets of the eastern region; a considerable number of frost days in central Afghanistan; and predominantly frost days at higher altitudes in central and north-eastern regions.

A map showing the average number of annual 'frost' days during 1981–2010 is given in Figure 49.

Average number of "frost" days (Tmin < 0 °C)

Period 1981–2010

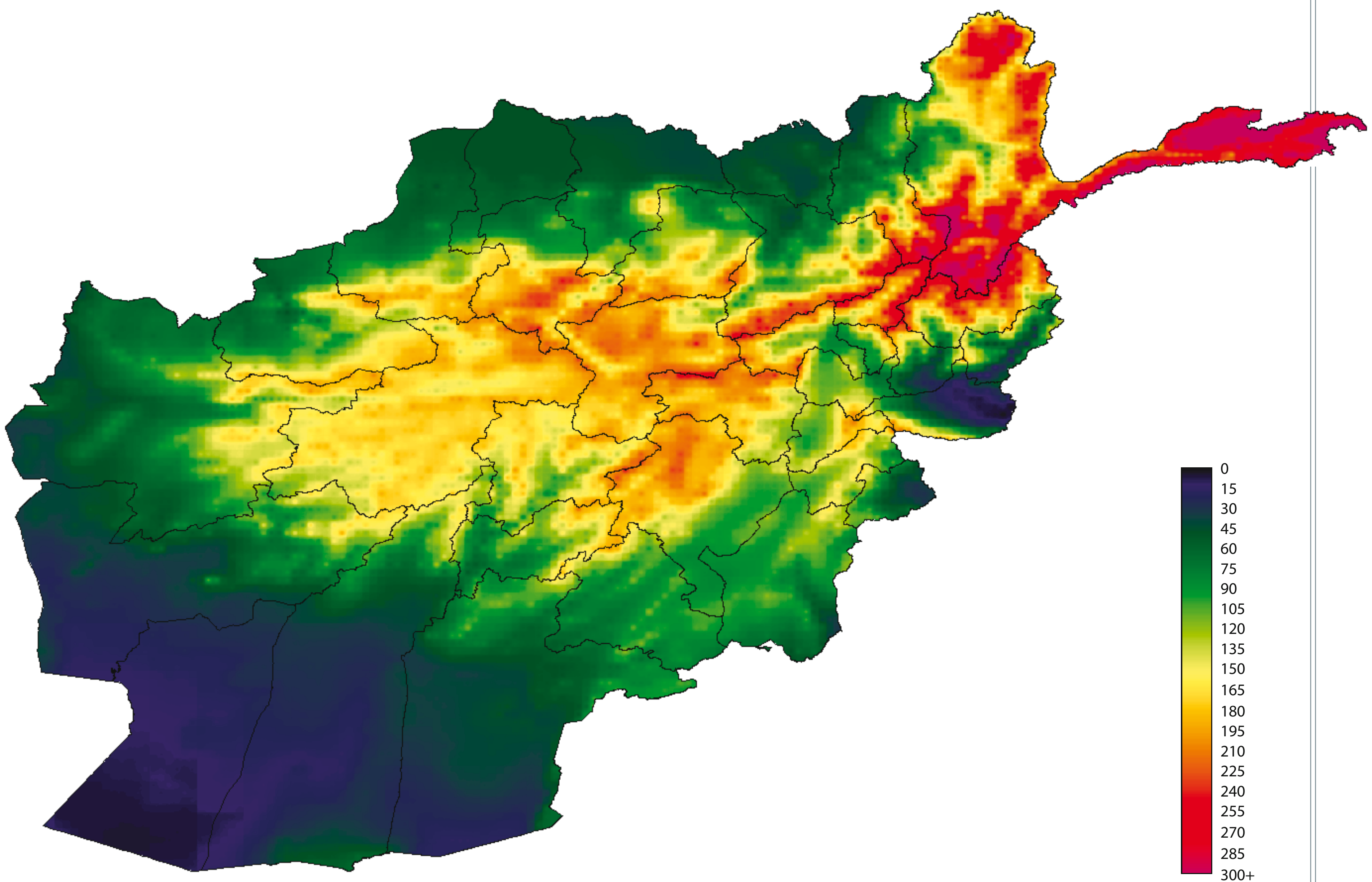

Source: IIASA, 2019

Figure 49

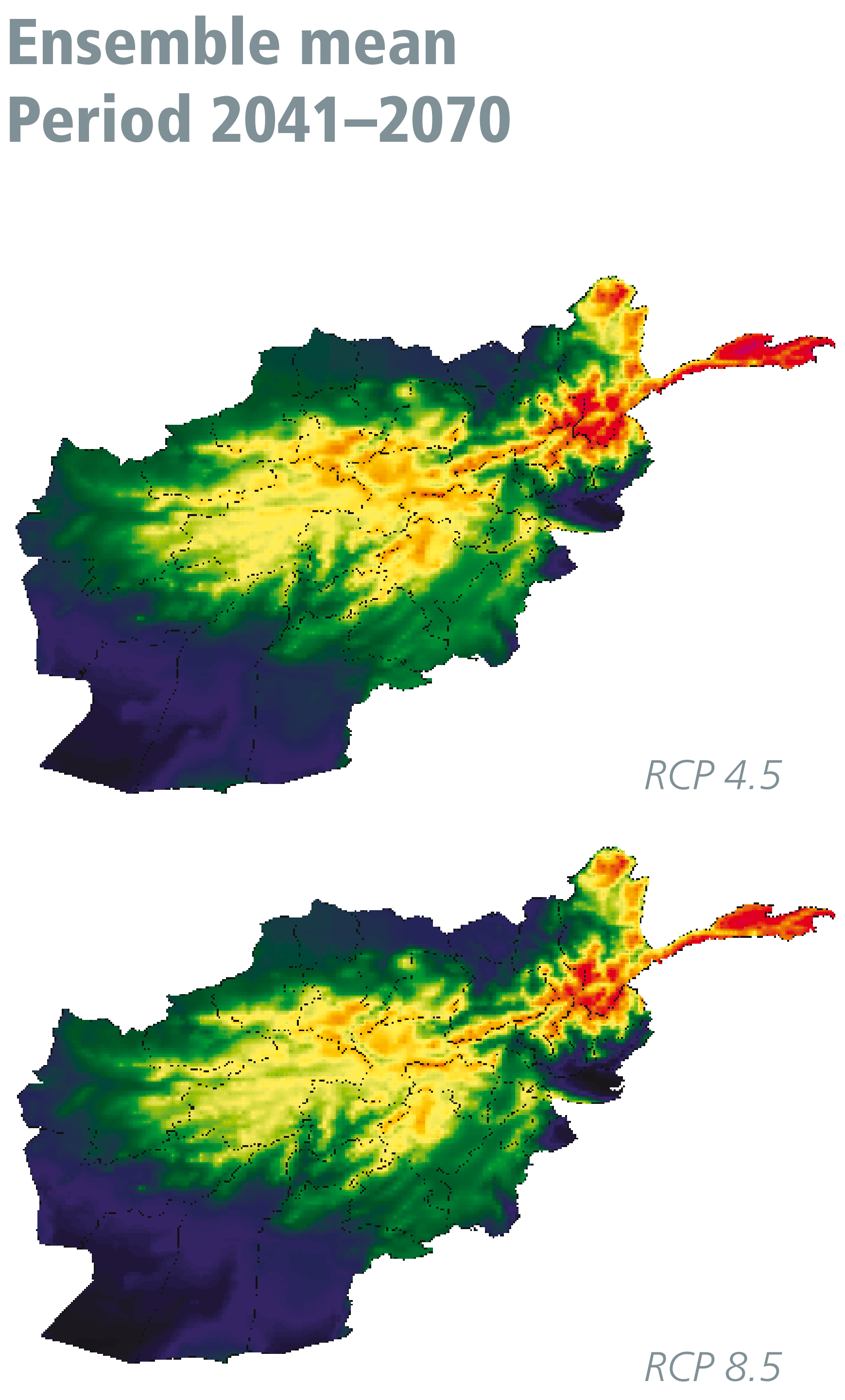

Source: IIASA, 2019

Figure 50

With climate change, the occurrence of frost days is obviously decreasing, as shown in Figure 50 for the 2050s under RCP 4.5 (top) and RCP 8.5 (bottom), respectively.

The annual number of days with frost, averaged over all the grid cells in a particular region, is listed in Table 14.

Of the eight geographical regions, the lowest number of 'frost' days during 1981–2010 is listed for the south-western region (47 days).

The average for the central regions was about 160 days and totals more than 170 days for the north-eastern region. Depending on RCP assumptions, the number of 'frost' days in the 2050s will be reduced by -12 days to -18 days in the south-western region; and by as much as -33 days to -45 days in the north-eastern region.

For the 2080s the changes of average number of 'frost' days are -16 days to -28 days in the south-western region; and -40 days to -69 days in the north-eastern region.

Table 14 - Changes of average number of "frost" days (with Tmin < 0 °C) period 2020s, 2050s and 2080s vs historical

Regions	Area (km²)	Historical		Ensemble mean RCP 4.5						Ensemble mean RCP 8.5					
		1961–1990	1981–2010	2020s	2050s	2080s	Days difference with 1981–2010			2020s	2050s	2080s	Days difference with 1981–2010		
							2020s	2050s	2080s				2020s	2050s	2080s
North Eastern	80 718	175	171	154	138	131	-17	-33	-40	150	126	102	-21	-45	-69
North Western	77 271	108	102	94	86	81	-8	-16	-21	92	78	63	-10	-24	-39
Eastern	25 059	117	115	97	84	77	-18	-31	-38	93	73	55	-23	-42	-61
Central	31 072	159	159	145	132	126	-13	-27	-33	142	121	97	-16	-38	-62
West Central	55 719	167	160	152	139	134	-8	-21	-27	150	129	104	-10	-31	-56
Western	160 581	108	96	91	82	78	-6	-14	-18	90	75	59	-7	-21	-37
South Eastern	28 472	97	94	84	73	67	-10	-21	-27	82	61	42	-12	-33	-52
South Western	183 421	59	47	41	36	31	-6	-12	-16	40	29	20	-8	-18	-28

Source: Calculations based on 30 arc-second NAEZ Afghanistan climate inventory.

Number of 'hot' days (with Tmax > 35 °C)

Several indicators are calculated in NAEZ to capture the risks of high temperature events occuring. For instance, NAEZ agro-climatic analysis produces a count of the number of 'hot' days, here defined as days when daily maximum temperature exceeds 35 °C, which is indicative of periods when temperature may damage development and yields of cool-weather crops such as wheat.

Wheat belongs to the C3 crop group (C3 I) which is characterized with optimum photosynthesis and growth at temperatures between 15 °C and 20 °C. Temperatures above 30 °C cause growth cycle curtailment and severe heat stress, both leading to lower yields.

Figure 51 presents a map showing the historical climate for period 1981–2010 and the average number of 'hot' days. It indicates large areas where high temperatures above 35 °C were rarely experienced in the past.

The highest counts of the average number of 'hot' days, some 178 days, occurred in selected areas of the south-western region.

Average number of "hot" days (Tmax > 35 °C)

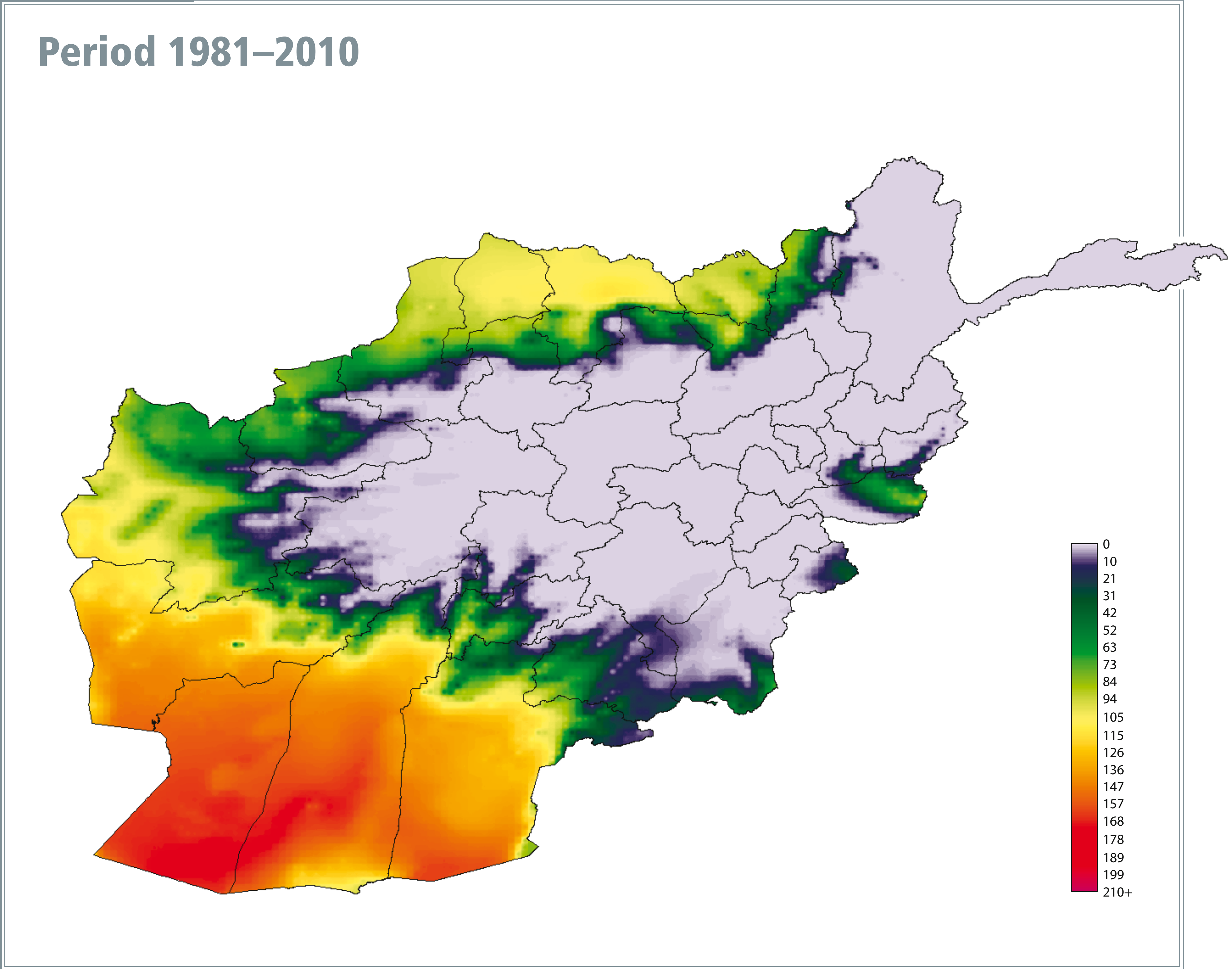

Source: IIASA, 2019

Figure 51

Ensemble mean Period 2041–2070

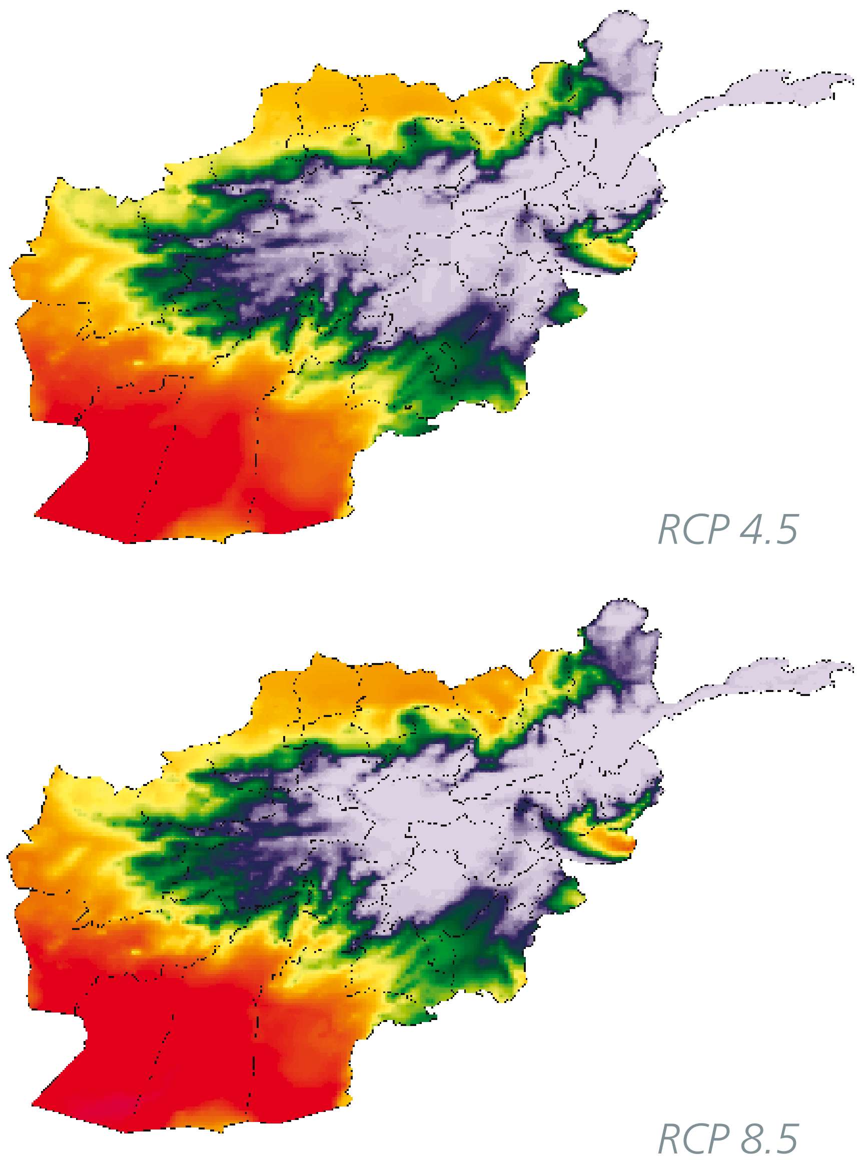

Source: IIASA, 2019

Figure 52

Figure 52 shows the number of 'hot' days in the 2050s under RCP 4.5 (top) and RCP 8.5 (bottom) projections.

The average number of 'hot' days by region is listed in Table 15. While 'hot' days rarely occurred in central Afghanistan and at higher altitudes of north-eastern, eastern and south-eastern regions, such temperatures most often occurred in the south-western region (which averaged 117 'hot' days during 1981–2010).

With climate change, in the 2050s the number of 'hot' days will increase in all regions, but will still remain rare in central Afghanistan.

For the south-western region, the average count of 'hot' days will increase from 117 days during 1981–2010 to 140 days (RCP 4.5) and 149 days (RCP 8.5), respectively. By the 2080s, maximum temperature on nearly half of all days will exceed 35 °C.

Table 15 - Changes of average number of "hot" days (with Tmax > 35 °C) period 2020s, 2050s and 2080s vs historical

Regions	Area (km²)	Historical		Ensemble mean RCP 4.5						Ensemble mean RCP 8.5					
		1961–1990	1981–2010	2020s	2050s	2080s	Days difference with 1981–2010			2020s	2050s	2080s	Days difference with 1981–2010		
							2020s	2050s	2080s				2020s	2050s	2080s
North Eastern	80 718	14	15	20	27	31	6	12	16	22	32	46	7	17	31
North Western	77 271	48	52	63	76	81	12	24	30	65	82	103	14	31	52
Eastern	25 059	10	10	18	27	32	8	17	23	19	34	54	9	24	44
Central	31 072	0	0	1	2	3	1	2	3	1	2	9	1	2	9
West Central	55 719	1	1	5	10	13	3	8	11	5	12	28	4	10	26
Western	160 581	53	61	73	95	91	12	24	30	75	93	118	14	32	57
South Eastern	28 472	7	7	15	26	33	8	19	26	17	33	63	10	27	56
South Western	183 421	106	117	127	140	147	10	24	30	129	149	173	13	33	57

Source: Calculations based on 30 arc-second NAEZ Afghanistan climate inventory.

Number of 'very hot' days (with Tmax > 40 °C)

Besides counting days with maximum temperature above 30 °C, 35 °C and 45 °C, the NAEZ analysis also produces a count of 'very hot' days, defined as daily maximum temperature exceeding 40 °C. This threshold was chosen to indicate days with a risk that even thermophilic crops like maize may suffer from high temperatures.

A map of the average number of 'very hot' days for historical climate of 1981–2010 is shown in Figure 53. Future outcomes in the 2050s under RCP 4.5 (left) and RCP 8.5 (right) are portrayed in Figure 54.

Map analysis reveals that during 1961–1990, 64.9 percent of the territory experienced, on average, 10 or less days with maximum temperatures exceeding 40 °C.

During period 1981–2010, this share fell to to 61.5 percent. On the other side of the distribution, only 0.1 percent of the land in Afghanistan had an average of 100 days or more with maximum daily temperature exceeding 40 °C, which increased to 2.9 percent of the land during 1981–2010.

By the 2050s, an average of 10 or less 'very hot' days will occur in 49.7 percent (RCP 4.5) to 46.7 percent (RCP 8.5) of the territory; and will exceed 100 days in, respectively, 16.6 percent (RCP 4.5) to 20.6 percent (RCP 8.5) of the land.

For the period 2070–2099 under RCP 8.5 assumptions, projections are that more than one-third of Afghanistan will experience, on average, 100 or more 'very hot' days, with a maximum of 178 'very hot' days – nearly half of the year – in some locations of the south-western region.

Average number of "very hot" days (Tmax > 40 °C)

Period 1981–2010

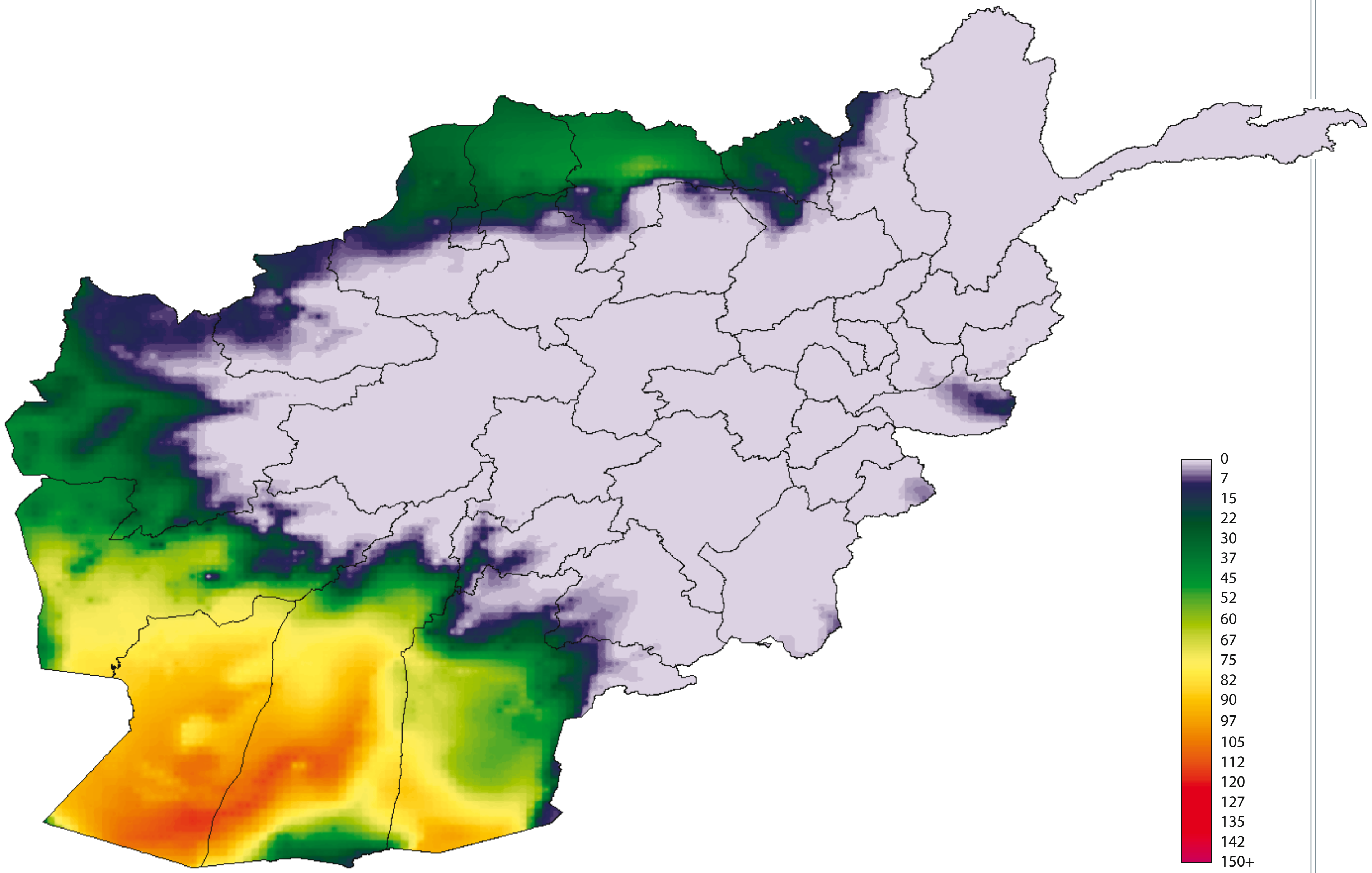

Source: IIASA, 2019

Figure 53

Ensemble mean Period 2041–2070

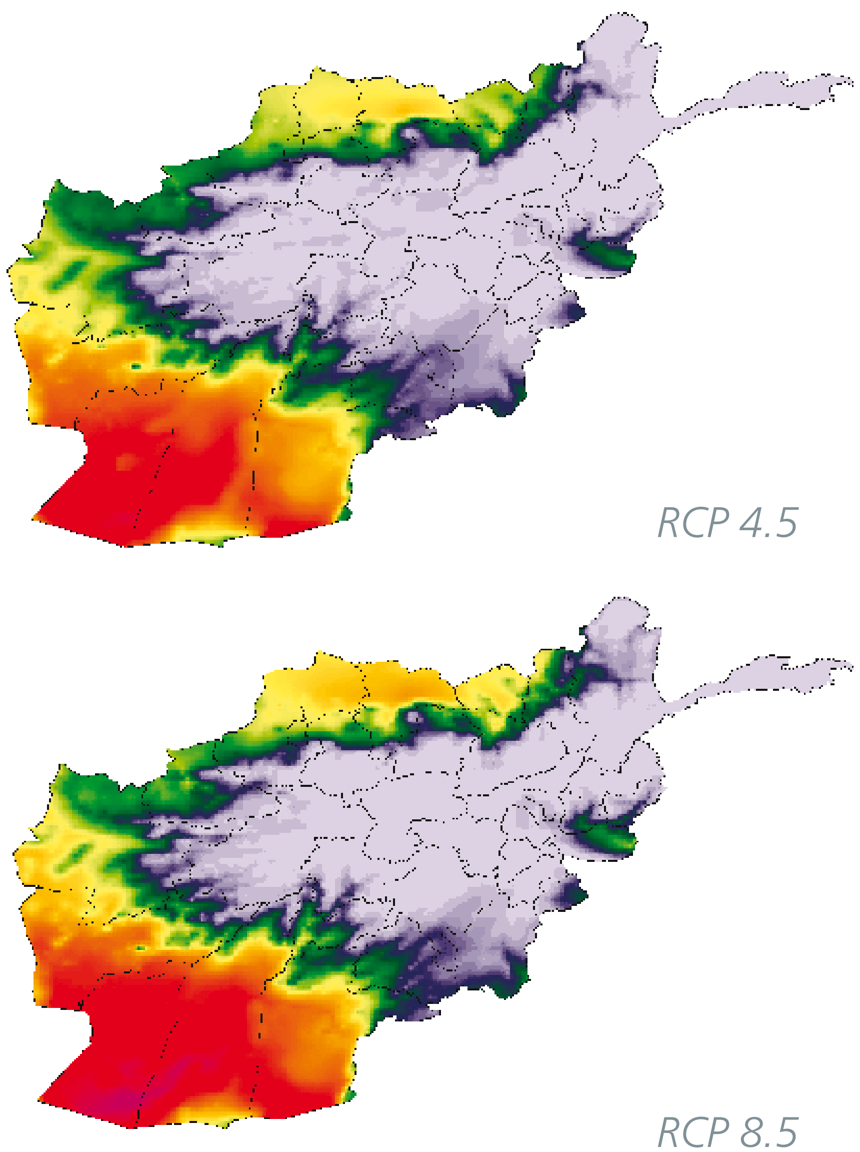

Source: IIASA, 2019 **Figure 54**

Table 16 gives average counts of 'very hot' days for the land in each region. While 'very hot' days on average were rare during 1981–2010 in central, eastern, south-eastern and north-eastern regions, a number of such days occurred in north-western and western regions. Most occurred in the south-western region.

Under climate change, by the 2050s the average number of 'very hot' days will increase in all regions, but will still remain a quite rare event in higher altitude regions. It is worth noting that the average number of 'very hot' days in the 2080s under RCP 8.5 will be higher than the occurrence of 'hot' days (with maximum temperature exceeding 35 °C) during period 1981–2010 (see also Table 15).

Table 16 - Changes of average number of "very hot" days (with Tmax > 40 °C) period 2020s, 2050s and 2080s vs historical

Regions	Area (km^2)	Historical		Ensemble mean RCP 4.5						Ensemble mean RCP 8.5					
		1961–1990	1981–2010	2020s	2050s	2080s	Days difference with 1981–2010			2020s	2050s	2080s	Days difference with 1981–2010		
							2020s	2050s	2080s				2020s	2050s	2080s
North Eastern	80 718	2	2	6	10	12	3	8	10	6	13	24	4	11	21
North Western	77 271	12	14	25	36	42	11	22	28	26	42	62	12	29	48
Eastern	25 059	1	1	2	4	6	1	4	6	3	7	18	2	6	17
Central	31 072	0	0	0	0	0	0	0	0	0	0	1	0	0	1
West Central	55 719	0	0	0	1	1	0	1	1	0	1	5	0	1	5
Western	160 581	14	19	29	39	44	10	20	25	30	47	70	11	27	50
South Eastern	28 472	0	0	1	3	5	1	3	5	2	4	15	2	4	14
South Western	183 421	46	56	69	85	91	13	28	35	72	93	120	16	37	64

Source: Calculations based on 30 arc-second NAEZ Afghanistan climate inventory.

Concluding remarks

The FAO/IIASA NAEZ system for Afghanistan has been used to assess likely spatial shifts in agro-climatic characteristics of land due to projected climate change in the period 2041–2070 (the 2050s) and 2071–2100 (the 2080s). Climatic conditions in Afghanistan will become warmer and mostly dryer in the future. This can create new opportunities in the North-Eastern region but will have negative impacts on water resources and rain-fed cropping in most other regions.

Temperature

- Comparison of 1981–2010 baseline climate with climate conditions projected for the 2050s, depending on a range of possible radiative forcing assumptions, suggests substantial temperature increases in Afghanistan by respectively 2.0 °C in the Western region to 2.8 °C in the Eastern region under representative concentration pathway RCP 4.5 and by 2.9 °C to 4.0 °C under RCP 8.5.
- For the 2080s under RCP 4.5 the increases in comparison with the 1981–2010 historical period vary from 2.6 °C (South-Western region) to 3.6 °C (Eastern region). Under RCP 8.5 the regional increases range from 5.1 °C to 6.3 °C.

Precipitation

- Same comparisons for precipitation reveal that for the 2050s under RCP 4.5 assumptions the average regional precipitation remains at approximately historical levels in the North-Eastern region but decreases by 5 to 15 percent in the other regions. Under RCP 8.5 assumptions, regional precipitation amounts decrease from about 5 percent (North-Eastern region) to as much as 18 percent (Central and West-Central regions).
- For the 2080s under RCP 4.5 the precipitation decreases in comparison with the 1981-2010 historical period vary from 2 percent (North-Eastern) to 18 percent (West-Central). Under RCP 8.5 the decreases occur in all regions varying from 7% (North-Eastern) to 26 percent (West-Central).

Growing period days

- The number of reference growing period days is a measure of the time during a year when both temperature and soil moisture conditions can support crop cultivation. Due to higher evapotranspiration rates and longer temperature growing periods due to warming but fairly constant or lower precipitation under climate change, the number of reference growing period days decreases generally with the exception of the North-Eastern region and some central highland areas where temperature growing period increases dominate.

- For the 2050s under RCP 4.5 assumptions, growing periods increase in the North-Eastern region on average by 14 percent while in the arid South-Western region growing periods decrease by up to 23 percent (from an average 63 days to 48 days). Under RCP 8.5 assumptions the changes in growing period days range from an increase by 15 percent (North-Eastern) to decreases of up to 25 percent (South-Western).
- For the 2080s under RCP 4.5 the annual number of growing period days changes in comparison with the 1981-2010 historical period by +15 percent (North-Eastern) to -27 percent (South-Western). Under RCP 8.5 the respective changes range from +20 percent to -35 percent.

Temperature extremes

- Temperature extremes change substantially from the 1981-2010 period as reflected by an overall decrease in number of frost days and increases of occurrences of hot and very hot days.
- Average annual numbers of frost days (minimum daily temperatures below 0 °C) for the 2050s under RCP 4.5 assumptions decrease by about 30 days in the cooler North-Eastern, Central and Eastern regions. Under RCP 8.5 the decreases in these regions are even larger, namely 30 to 40 frost days less, a reduction by approximately a quarter to a third.
- For the 2080s under RCP 4.5 the number of frost days decreases in comparison with the 1981-2010 historical period by up to 40 days. Under RCP 8.5 the decreases are up to 69 days, a reduction by 40 percent to 50 percent compared to 1981-2010.
- The average annual numbers of hot days (maximum daily temperatures more than 35 °C) for the 2050s under RCP 4.5 assumptions remain very low in Central Afghanistan but increase from 117 days to 140 days in the South-Western region. Under RCP 8.5 the regional increases of hot days reach up to 33 additional days (e.g. South-Western region).
- For the 2080s under RCP 4.5 the number of hot days increases in comparison with the 1981-2010 historical period by up to 30 days (South-Western, Western and North-Western regions). Under RCP 8.5 the increases are up to 57 days, reaching 118 hot days and 173 hot days respectively in the Western and South-Western region.

Multiple cropping

- Where natural soil moisture limitations can be overcome with irrigation, the prevailing temperature regime allows for triple cropping in South-Western Afghanistan and in pockets of Eastern and South-Eastern Afghanistan. In most of the Central region and part of the North-Eastern region only one sequential or no crop is possible due to limited heat provision at higher altitudes. In the North-Western, Western and South-Eastern regions dominantly double cropping can be practiced where water is available. With climate change, and where irrigation water can be supplied, the multiple cropping potential is expected to increase country-wide due to warming. The enhancement of multi-cropping potential will be rather distinct in the North-Eastern, North-Western, Central and Eastern regions of Afghanistan.
- Under purely rain-fed conditions only one crop, if at all, can be grown in most of Afghanistan. Due to a deteriorating soil moisture balance rain-fed double cropping in most of Afghanistan will also not be possible in the future.

Net primary production

- Net Primary Production (NPP) as used here is an agro-climatic indicator of potential biological activity. During the 1981-2010 period highest average rain-fed based NPP is found in the Eastern region of Afghanistan (almost 5 tons C/ha). Lowest average rain-fed NPP is found in the arid South-Western region (about 0.8 tons C/ha).
- For projected future climate the average rain-fed NPP potential is found to decrease in all regions with the exception of the North-Eastern region where due to warming and sufficient precipitation a slight increase is expected. For the 2050s under RCP 4.5 assumptions rain-fed NPP decreases by some 10 percent (Eastern region) to 28 percent (South-Western region). Under RCP 8.5 assumptions in the 2050s the respective changes of rain-fed NPP potential fall in a similar range of -13 percent (Eastern region) to -31 percent (West-Central region).
- For the 2080s under RCP 4.5 rain-fed NPP potential increases slightly in the North-Eastern region and decreases in all other regions in comparison with the 1981-2010 historical period by between 12 percent (Eastern region) and 30 percent (West-Central region) and with similar trends under RCP 8.5.
- For irrigated NPP (assuming no water stress) the results look different. When taking the average over the current cropland areas, the irrigated NPP potential increases in all regions due to warming, the least in the low-lying areas of the South-Western region and the most at higher altitudes of the Central and North-Eastern regions. Under RCP 4.5 conditions in the 2050s the improvements range from 2 percent (South-Western) to 7% (Central, Eastern and North-Eastern). Under RCP 8.5 the range of increases becomes 4 percent to 11 percent. In the 2080s the potential benefits from warming amount to a range of 4 percent to 10 percent under RCP 4.5 and to 10 percent to 18 percent under RCP 8.5 respectively. Note that such benefits do not account for possibly more frequent occurrence of extreme weather events and improvements can only materialize if irrigation water is available to meet the additional crop water requirements resulting in a future climate due to longer temperature growing periods and higher evaporative demand of crops per unit area.

1. Appendix

Agro-ecological zoning procedure for calculation of reference evapotranspiration

The calculation of reference evapotranspiration (ET_O), i.e. the rate of evapotranspiration from a hypothetic reference crop with an assumed height of 12 cm, a fixed canopy resistance of 70 ms^{-1}, an albedo of 0.23 (closely resembling the evapotranspiration from an extensive surface of green grass) and assuming well-watered growing conditions, is done according to the Penman-Monteith equation (*Monteith 1965; Monteith 1981; FAO 1992; FAO 1998*). The calculation procedure uses a standardized set of monthly, decadal or daily climatic input parameters, as follows:

$Tmax$	maximum daily temperature (°C)
$Tmin$	minimum daily temperature (°C)
RH	mean daily relative humidity (%)
$U2$	wind speed measurement (ms^{-1})
SD	bright sunshine hours per day (hours)
A	elevation (m)
L	latitude (deg)
J	Julian date, i.e., number of day in year

The Penman-Monteith combination equation can be written in terms of an aerodynamic and a radiation term:

$$ET_O = ET_{ar} + ET_{ra} \quad (1)$$

where the aerodynamic term can be approximated by

$$ET_{ar} = \frac{\gamma}{\vartheta + \gamma^*} \cdot \frac{900}{T_a + 273} \cdot U2 \cdot (e_a - e_d) \quad (2)$$

and the radiation term by

$$ET_{ra} = \frac{\vartheta}{\vartheta + \gamma^*} \cdot (R_n - G) \cdot \frac{1}{\lambda} \quad (3)$$

where variables in (2) and (3) are as follows:

γ	psychrometric constant (kPa $°C^{-1}$)
γ^*	modified psychrometric constant (kPa $°C^{-1}$)
ϑ	slope of vapor pressure curve (kPa $°C^{-1}$)
Ta	average daily temperature (°C)
ea	saturation vapor pressure (kPa)
ed	vapour pressure at dew point (kPa)
$(ea - ed)$	vapour pressure deficit (kPa)
$U2$	wind speed measurement (ms^{-1})
Rn	net radiation flux at surface (MJ m^{-2} d^{-1})
G	soil heat flux (MJ m^{-2} d^{-1})
λ	latent heat of vaporization (MJ kg^{-1})

In the calculation procedure for the reference crop we use the following relationships to define terms in (2):

Average daily temperature:

$$T_a = 0.5(T_{max} + T_{min}) \quad (4)$$

Latent heat of vaporization:

$$\lambda = 2.501 - 0.00236 \quad (5)$$

Atmospheric pressure (kPa) at elevation A:

$$P = 101.3\left(\frac{293 - 0.0065\,A}{293}\right)^{5.256} \quad (6)$$

Psychrometric constant:

$$\gamma = 0.0016286 \cdot \frac{P}{\lambda} \quad (7)$$

Aerodynamic resistance:

$$r_a = \frac{208}{U2} \quad (8)$$

Crop canopy resistance:

$$r_c = \frac{R_l}{0.5\,LAI} \quad (9)$$

where under ambient CO_2 concentrations the average daily stomata resistance of a single leaf, variable R_l (sm^{-1}), is set to R_l = 100, and the leaf area index of the reference crop is assumed as LAI = 24·0.12=2.88.

Modified psychrometric constant:

$$\gamma^* = \gamma\left(1+\frac{r_c}{r_a}\right) \quad (10)$$

Saturation vapour pressure e_a for temperatures and

$$e_{ax} = 0.6108\exp\left(\frac{17.27\,T_{max}}{237.3+T_{max}}\right) \quad (11)$$

$$e_{an} = 0.6108\exp\left(\frac{17.27\,T_{min}}{237.3+T_{min}}\right) \quad (12)$$

$$e_a = 0.5\,(e_{ax}+e_{an}) \quad (13)$$

Vapour pressure at dew point, e_d :

$$e_d = \frac{RH}{100}\cdot\frac{0.5}{\left(\frac{1}{e_{ax}}+\frac{1}{e_{an}}\right)} \quad (14)$$

Slope of vapour pressure curve, ϑ, for given temperatures $Tmin$ and $Tmax$:

$$\vartheta_x = \frac{4096\,e_{ax}}{(237.3+T_{max})^2} \quad (15)$$

$$\vartheta_n = \frac{4096\,e_{an}}{(237.3+T_{min})^2} \quad (16)$$

$$\vartheta = (\vartheta_x + \vartheta_n) \quad (17)$$

Using (4)-(17) all variables in (2) can be calculated from the input parameters. To determine the remaining variables R_n and G used in the radiation term ET_{ra} of equation (3), we proceed with the following calculation steps:

Latitude expressed in rad:

$$\varphi = \frac{L\pi}{180} \quad (18)$$

Solar declination (rad):

$$\delta = 0.4093\sin\left(\frac{2\pi}{365}J - 1.405\right) \quad (19)$$

Relative distance Earth to Sun:

$$d = 1 + 0.033\cos\left(\frac{2\pi}{365}J\right) \quad (20)$$

Sunset hour angle (rad):

$$\psi = arc\cos(-\tan\varphi\tan\delta) \quad (21)$$

Extraterrestrial radiation (MJ m^{-2} d^{-1}):

$$R_a = 37.586\,d\,(\psi\sin\varphi\sin\delta + \cos\varphi\cos\delta\sin\psi) \quad (22)$$

Maximum daylight hours:

$$DL = \frac{24}{\pi}\psi \quad (23)$$

Short-wave radiation (MJ m^{-2} d^{-1})

$$R_s = \left(0.25 + 0.5\frac{SD}{DL}\right)R_a \quad (24)$$

For a reference crop with an assumed albedo coefficient $\alpha=0.23$ net incoming short-wave radiation (MJ m^{-2} d^{-1}) is:

$$R_{ns} = 0.77\,R_s \quad (25)$$

Net outgoing long-wave radiation R_{nl} (MJ m^{-2} d^{-1}) is estimated using:

$$R_{nl} = 4.903\cdot10^{-9}\left(0.1+0.9\frac{SD}{DL}\right)\left(0.34-0.139\sqrt{e_d}\right)\frac{(273.16+T_{max})^4+(273.16+T_{min})}{2} \quad (26)$$

Using (25) and (26), net radiation flux at surface, R_n, becomes

$$R_n = R_{ns} - R_{nl} \quad (27)$$

Finally, soil heat flux is approximated using

$$G = 0.14\,(T_{a,n} - T_{a,n-1}) \quad (28)$$

Where Ta,n and $Ta,n\text{-}1$ are average monthly temperatures of current and previous month, respectively. With equations (5), (10), (17), (27) and (28) all variables in (3) are defined and can be calculated from the input parameters described at the beginning of this Appendix.

2.

Appendix

Agro-ecological zoning soil moisture regime

In Module 1, AEZ calculates a daily reference soil-water balance for each grid-cell and estimates actual evapotranspiration for a reference crop. In the Module 2, soil moisture balance calculations are performed considering specific crop/LUTs.

Soil moisture balance

Daily soil moisture balance calculation procedures follow the methodologies outlined in *CROPWAT (FAO 1976, 1992)* and the paper: *"Crop Evapotranspiration" (FAO, 1998)*. The quantification of a crop-specific water balance determines crop "actual" evapotranspiration (ETa) used for water-constrained crop yield estimation.

The volume of water available for plant uptake is calculated by means of a daily soil water balance (Wb). The Wb accounts for accumulated daily water inflow from precipitation (P) or snowmelt (Sm) and outflow from actual evapotranspiration (ETa), and excess water lost due to runoff and deep percolation.

$$Wb_j = \min(Wb_{j-1} + Sm_j + P_j - ETa_j, Wx)$$

where j is the day of the year; Wx is the maximum water available to plants. The snowmelt (Sm) is accounted within the snow balance calculation procedures and water in excess of Wx is booked as lost from soil moisture due to runoff and deep percolation.

The upper limit Wx of the water available to plants depends on the soil's physical and chemical characteristics that influence total soil water holding capacity (Sa). By definition, Wx is the product of total soil water holding capacity (Sa) and rooting depth (D).

$$Wx = Sa \times D$$

The Sa value is a soil-specific attribute defined as the difference between soil moisture content at field capacity (Sfc) and permanent wilting point (Swp) over the rooting zone. For reference soil moisture balance calculations, a total water holding capacity of 100 mm is assumed. Therefore, at any given day, actual soil water content (Wb) will be available to plants if $Swp < Wb < Sfc$ (Figure below).

However, water extraction becomes more difficult as soil water content (Wb) is less than a critical threshold (Wr) defined by p, the "soil water depletion factor", and the soil water holding capacity (Sa). When sufficient easily extractable water is available in the soil, actual evapotranspiration ETa will match maximum potential evapotranspiration ETm. In the reference water balance of AEZ Module 1, maximum potential evapotranspiration ETm is taken to be the Penman-Monteith reference evapotranspiration ETo. In crop water balance calculations of specific crops/LUTs, crop-stage specific parameters are applied to ETo to estimate respective ETm values.

For actual soil moisture falling below the threshold of easily extractable water, the value of ETa will be less than ETm and a crop water deficit $WDe = ETm - ETa$ occurs.

Schematic representation of water balance calculations.

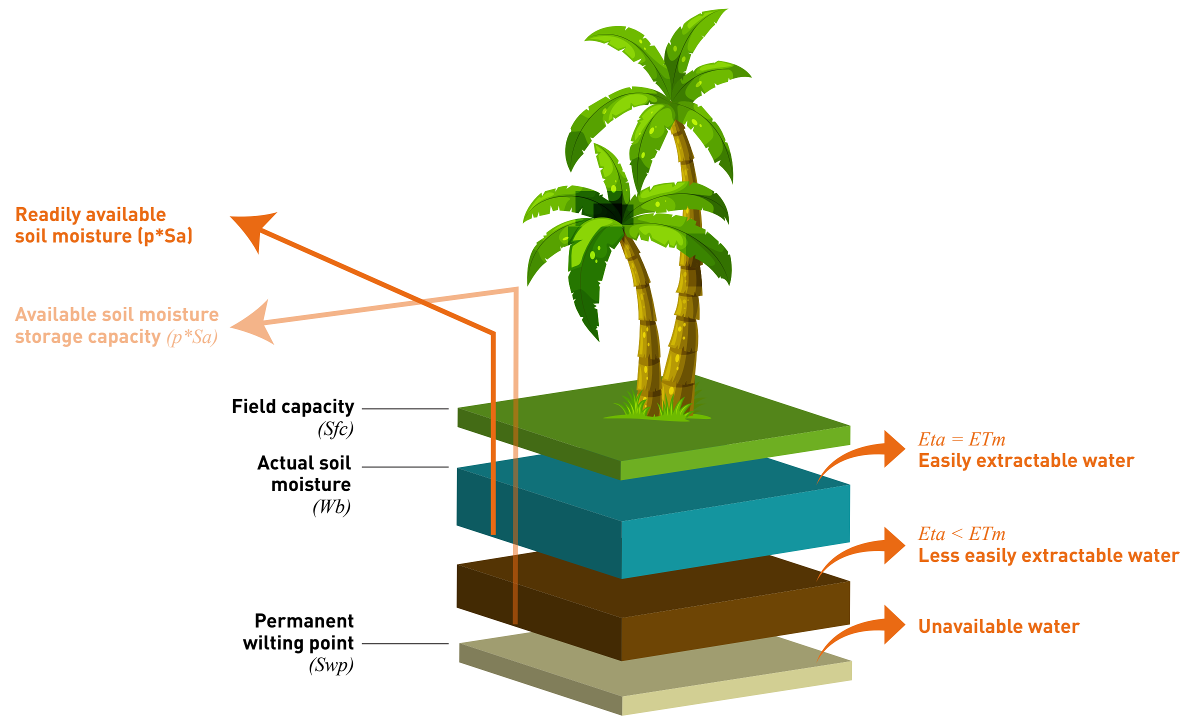

3.

Appendix

Agro-ecological zoning net primary production potential indicator

Net primary production (NPP) is estimated in AEZ as a function of incoming solar radiation and soil moisture at the rhizosphere. Actual crop evapotranspiration (ETa) has a close relationship with NPP of natural vegetation as it is quantitatively related to plant photosynthetic activity which is also driven by radiation and water availability. NPP is estimated according to Zhang & Zhou (1995) as follows:

$$NPP = \sum ETa \times \frac{A_0}{d}$$

The $\sum ETa$ are accumulated estimates of daily ETa from the AEZ water balance calculations. The variable A0 denotes a proportionality constant depending on diffusion conditions of CO_2 and d is an expression of sensible heat. The ratio $A0/d$ can be approximated by a function of the radiative dryness index (RDI) (*Uchijima & Seino, 1988*).

$$\frac{A_0}{d} \approx f(RDI) = RDI \times \exp\left(-\sqrt{9.87 + 6.25 \times RDI}\right)$$

with:

$$RDI = \frac{\sum_{j=1}^{12} Rn_j}{\sum_{j=1}^{12} P}$$

Where, $\sum Rn$ is accumulated net radiation for the year and $\sum P$ is precipitation for the year.

Two separate evaluations of the NPP function are performed:

1. For NPP estimates under natural, i.e rain-fed conditions, RDI is calculated from prevailing net radiation and precipitation of a grid cell and ETa is determined by the AEZ reference water balance:

$$NPP_{rf} = \sum ETa \times RDI \times \exp\left(-\sqrt{9.87 + 6.25 \times RDI}\right)$$

2. For an NPP estimate applicable under irrigation conditions, ETa = ETm is assumed and a RDI of 1.375 is used, which results in a maximum for the function term approximating the $A0/d$ ratio:

$$NPP_{ir} = \sum ETa \times 1.375 \times \exp\left(-\sqrt{9.87 + 6.25 \times 1.375}\right)$$

NPP is computed based on estimated actual evapotranspiration of the reference water balance and serves as a climate related indicator of rain-fed biological activity.

References

FAO. 1976. *CROPWAT. A computer program for irrigation planning and management. Irrigation and Drainage Paper 46.* Land and Water Development Division. Rome, FAO.

FAO. 1992. *CROPWAT. A Computer Program for Irrigation Planning and Management. Irrigation and Drainage Paper 46.* Land and Water Development Division. Rome, FAO.

FAO. 1998. *Crop Evapotranspiration: Guidelines for computing crop water requirements. FAO Drainage and Irrigation Paper 56.* Rome, FAO.

FAO. 1992. *Report on the Expert Consultation on Revision of FAO Methodologies for Crop Water Requirements.* Land and Water Development Division. Rome, FAO.

Hempel, S., Frieler, K., Warszawski, L., Schewe, J., & Piontek, F. 2013. *A trend-preserving bias correction – the ISI-MIP approach.* Earth Syst, Dynam. Discuss., 4, 49-92, 2013.

Monteith, J. L. 1965. *Evapotranspiration and the environment. The State and Movement of Water in Living Organisms.* XIXth Symposium, Cambridge, UK. Society for Xp. Biology, Swansea: 205-234.

Monteith, J. L. 1981. *Evapotranspiration and surface temperature.* Quarterly Journal Royal Meteorological Society, 107:1–27.

Taylor, K.E., Stouffer, R.J., & Meehl, G.A., 2011. *An Overview of CMIP5 and the experiment design.* Bull. Amer. Meteor. Soc., doi:10.1175/BAMS-D-11-00094.1, 2011.

Uchijima, Z., & Seino, H. 1988. *An agroclimatic method of estimating net primary productivity of natural vegetation.* Japan Agricultural Research Quarterly. 21: 244–250.

Van Vuuren, D.P., Edmonds, J.A., Kainuma, M., Riahi, K., & Weyant, J. 2011. *A special issue on the RCPs.* Climatic Change 109, 1-4, DOI: 10.1007/s10584-011-0157-y.

Zhang, X., & Zhou, G. 1995. A *New NPP Model. China Contribution to Global Change Studies*, China Global Change Report No. 2. (eds: Duzheng, Y. and Hai, L.), Science Press, Beijing. ISBN 7-03-995935-5/P.

THIS ACTIVITY IS FUNDED BY

The views expressed herein can in no way be taken to reflect the official opinion of the European Union

ISBN 978-92-5-131925-3

9 789251 319253

CA6889EN/1/11.19